Amélioration des modèles de cultures du blé par leurs réponses à la température : Phyllochrone et photosynthèse.

Maëva Baumont

THÈSE POUR OBTENIR LE GRADE DE DOCTEUR DE MONTPELLIER SUPAGRO

En Ecophysiologie

École doctorale GAIA – Biodiversité, Agriculture, Alimentation, Environnement, Terre, Eau
Portée par

Unité de recherche LEPSE

Amélioration des modèles de cultures du blé par leurs réponses à la température : Phyllochrone et photosynthèse.

Présentée par Maeva BAUMONT
Le 14 décembre 2018

Sous la direction de Pierre MARTRE
et Boris PARENT

Devant le jury composé de

John Roy PORTER, PR, University of Copenhaguen	Président
Daniel EPRON, PR, Université de Nancy	Rapporteur
Anne-Sophie VOISIN, CR, INRA Dijon – UMR Agroécologie	Rapporteur
Hélène MARROU, MC, Montpellier SupAgro – UMR System	Examinateur
Gaëtan LOUARN, CR, INRA Lusignan – UMR F3P	Examinateur
Pierre MARTRE, DR, INRA Montpellier – UMR LEPSE	Directeur de thèse

UNIVERSITÉ DE MONTPELLIER

Montpellier SupAgro

Résumé

Les modèles de cultures sont des outils très utilisé pour prédire le rendement des cultures dans des climats fictifs. Ils permettent d'anticiper les effets du changement climatique et d'autres contraintes et de prévoir des solutions pour améliorer notre agriculture. Mais les modèles actuels n'ont qu'une prise en compte limitée de l'impact de l'histoire thermique sur les capacités des plantes, ce qui pourrait être une limite majeure à leurs performances. Le travail présenté ici propose des pistes d'amélioration des modèles de culture, en particulier sur l'impact de l'histoire thermique des plantes sur la réponse du rythme d'apparition des feuilles et celle de la photosynthèse. Le premier axe de cette étude remet en question la modélisation actuelle du rythme d'apparition des feuilles. Ce dernier est majoritairement prédit via des équations empiriques qui ne traduisent généralement pas tous les effets connus de la lumière, photopériode, température, concentration en CO2, ou même du stade de développement sur le rythme d'émergence des feuilles de blé. Le premier chapitre de cette étude présente donc une nouvelle façon de modéliser le rythme de développement du blé basé sur la teneur en carbone de la plante. Cette hypothèse a pu être testée et validée par des expériences impliquant différentes températures, intensités lumineuses, photopériodes et teneurs atmosphériques en CO2. Les résultats ont été traduits en un modèle écophysiologique qui a montré de très bonnes performances dans des conditions de cultures en champs variées. Le deuxième axe de cette thèse s'intéresse à l'acclimatation de la photosynthèse du blé à un changement de température. Les expériences menées ici ont permis de développer un jeu de données regroupant un nombre important de scénarios de changement de température avec des suivis temporels de l'acclimatation de la photosynthèse. Nous avons pu différencier deux mécanismes d'acclimatation de la photosynthèse à la température : le premier est le résultat de l'effet de la température sur la vélocité du métabolisme, alors que le deuxième reflète la réponse des stomates aux changements de température. Ces hypothèses ont pu être approfondies dans un troisième axe d'étude où nous avons utilisé nos résultats dans un modèle de photosynthèse. Le but était ici d'abord de comprendre l'implication de la conductance stomatique dans la réponse de la photosynthèse à un changement température, qu'il soit immédiat ou sur du plus long terme ; puis de définir les limites du modèle à prédire l'acclimatation à la température. Ce travail démontre l'intérêt d'une prise en compte de l'aspect temporel sur la réponse des cultures à la température, que ce soit pour la photosynthèse ou pour le rythme de développement. Il montre aussi les limites des modèles

empiriques et démontre que l'amélioration des modèles passe par la construction d'équations se rapprochant des connaissances biologiques.

Mots clés : Modèles de culture, acclimatation, histoire thermique, température, intéraction carbone.

Abstract

Crop models are tools used to predict crop yield in virtual climates. They enable to anticipate the effects of climate change and other constraints and to provide solutions to improve our agriculture. However, current models have a limited consideration of the impact of thermal history on plant capacities, which could be a major limit to their performances. The work presented here provides areas for improving wheat crop models by formalisms of leaf appearance rate and carbon assimilation response to temperature and its variations. The first chapter of this study questions the actual modelling of leaf appearance rate. It is mostly predicted through empirical equations, which do not account for all known effects of temperature, light intensity, photoperiod, atmospheric CO2 concentration and development stage on wheat development rhythm. We present here a new way of modelling wheat leaf appearance rate (LAR) based on plant carbon status. This hypothesis of a carbon-driven development rate was supported by an experiment implying different levels of temperature, light intensity, photoperiod and atmospheric CO2. Results have been translated into an ecophysiological model which showed good performances in predicting LAR in contrasted field growth conditions. The second focus of this thesis was the acclimation of wheat photosynthesis to a temperature change. Experiences carried out in this thesis allowed the development of a data set of assimilation capacities under a large number of temperature change scenarios. We were able to differentiate two types of acclimation mechanisms. The first one is the direct result of temperature effect on the photosynthesis metabolism rate, while the second one reflects the response of stomata to a change of temperature. These hypotheses have been studied deeper in the third chapter of this work, in which these results were reanalyzed through a gas exchange model. The objectives were first to understand the implication of stomatal conductance in wheat carbon assimilation response to long and short-term temperature changes; and then to define the limitation of the model to predict this acclimation. This thesis demonstrates the importance of improving formalisms of temperature effects on development rate and carbon assimilation. It also highlights the limits of empirical models and demonstrates that developing new equations closer to biological knowledge could improve predictions of crop growth models.

Key words: Crop models, acclimation, thermal history, wheat, temperature, carbon interaction.

Remerciements

Arriver au bout de cette thèse n'a certainement pas été une tâche facile. Il y a eu beaucoup, beaucoup de moments de doutes ou de découragements. Ceci n'aurait jamais aboutis sans votre soutien.

Je voudrai tout d'abord remercier mes encadrant, Pierre M. et Boris P. Merci d'avoir placé votre confiance en moi pour ce projet. Merci de m'avoir donné l'indépendance dont j'avais besoin, tout en étant là quand c'était nécessaire. Merci de m'avoir guidé tout au long de cette recherche. Merci aussi à Bertrand M. pour tes conseils, ton soutien et ton implication. Merci aussi pour cette conversation il y a quelques mois qui a été un grand déclic pour que j'arrive au bout de ce travail.

Le parcours me menant à ce projet de thèse a été assez improbable, et je dois cette opportunité en partie à Thierry S. et Angélique C. Merci à vous deux de m'avoir proposé ce stage à un moment clé, merci d'avoir permis que tout se présente comme une évidence. Angélique, merci d'avoir entrainé une grande amélioration de mon orthographe, et merci de ton soutien pendant tout ce temps.

Merci à XinYou Y. et aux autres partenaires du projet ModCarboStress pour leurs conseils et avis qui ont largement permis l'avancé de cette thèse. De même, merci à Delphine L., Tanguy L. et Jean-Louis D. pour votre présence à mes comités de suivis de thèse. Vos conseils et encouragement m'ont été précieux. Un merci particulier à Bernard G. pour avoir toujours su dégager du temps pour nous aider sur les interprétations, même un dimanche soir depuis le Japon. Merci pour tes conseils qui ont toujours été d'une grande aide.

Merci évidemment à toute l'équipe du LEPSE, parce que travailler ici c'est se sentir entouré et soutenu tous les jours. Merci à Loïc M. pour son aide et ses conseils sur les scripts de modèle, merci pour ta disponibilité et tes conseils. Un grand merci à Benoit S. et Stéphane B. pour le soutien technique, je me souviens particulièrement des pannes de chambre A pendant les vacances de Noel… Merci aussi à Gaëlle R., pour les nombreuses heures passées au labo à percer les secrets du dosage de fructanes, et à Myriam D., pour son soutien sans faille face à ces capricieux CIRAS. Merci à Marie-Claude, Marie-Françoise et Katy pour l'aide administratif. Désolé Marie-Claude pour ces ordres de missions à la dernière minute, promis c'est fini...! Merci pour

votre patience à tous, merci d'avoir supporté mes maladresses quotidiennes, merci pour vos encouragements et sourires.

Un grand merci aussi à Jacques R. et son équipe de l'unité CNRS – Ecotron ; ainsi qu'à Bernard G. et son équipe du CEA de Cadarache. Merci pour vos accueils, et pour m'avoir fait me sentir à ma place pour quelques mois. Merci pour votre disponibilité et vos conseils face à mes protocoles infinis.

Merci à chaque personne que j'ai pu croisé pendant des formations, des congrès ou des rencontres. Vous m'avez tous insuffler un élan d'inspiration, de détermination, de confiance qui m'ont fait arriver jusqu'ici. Et puisque l'inspiration peut se trouver parfois à des endroits plus incongru, merci aux auteurs, réalisateurs, journalistes, aux gens croisés au hasard de soirées, à toutes ces autres rencontres inspirantes, merci à vous tous de m'avoir insufflé ces élans de confiance et de détermination. Merci de m'avoir montré que quand on veut, on peut. Merci de m'avoir aidé à me dépasser.

Et pour tout ça, merci Soraya. Je sais que tu ne réalises pas à quel point tu m'as aidé à arriver au bout de ces derniers mois, à quel point tu m'as fait évoluer. Je ne suis pas sure moi non plus de le réaliser complètement mais en tout cas le résultat est là, et je t'en remercie. Merci aussi pour ton soutient ces dernières semaines, merci pour les repas, les encouragements et les débriefes quotidiens, ça m'a été précieux.

Milles merci à Laetitia pour ton soutient depuis toutes ces années. Merci pour les moments de bulles apaisants que tu m'offres, loin dans notre monde à nous. Merci pour le soutient aveugle que tu m'offres en toutes circonstances. Merci à Isa, Marie, Audrey, je n'aurais jamais été qui je suis sans vous, merci.

Merci aussi à Cassandre. Tu as été un support important à ma vie pendant ces années, tu m'as permis d'évoluer et d'avancer jusque-là et je t'en remercie du fond du coeur.

Milles merci à mes chers collègues et surtout amis d'avoir partagés ces presque 4 ans avec moi. Merci Sandy pour tes conseils toujours avisés. Merci Diane pour ta compréhension et ton écoute ces derniers mois. Merci Romain, depuis toutes ces années d'être là, tu auras suivi ces huit ans d'études. Eh bah on aura bien changé ! Merci pour ton soutien, pour tes conseil et merci pour les tonnes de souvenirs construits. Merci Monique pour ta lucidité et ton soutien, tu nous auras manquer ces dernières années… Et merci à Agathe. Qu'est-ce que j'aurais fait sans toi pendant

toutes ces années ? Je te réponds enfin : surement pas grand-chose... ! Merci pour ces parties de rigolades infinies, pour ces débats à n'en plus finir, merci pour ces soirées ciné, raclettes, jeux... ça ne sera jamais suffisant mais MERCI !

Et finalement merci à ma famille qui, de prêt ou de loin, en comprenant ou non ce que je fais, a toujours été là pour moi, depuis 26 ans maintenant. Merci Papa et Maman de n'avoir mis aucunes limites à mon développement, à mes choix. Merci à mes chers frères et soeur pour tous ces souvenirs, j'aime tellement vous voir débattre en finissant par en oublier la raison, à vouloir toujours avoir le dernier mot... Vous m'aurez mine de rien appris à construire mes arguments, ce qui m'aura été très utile ici !

Et finalement merci Maman, cette dernière ligne de revient. Merci pour ton soutien sans faille. Tu es vraiment la meilleure maman du monde, et je le dis à tous : ma maman c'est la meilleure ! Tout ce travail est pour toi, mais ça tu le sais déjà.

Table of content

General introduction

> The proper use of science is not to conquer nature, but to live in it.
>
> —Barry Commoner

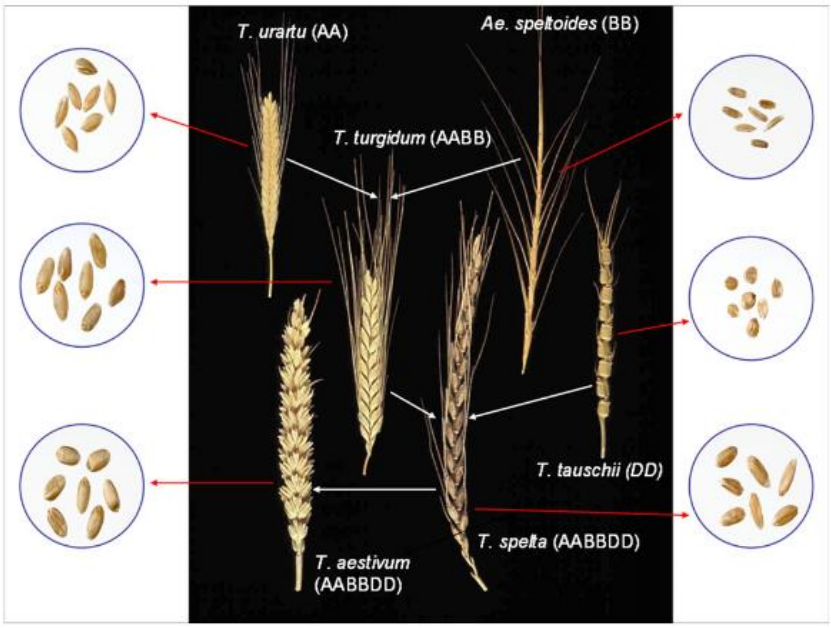

Figure 0.1: Cultivated bread and durum wheat and related wild diploid grasses morphologic and genetic differences. From Shewry (2009).

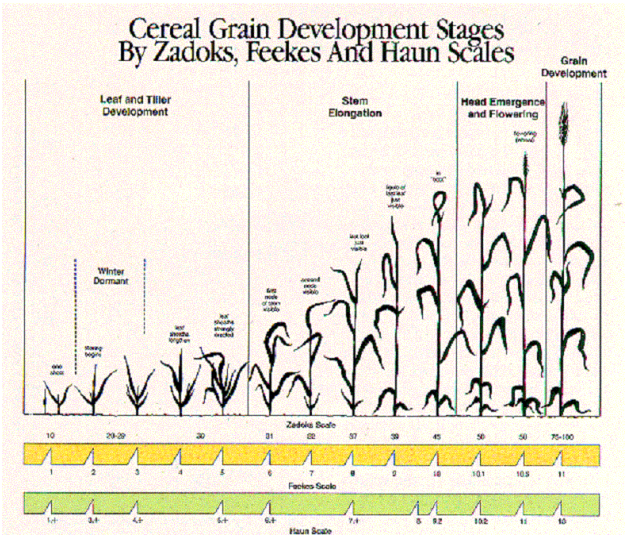

Figure 0.2: Main development stage in wheat.

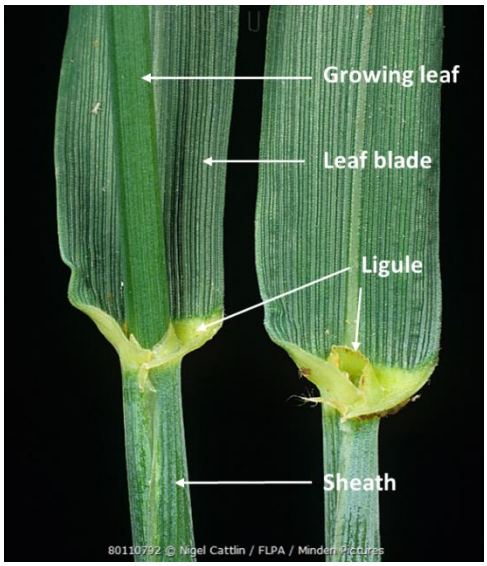

Figure 0.3: Illustration of wheat ligule and surrounding organs.

I. Climate change and wheat agronomy

1. Wheat as one of the major crop of the world diet

Wheat is the second most important world cereal crop, after maize (749 Mt produced in 2016). It is grown on all continents, as a rainfed crop under temperate climates, in the sub-tropics with winter rainfall, in the tropics near the equator, in the highlands with altitudes of more than 1500 m and in the tropics far from the equator where the rainy season is long and where it is grown as a winter crop. Wheat was domesticated at least 12 thousands years ago with the setting of agriculture during the Neolithic Revolution from still living diploid (genome AA) and tetraploid (genome AABB) ancestors respectively called einkorn (*Triticum monococcum*) and emmer (*T. dicoccum*) originated from the Near Est region (Shewry, 2009). On a physiological aspect, differences are larger seeds with hulls and non-shattering rachis for the last one, increasing its yield and facilitating its harvest (Fig. 0.1).

The genus *Triticum* includes a wide range of species, but only two species are grown commercially to a large extent; the hexaploid bread or common wheat (*T. aestivum* L.), representing over 90% of the wheat grown worldwide. Its main uses are for bread making and livestock feeding; the tetraploid durum or macaroni wheat (*T. turgidum* L. subsp. durum (Desf.) Husn.), with a higher protein content is mostly grown in the Mediterranean basin and is used for pasta production.

2. Wheat development

Like many grasses, wheat is an annual monocotyledon characterized by two main developmental phases (Simmons, 1987; Fig 0.2). The vegetative phase is characterized by the production of leaves and tillers (Haun, 1973; Tottman *et al.*, 1979). Leaves are produced from an apical meristem that remains close to the soil level as long as new leaves are produced. The growing leaf rises inside the sheath of the previous leaf until its emergence above the whorl of the older leaf. The leaf continues to extend until its ligulation (appearance of its ligule, see Figure 0.3). Leaf ligulation is an important stage since it is concomitant with the end of the leaf lamina elongation. Leaf is there considered mature, meaning it has reach its full photosynthesis capacities. During the vegetative phase, axillary meristems are formed at the base of mature leaves, giving rise to tillers that also produce leaves as does the main tiller. A widely used metric to describe grasses development is

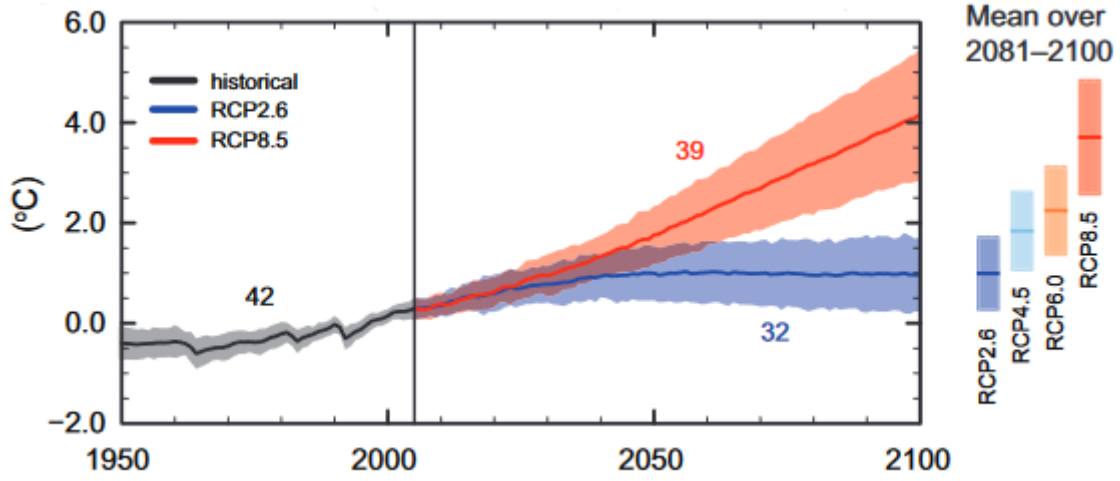

Figure 0.4: Time series simulated from multiples models from 1950 to 2100 for the evolution of the global annual mean temperature. Black represents the historical evolution and is modelled from historical data. Means and their uncertainties for the 2010-2100 period are presented for all Representative Concentration Pathway (RCP) scenarios with the colored vertical bars. Number of used models are indicated next to the lines. Source: Cubasch et al. (2013).

the Haun scale (abbreviated HS; Haun, 1973). Plant development stage is translated through a number with the unit being the number of ligulated leaves, and the decimal representing the ratio of the growing leaf compared to the youngest ligulated one (eg. HS = 3.5: three ligulated leaves, the fourth leaf reaching half of length of the third one).

The duration of the vegetative phase is determined by external factors such as vernalization (cold period needed for the plant to switch into the reproductive stage) and photoperiod; and by genetic factors, distinguishing cultivars requirements for vernalization or sensitivity to photoperiod (Flood and Halloran, 1986; Cao and Moss, 1991). Common wheat can thus be separated between spring wheat, which does not require vernalization, and winter wheat for which a vernalization period is required for floral transition.

The second development phase is reproductive. The elongation of internodes marks the transition between the two main phases. The last leaf is called flag leaf and displays special features like improved photosynthetic capacities (Evans, 1983). Flag leaf improved capacities have been related with wheat yield in several studies (Simpson, 1968; Evans, 1983). The ear then emerges and ages until anthesis (flowering during which pollination occurs), followed by kernels formation and maturation. Not every tiller will enter in a reproductive stage, differencing the fertile from the unfertile ones (Sharma, 1995; Frank and Bauer, 1996).

3. Range and impact of climate change

a. Current and future climate change

Since the onset of the industrial revolution, human activities induced a regular increase of greenhouse gases concentration, leading to considerable changes of the Earth climate (later referred as CC: climate change). Considerable research effort has been devoted during the last 2 decades to predict climate evolution for the next century (IPCC, WG I, 2013). Regularly updated, these scenarios predict different trajectories of the climate based on hypotheses related to the future release of Greenhouse gases emission (CO_2 on the first place, which increased from 340 to 400 ppm from 1980 to 2016). These trajectories predict a rise in air temperature of +2.0°C up to +3.7°C by 2100 as compared to the pre-industrial period (IPCC SR15; Christensen *et al.*, 2007) (Figure 0.4), while temperature today is on average 1°C higher than before the industrial revolution (early 20th century) (IPCC, WG II, 2014). Most scenarios predict a rise of temperature

variations as well as increased occurrence of extreme events such as heat waves, drought, flood or extreme cold.

b. Impacts of climate change on agriculture and on wheat production

Impacts of climate change on agricultural production have been extensively studied for more than three decades. While earlier experimental studies focused on the impact of atmospheric CO_2 concentration ($[CO_2]_{atm}$) (Long, 1991; Rosenzweig and Parry, 1994; Moore *et al.*, 1999; Wall *et al.*, 2000), elevated temperature and drought independently (Henckel, 1964; Chaves *et al.*, 2002; Farooq *et al.*, 2009), most recent studies tend to combine stresses associated with climate change because they are likely to co-occur (Crous *et al.*; Gifford, 1995; Vile *et al.*, 2012; Perdomo *et al.*, 2014). Because their occurrence is also likely to increase with CC, extreme events are also the matter of several studies (Kratsch and Wise, 2000; Thomashow, 2003; Porter and Semenov, 2005; Barnabás *et al.*, 2008). The outcome of simulations combining both a regular trend in temperature increase and a rise in the occurrence of extreme temperatures could lead to a decrease of wheat production by 50% (Asseng *et al.*, 2011). Other studies associate yield loss to the reduction of the period compatible with wheat cultivation resulting from the rise of temperature(Zhao *et al.*, 2017). By contrast with elevated temperature, an increase of $[CO_2]_{atm}$ could improve yield and lead to a partial compensation of the loss due to increased temperature (Wheeler *et al.*, 1996). Finally, aside from yield modifications, a change in wheat flour end-use value through changes on protein concentration are also expected (Porter and Semenov, 2005), or nutritional value (Müller *et al.*, 2014).

Interestingly, the effect of the increase in temperature variation*s* has been much less studied. The impact of amplitude, rhythm and temperature range on major plant processes is still poorly understood and it is acknowledged that research effort should be devoted to better understanding crop response to such variations (Rötter *et al.*, 2011; Rosenzweig *et al.*, 2014).

II. Crop models: a useful but limited tool

1. Definition

Simulation models can be defined as a series of mathematical equations based on laws driving a system, which aims at predicting an output from an input. They exist in many disciplines, from social science to astrophysics. If Stephen Hawkins says in its books *The Grand Design* that everything respond to law ("*all the evidence is that [nature] evolves in a regular way according to certain laws*"), he also noted that these laws and interactions are complex. It is so hard to perfectly describe a system with a model, and the difficulty rises with the system complexity: "*whenever we deal with macroscopic systems, the number of particles is always too large for there to be any chance of solving the fundamental equations* [*nb*: the physical equations describing the behavior of these particles]. *What we do instead is use effective theories*". Stephen Hawkins thus suggests that the better the system is understood, the better founded the theories and so the better the model will be. However, models do exist without translating a system understanding. They are composed of equations describing empirical relations, which do not translate the reason binding this relation. A good example in biology is the use of thermal time to describe plant development rate (Wang and Engel, 1998; Bonhomme, 2000). This example and its limits are further discuss in the third part of this chapter.

A model offers an environment control going far ahead from what experimentation allows, in terms of range of variables and in terms of possible control and decoupling of these variables. Thus, models are used to predict the behavior of plant processes in specific environments (Sinclair and Horie, 1989; Wheeler *et al.*, 1996; Long and Bernacchi, 2003; Evers *et al.*, 2010). Biological systems can be modelled at many scales, from molecules to ecosystems. Ecophysiological models describe specific plant processes response to environmental variables such as climate components (temperature, irradiance, wind…) or soil properties (compositions, nutrient availabilities…). They are used for instance to predict carbon assimilation or transpiration rate (Farquhar *et al.*, 1980; Collatz *et al.*, 1991). Ecophysiological models can be combined to simulate crop behavior (Bernacchi *et al.*, 2013; Zhu *et al.*, 2018), then constituting a crop model. Crop model are used to predict crop yield and development in a given environment. It uses environmental variables inputs – translating the studied climate, soil and geographical location – as well as specific parameters calibrated according to the studied species and even cultivar for some specific processes.

Early crop models each have their own structures with specific considered variables and logic, resulting in very few applications. With the development of their use, the need of efficient and transposable crop models emerged (Reynolds and Acock, 1997). This is reached by dividing the modelled system into biologically meaningful units called modules. Then, each module constitutes an ecophysiological model, since it translates a response of a target plant process to the environment. According to Reynolds and Acock, (1997) modules should: 1) relate directly to the real world processes; 2) have input and output that are measurable values; 3) communicate via these inputs or outputs. Some examples of modules of crop models are photosynthesis, leaf emission, leaf growth, seed filling etc… In such modular models, modules can be easily transposed, replaced or modified, making them adaptable to the working hypothesis.

Crop models falls in two categories depending on the role given to carbon as a driver (Parent and Tardieu 2014). In source-limited models, processes are organized in series with carbon assimilation being on the top of the chain and most other processes being dependent on this assimilation, including leaf growth. Here, a stress such as water deficit will impact the system primarily through photosynthesis (Kaiser, 1987; Lawlor and Cornic, 2002) which in turns affects other processes. In contrast, in sink-driven models leaf growth and C assimilation are modeled in parallel and can be uncoupled which better fits with experimental evidence (Muller et al 2011).

2. Crop model uses and limits

Crop models have multiple uses. They are used as analytical tools to test hypotheses of crop behaviors (Parent *et al.*, 2018) under various conditions or to design new crop management strategies or cropping systems (De Reffye *et al.*, 1995; Dupraz *et al.*, 2011). Crop models are also used to project the impacts of future climate scenarios and test climate change adaptation and mitigation strategies (Hoogenboom, 2000; Challinor and Wheeler, 2008; Bassu *et al.*, 2009; Rosenzweig *et al.*, 2014; Martre *et al.*, 2017). They can also be used as tools for crop management and decision-making. The incorporation of genetic variability (most often through genotype-dependent parameters) in these crop models is not systematic although it helps genetic studies in many ways. They can be used to assess the importance of specific genetic regions to different climatic scenarios (Chenu *et al.*, 2009; Millet *et al.*, 2016), to quantify environmental co-variables cultivar responses (Heslot *et al.*, 2014; Ly *et al.*, 2017) or to target interesting phenotyping traits (Tardieu *et al.*, 2017; Chenu *et al.*, 2018). Integrating genotype effects in crop models allow the

identification of ideotypes (*ie* cultivars gathering a series of favorable traits in a given environment), guiding plant breeding in front of climate change (Hammer *et al.*, 2002; Slafer, 2005; Lisson *et al.*, 2005; Chenu *et al.*, 2017).

Using crop models to estimate the performances of crops under futures climates raises their limitations when working with multiple stresses. Some of these limits comes from their way of managing time. Indeed, daily mean temperature, calculated as the mean of the daily maximal and minimal temperature, is the most commonly used input when time is needed. In a few models, the daily mean is decomposed in hourly mean, generally used as input in some very specific modules generally linked for instance to photosynthesis. However, some processes are known to have more complex responses to variations of environmental variables, and a daily input is not enough. This is the case for processes such as carbon assimilation, which are known to acclimate to a change of temperature for instance (Atkin and Tjoelker, 2003; Asseng *et al.*, 2013; Yamori *et al.*, 2013). This will be further discuss in the section III.4 of this chapter. To account for these effects of climate history and variation effects on plant performances, model time-scale needs to be more precise (Thornley, 1998).

Another source of models errors come from a lack of biological knowledge. First, because our lack of understanding of the ecophysiological mechanisms leads to empirical representations that limit models uses (Yin and Struik, 2010). Then, because data available to quantify or understand the effect of a variable on another are often not enough to develop a model. This is the case for example for plant response to combined drought, temperature, and elevated atmospheric CO_2. Another example is the understanding of plant acclimation to temperature. Recent studies highlighted the importance of a good modelling of plant response to temperature to ensure good crop model simulations (Asseng *et al.*, 2011; Yamori *et al.*, 2013; Way and Yamori, 2014; Li *et al.*, 2015).

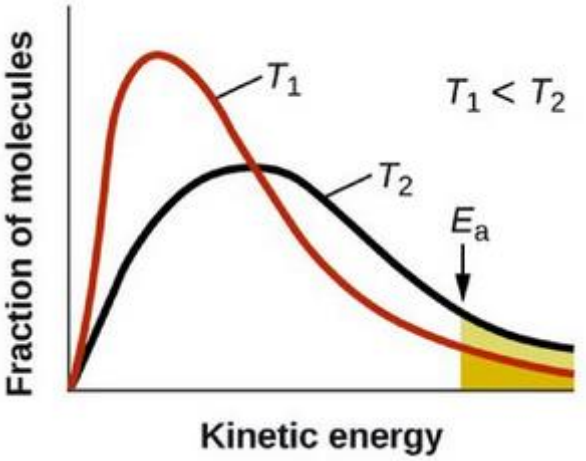

Figure 0.5: Representation of the kinetic energy formed by a reaction according to the Arrhenius equation at two temperatures T_1 and T_2. E_a: activation energy.

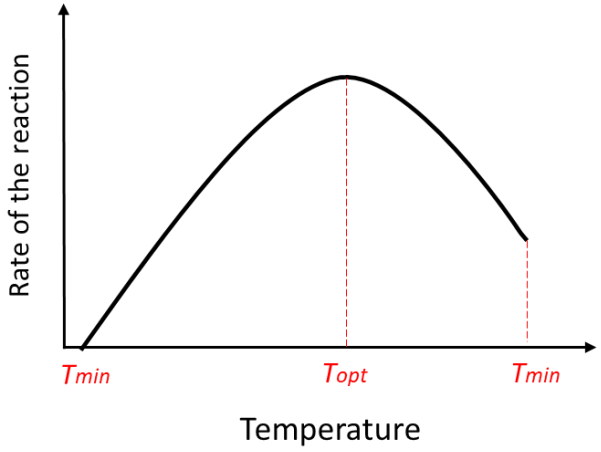

Figure 0.6: Schema of the general response of biological process response to temperature. T_{min} is the minimal temperature needed to obtain a reaction, T_{opt} is the temperature were the reaction is at its maximal velocity, and T_{max} is the maximal temperature beyond which no reaction is possible.

III. Impact of temperature on plants

1. General equations to model plant processes response to temperature

Temperature is a physical variable defined by the state of particles agitation: the more the particles are agitated, the more they collide, the more thermal energy is released, and the higher is temperature. This particle agitation state is translated in biology by a meeting potential between two molecules. For instances, the higher the temperature, the more an enzyme is likely to meet its substrate. This is true up to a given temperature beyond which links giving its configuration to a molecule are weakened and molecules are denatured. A minimal particle agitation is needed to obtain a reaction, translating a necessary activation energy specific to each reaction. Thus, enzymatic reaction and linked processes respond to temperature first by an increased rate attributed to a rise of implied enzyme velocity (Daniel *et al.*, 2008); then by a decreased rate linked to a loss of protein and membrane integrity (Upchurch, 2008).

Links between temperature and energy have been translated into a widespread equation expressing the relation between reaction rate and temperature: the Arrhenius equation, developed in 1889 by Svante August Arrhenius. This model describe well the temperature effects on almost all biological systems (Dell *et al.*, 2011) (Fig 0.5).The initial equation only accounts for reaction rate increase with temperature, depending on an activation energy. It has later been modify to include the observed decrease at higher temperature (Johnson *et al.*, 1942). This modify Arrhenius equation is now commonly used to describe biological and biochemical reaction response to temperature (Farquhar *et al.*, 1980; Parent *et al.*, 2010; White *et al.*, 2012; Bernacchi *et al.*, 2013).

Another commonly used equation to describe processes response to temperature is the beta function equation proposed by Wang and Engel (1998). The response is here characterized by three cardinal temperatures: a minimum temperature (also called based temperature; T_{min}) required to obtain a reaction, an optimal temperature (T_{opt}) at which the reaction rate reaches its maximum, and a maximal temperature (T_{max}) beyond which no reaction is possible (Gillooly *et al.*, 2001) (Fig. 0.6). The use of this equation to describe the temperature of plant development, leaf expansion, and carbon assimilation greatly reduces the uncertainty of crop model response to temperature (Wang *et al.*, 2017).

2. Rate of development and temperature

a. The thermal time concept

Every phase of development requires a minimum accumulation of temperature before that phase can be completed and the plant can move to the next stage (Gallagher, 1979). The higher the temperature, the faster the plant will reach this minimum accumulation and develop. This strong dependence of development rate on temperature has been translated into the thermal time concept (Wang, 1960). The principle of the thermal time concept is the following. First, the daily thermal-time (TT; expressed in degree-days, °Cd) is calculated. It represent the daily mean temperature above the plant development base temperature (T_b; minimal temperature required to observe a plant development).

$$TT = T_{mean} - T_b \quad (0.1)$$

Under the supposition of a constant effect of temperature on development rhythm, this daily thermal time is added over a time period to get the cumulated thermal time (°Cd) at day *d* since a given day d_0:

$$TTc_d = \sum_{i=d_0}^{d} TT_i \quad (0.2)$$

The base temperature is generally determined by a linear extrapolation of development rate response at low temperature (Bonhomme, 2000) but shows some variability with growth temperature and development stage, precisely because of its non-linear response to temperature as discussed in the next paragraph (Slafer and Rawson, 1995; Craufurd *et al.*, 1998; White *et al.*, 2012). For wheat, the base temperature for development is commonly assumed to be 0°C (Wang *et al.*, 2017).

Development according to cumulated thermal time has been acknowledged to be linear for a long time (Friend, 1965; Masle *et al.*, 1989*a*). However, recent studies have shown that when larger ranges of temperature are considered, responses are non-linear and this was integrated into a new concept of time spent at a given reference temperature. Thermal time is then calculated with a non-linear effect of temperature on development rate, with Johnson's similar equation described in Parent and Tardieu, (2012):

$$TT = T_{mean} \times A \frac{T_{mean} e^{-E/RT_{mean}}}{1+(e^{-E/RT_{mean}})^{\alpha(1-\frac{T_{mean}}{T_0})}} \quad (0.3)$$

Where E is the activation energy of the reaction; α is the ratio of E/D with D being the deactivation energy of the reaction; T_0 is the D/S ration, with S being an entropy term of the reaction deactivation; and A is the trait-scaling coefficient.

b. Simulating development through the phyllochron

Phyllochron is a widely used metric to quantify plant development. It represents the time interval between the setting-up of two successive organs (Wilhelm and McMaster, 1995). Many growth models use the phyllochron to model both vegetative and reproductive development (Rickman and Klepper, 1995; Fournier *et al.*, 2005; Evers *et al.*, 2010). This success relies on the robust linear relationship between leaf appearance rate (LAR) and temperature, and thus on its constancy when expressed in thermal time. However, even when expressed per degree-days, LAR has been shown to be non-constant in many situation, limiting its value to predict development rate. For instance, LAR increases with photoperiod (Baker *et al.*, 1980; Cao and Moss, 1989; Masle *et al.*, 1989*b*; Slafer *et al.*, 1994), irradiance (Rickman *et al.*, 1985; Volk and Bugbee, 1991; Bos and Neuteboom, 1998; Birch *et al.*, 1998), and atmospheric CO_2 concentration (Boone *et al.*, 1990; McMaster *et al.*, 1999) for several grasses including wheat. It is also known to decrease with plant density (Abichou *et al.*, 2018), red/far-red ratio and blue light (Gautier and Varlet-Grancher, 1996), and nitrogen or water deficit (Longnecker and Robson, 1994). It has also been reported to change with plant ontogeny (Hay and Delécolle, 1989; Slafer and Rawson, 1995; Miralles and Richards, 2000).

Whereas all these results are well-known, little efforts have been made to include them into crop models. Currently, development models represent these effects through empirical equations, making them hard to use in various condition. However, development rhythm determines the timing of all other processes and thus there is a real need to develop and improve development models to be able to improve crop model predictions.

Another process largely driven by temperature because of the numerous implied enzyme is the photosynthesis.

3. Carbon acquisition and temperature

a. Carbon assimilation mechanisms

Through photosynthesis, plants fix carbon from atmospheric CO_2. Two reactions are distinguished: i) the light-dependent reaction during which photon energy excites the photosystems on the

chloroplast membrane, leading the transfer of electrons that will triggers the oxydation of water, generating ATP and NADPH and releasing oxygen to the atmosphere; ii) the dark reaction during which the enzyme RuBisCO (Ribulose-1,5-bisphophate carboxylase/oxygenase) captures the atmospheric CO_2 which enter in the Calcin-Benson cycle. This cycle uses the newly formed ATP and NADPH and, in the case of C3 species, such as wheat, releases three carbon sugar exported from the chloroplast. Trioses are later combined to form soluble sugar such as glucose, fructose or sucrose that will enter the primary metabolism or will be derived to store C in the form of sugar polymers such as starch or fructans. Thus, the rate of photosynthesis depends on the electron transport rate, on the Rubisco carboxylation rate, and on the RuBP (carbon acceptor molecules) regeneration rate.

These reactions directly implies a dependence of photosynthesis rate to light intensity (defining photon availability), atmospheric CO_2 availability, and nitrogen availability (linked to the photosynthesis enzyme content and so to their reaction velocity (Sinclair and Horie, 1989). Temperature have also a large effect on photosynthesis since it directly acts on RuBisCO and Calvin-Benson cycle enzyme velocity (Farquhar *et al.*, 1980). It also triggers changes in membrane fluidity, structure and composition (Nishida and Murata, 1996; Upchurch, 2008), as well as in the activation state of the photosystems (Yamasaki *et al.*, 2002), affecting the electron transport rate.

The enzyme RuBisCO has a carboxylase site, allowing the carboxylation of RuBP, as well as an oxygenase site, allowing the oxidation of RuBP with atmospheric O_2 integrated in the Calvin cycle to form hydrogen peroxide, glycolate and serine. Those molecules are later recycled, releasing atmospheric CO2 and ammoniac. This reaction stemming from RuBisCO oxygenase is called photorespiration. Photorespiration is a wasteful process for the plant because it reduces photosynthesis rate and has a higher metabolism cost compared to RuBisCO carboxylase activity. Temperature changes the affinity of RuBisCO for carbon or oxygen, the carboxylase to oxygenase quotient will be higher at higher temperature, decreasing photosynthesis rate.

Assimilation response to temperature is a predominant subject of this work. It was study through experimental data and thanks to one photosynthesis among other: the Farquhar-von Cammerer and Berry model.

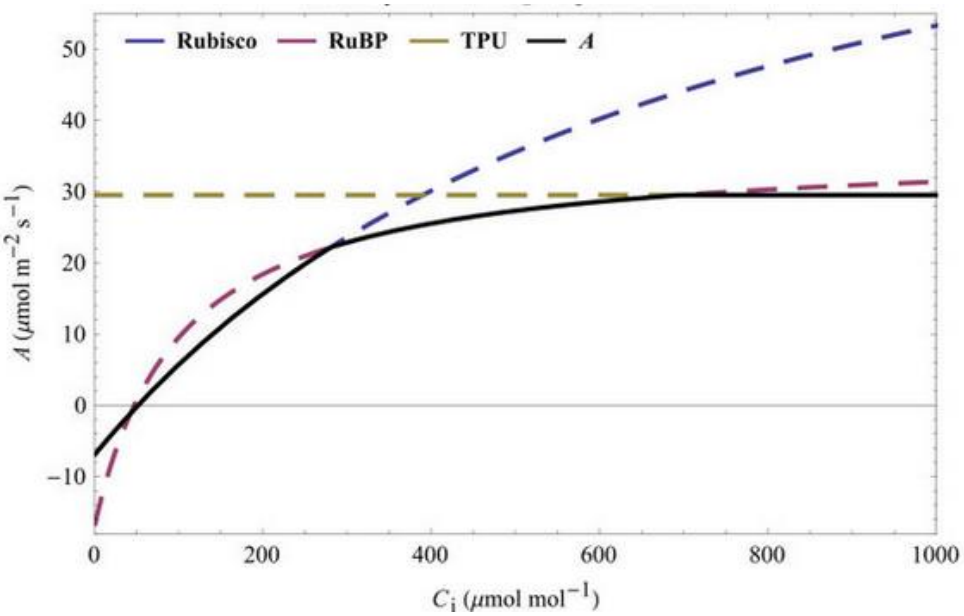

Figure 0.7: Assimilation (A) at saturating light response to leaf intern CO_2 concentration (C_i) using the leaf Farquahr model (Farquhar *et al.*, 1980). Modelled A is determined by whichever process is the most limiting (solid black line). Blue dotted line represent limit imposed by the maximum Rubisco carboxylation rate (limitation typically arising from CO_2 availability); red dotted line is the RuBP regeneration rate limitation (limited by photon availability); and gold dotted line is the limitation by the triose-phosphate use (TPU, limited by the ability to convert triose phosphate – molecule on which the new C atom is binded – into other sugars). Source: Bernacchi *et al.*, 2013.

b. The Farquhar-von Cammerer and Berry model of photosynthesis

The Farquhar, von Cammerer and Berry model (here after called the FvCB model) (Farquhar *et al.*, 1980) is a widely used model to describe carbon assimilation through its biological limits. It calculates net assimilation as the minimum of assimilation limited by the RubisCO carboxylation rate (A_c), by the electron transport rate implied in the Ribulose-1,5-bisphosphate (RuBP) regeneration rate (A_j), or by the triose-phosphate (TPU) use (A_T) (Fig 0.7). A_T is only reached for high CO_2 concentration and will not be considered in this study, therefore A is given as.

$$A = \min(A_c, A_j) \tag{0.4}$$

Ac is calculated as a function of the maximal rate of RuBisCO carboxylation ($V\mathrm{c}_{\max}$) by:

$$A_c = \frac{(C_c - \Gamma_*)V\mathrm{c}_{\max}}{C_c + K_{\mathrm{mC}}(1 + {}^{O}/_{K_{\mathrm{mO}}})} - R_d \tag{0.5}$$

where C_c (µbar) is the CO_2 partial pressure at the carboxylation sites of Rubisco; O (µbar) is the oxygen partial pressure; K_{mC} and K_{mO} are the Michaelis-Menten constant of Rubisco for CO_2 and O_2, respectively (µbar); J (µmol photons m^{-2} s^{-1}) is the electron transport rate; R_d (µmol CO_2 m^{-2} s^{-1}) is the day respiration (respiratory CO_2 release other than by photorespiration); and Γ_* (ppm) is the CO_2 compensation point in the absence of R_d.

Mitochondrial respiration (R_d) is common to all living organisms. Mitochondria are cellular organelles inside which glucose is oxidized, releasing energy under the form of ATP and $NADP^+$, necessary to all biochemical reactions. It also release CO_2, here again altering the net assimilation rate (raw assimilation being the assimilation rate when no mitochondrial respiration is considered). Like photosynthesis, it involves many enzymes and membranes, making it a process also dependent on temperature. Rd is so known to rise with temperature (Atkin *et al.*, 2005).

The temperature dependence of R_d and kinetic properties of Rubisco ($V\mathrm{c}_{\max}$, K_{mC} and K_{mO}) in Eq. (0.5) is described by an Arrhenius function normalized with respect to their values at 25°C:

$$Parameter = Parameter_{25} \times e^{\frac{(T-25)E}{[298R(T+273)]}} \tag{0.6}$$

where T (°C) is the leaf temperature, E (J mol^{-1}) is the activation energy, defining the responsiveness of the relevant parameter to temperature; R (J K^{-1} mol^{-1}) is the universal gas constant.

The FvCB model assumes 100% non-cyclic electron transport, thus excluding cyclic electron transport around photosystem I, and A_j can be calculated as:

$$A_j = \frac{(C_c - \Gamma_*)J}{4C_c + 8\Gamma_*} - R_d \quad (0.7)$$

In most applications of the FvCB model the relationship between *J* in equation (0.7) and irradiance is described by a non-rectangular hyperbolic function of irradiance by Farquhar and Wong (1984):

$$J = \frac{\left(\alpha_{(\mathrm{LL})} I_{\mathrm{abs}} - \sqrt{\left(\alpha_{(\mathrm{LL})} I_{\mathrm{abs}} + J_{\max}\right)^2 - 4\theta J_{\max} \alpha_{(\mathrm{LL})} I_{\mathrm{abs}}}\right)}{2\theta} \quad (0.8)$$

where $\alpha_{(\mathrm{LL})}$ (mol (electons) mol^{-1} (photons)) is the electron transport under low light; I_{abs} (µmol photon m^{-2} s^{-1}) is the photon flux density absorbed by leaf photosynthetic pigments; θ (dimensionless) is the convexity of the response curve of *J* to I_{abs}.

The optimum response of J_{max} to temperature is often described by a modified Arrhenius function (Medlyn *et al.*, 2002) (Fig. 0.6):

$$Parameter = Parameter_{25} \times e^{\frac{(T-25)E}{[298R(T+273)]}} \times \frac{1 + e^{\frac{(298.S - D)}{298.R}}}{1 + e^{\frac{(T+273)S - D}{R(T+273)}}} \quad (0.9)$$

where *S* (J K^{-1} mol^{-1}) is an entropy term; and *D* (J mol^{-1}) is the energies of deactivation, defining the responsive shape of the supra- optimal ranges.

The parameters composing this model thus relies on both metabolism capacities and implies energies. They can all be related to climate variables that are known to affect these parameters, like atmospheric CO_2 concentration or temperature. The FvCB model is often completed with complementary calculation, for example to account for stomatal and mesophyll conductance limitation on photosynthesis (Bernacchi, 2002; Flexas *et al.*, 2014).

Indeed, gas exchanges associated with photosynthesis (CO_2 entrance and O_2 release) happen through active pores on leaf epidermis, called stomata. Stomata opening determines gas transfer rate and is quantified via the leaf conductance (g_s,stomatal conductance, µmol H_2O m^{-2} s^{-1}). It is related to plant hydraulic status as well as to vapor pressure deficit (VPD, kPa) between leaf (within sub-stomatal cavities) and surrounding air (Osonubi and Davies, 1980; Morison and Gifford, 1983; Tardieu and Simonneau, 1998), themselves depending on temperature. This control of leaf gas exchange triggers a strong correlation between carbon assimilation rate and stomatal

conductance at the leaf scale (Nijs *et al.*, 1997; Del Pozo *et al.*, 2005), for many speciesand different growth conditions (Crafts-Brandner and Salvucci, 2000; Haldimann and Feller, 2004).

In the model used in this study, described in Yin *et al.* (2009)Yin and Struik (2009), *A* can be predicted with g_s as an input through a quadratic equation described in chapter 3. *A* can also be resolve without the intervention of GS, with an analytic solution described in Yin *et al.* (2009) and later in the chapter 3. g_s is then calculated as:

$$g_s = g_0 + \frac{(A+R_d)\times f(VPD)}{Ci - Ci_*} \quad (0.10)$$

Where g_0 is the residual stomatal conductance at extremely low light, Ci_* is the Ci compensation point in the absence of R_d, and $f(VPD)$ is a function translating the effect of VPD on g_s.

To understand the underlying process of carbon assimilation response to temperature, it is important to uncorrelate one from another, or at least to quantify the impact of one on the other (Leuning, 1995; Flexas *et al.*, 2014). This can be partly allowed by a good control of climate variables during gas exchange measurements (Long and Bernacchi, 2003). This issue can also be partly solved using models (Leuning, 1995).

This makes the FvCB model a very useful tool to characterize environment impacts on carbon assimilation and to make hypotheses on the underlying metabolism limitation in a given situation.

IV. Acclimation capacity of plants

1. Definition

To cope with climate variations that they experience at any time scale, from seconds to days or weeks, plants are able to acclimate to new environmental conditions. Acclimation of photosynthesis was first defined by Berry and Bjorkman (1980) as an “environmentally induced change in photosynthetic characteristics that results in an improved performance under the new growth regime”. This concept has been extended to other processes (*eg* respiration) showing modifications after change of the environment (Arnone and Körner, 1997; Atkin *et al.*, 2006). Acclimation needs to be distinguished from adaptation, being adjustment to the environment across generations (Arnone and Körner, 1997). As Way and Yamori (2014) noticed it, we need to adjust our definition when talking about acclimation. In this work, we will consider that there is

acclimation when the plant capacities change in response to an environment modification to reach capacities of plant fully grown in the new growth condition, regardless if this new condition lead to improved capacities or not.

Acclimation happens in response to diverse environmental variables like light intensity (Murchie and Horton, 1997; Evans and Poorter, 2001; van Rooijen *et al.*, 2015), atmospheric CO_2 concentration (Long, 1991; Sage, 1994; Gifford, 1995) and temperature (Atkin and Tjoelker, 2003; Hikosaka *et al.*, 2006; Smith and Dukes, 2017); and this for all type of plants, from fern to angiosperm, from C3 and C4-types (Yamori *et al.*, 2013). This work focus on the acclimation of wheat to temperature, and particularly on photosynthesis acclimation.

2. The time scale to consider

Another issue to assess when talking about process response to a change of growth environment is the considered time scale. We generally need to distinguish response of immediate changes from longer-term changes. For instance, studies of carbon assimilation response to temperature often assess the carbon assimilation response to immediate changes of temperature (A/T). This variable is obtained by measuring assimilation capacities (A) at either leaf, plant or crop level at different imposed temperatures. However, the temperature is generally imposed for a few minutes only, resulting in the measurement of assimilation capacities response to an immediate temperature change. In this case, we consider that no acclimation occurs. On the contrary, assessing assimilation capacities for a plant that undergone a longer temperature change (change of growth temperature; Tgrowth) will probably trigger acclimation. The lake of study monitoring the dynamic of a process response to long-term temperature changes does not allow to determinate how much time is needed to consider that acclimation happens, and that the observed result is not only a response to an immediate change. It is also important to distinguish immediate non-acclimated response of assimilation to temperature (noted A/T in this study) from response of assimilation to Tgrowth, the latter being fully-acclimated response (referred as a response to Tgrowth in this work).

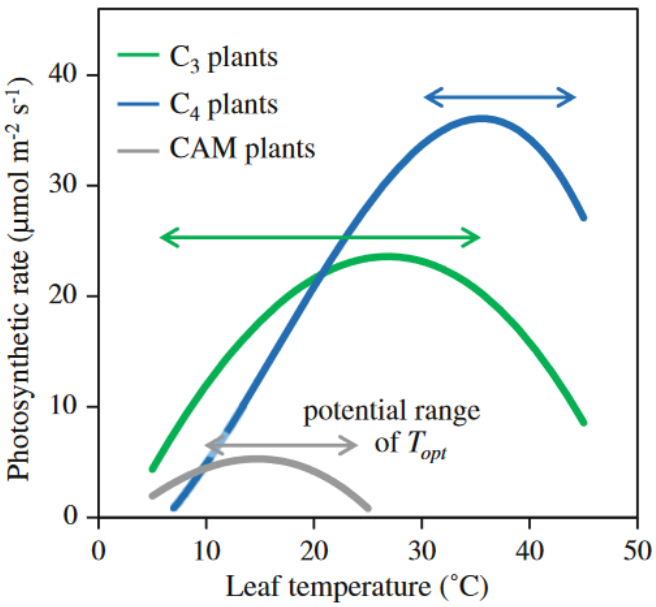

Figure 0.8: Typical temperature response of photosynthesis in C3, C4 and CAM plants. Source: Yamori *et al.*, 2013.

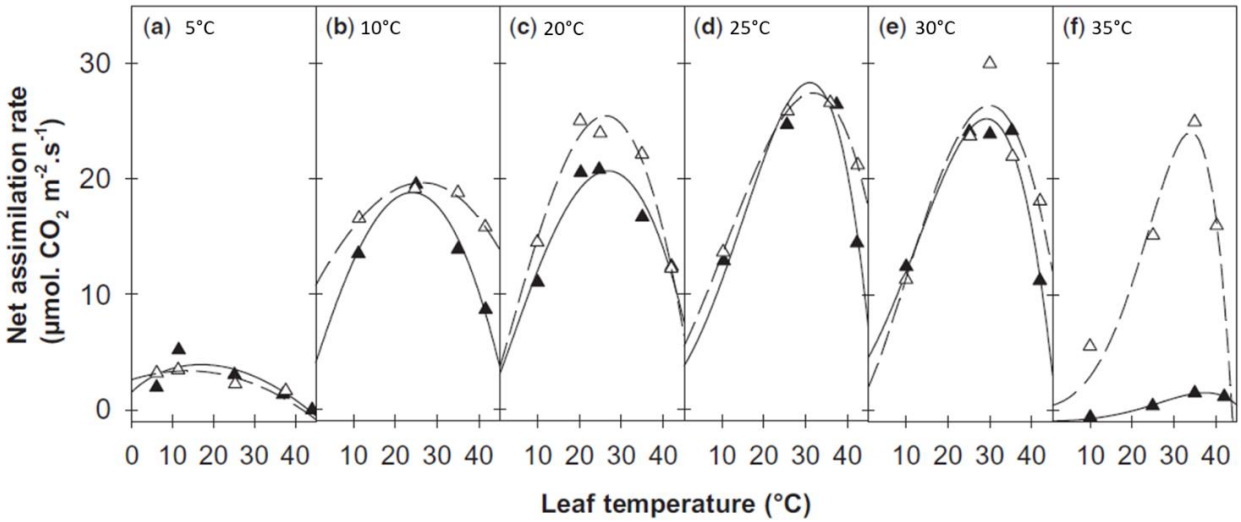

Figure 0.9: Temperature response of the net assimilation rate at ambiant CO2 for several growth temperateur (noted on the figure) for two alfalfa cutting of Mediterranean (filled triangles, full-lines) and temperatre (open triangle, dotted lines) origins. Source: Zaka *et al.*, 2016.

3. Photosynthesis acclimation to temperature

The importance of photosynthesis acclimation to temperature for plant success in fluctuating temperature conditions has made it an important studied subject this last decade (Berry and Bjorkman, 1980; Asseng *et al.*, 2011). Temperature response of carbon assimilation (*A*/*T*) is well known to depend on thermal regimes (assimilated to T_{growth}) in the natural habitats of wild plants or in regions where crops are adapted to (Sage and Kubien, 2007; Yamori *et al.*, 2013). Species from different climate origin show contrasted *A*/*T* response curves, with species adapted to cold climate having lower T_{opt} values than warm-originated ones (Slayter and Morrow, 1977; Yamori *et al.*, 2013; Zaka *et al.*, 2016) (Fig. 0.8). Differences of *A*/*T* curves are also found at the intra-specific level since widely spread cultivars of a same species can show contrasted assimilation response to temperature (Slayter and Morrow, 1977; Zaka *et al.*, 2016; Fig 0.9). A shift in growth temperature results in a modification of T_{opt} toward the new growth temperature and in a modification of the general carbon assimilation capacities (Yamasaki *et al.*, 2002; Way and Yamori, 2014; Zaka *et al.*, 2016).

A the molecular scale, this acclimation could result from a RuBisCO activation state or carboxylation properties change (Gutteridge and Gatenby, 1995; Crafts-Brandner and Salvucci, 2000), or a regulation through stomatal conductance adjustments (Farquhar and Sharkey, 1982; Ball *et al.*, 1987; Del Pozo *et al.*, 2005). Yamori *et al.*, (2005) attributed this shift in T_{opt} to a change in the balance of the RuBP (substrat receiving the newly fixed C, see part III.2.a) regeneration rate and the RuBisCO carboxylation rate, while others linked it to modifications of photosystem II (Yamasaki *et al.*, 2002), or to modifications of biochemistry relation to nitrogen (Cai *et al.*, 2018). The underlying mechanisms of photosynthesis acclimation are not certain and may depend on the most limiting biochemical processes which differ between plant types and growth conditions (Sage and Kubien, 2007; Smith and Dukes, 2017).

Some attempts have been made to model photosynthesis acclimation through an integration of T_{growth} effects on Vc_{max} and J_{max} (Kattge and Knorr, 2007) or through a coupled acclimation of assimilation and respiration (Dewar *et al.*, 1999; Smith and Dukes, 2013). Some authors suggested that acclimation of photosynthesis to temperature could be modeled as changes in the parameters describing the direct effect of T_{growth} on photosynthetic capacity (activation or deactivation energy, entropy parameter) (Scafaro *et al.*, 2017; Stinziano *et al.*, 2018). To predict the effect of temperature variations on carbon assimilation and more generally on crops, we need

to have a better understanding of the effect of T_{growth} on photosynthesis-linked parameters (Perdomo *et al.*, 2016; Smith *et al.*, 2017). Models of photosynthesis acclimation make strong assumptions about the dynamic of the processes acclimation but limited experimental studies are available to support these hypotheses. Many studies have assessed thermal acclimation by measuring photosynthesis of plants grown at diverse T_{growth} but only a few analyzed the dynamic of this change (Bunce, 1985; Boese and Huner, 1990).

V. Uncoupling development and carbon acquisition

If developmental processes show a coordination of their response to temperature (Parent *et al.*, 2010; Zaka *et al.*, 2017), carbon assimilation differs. Indeed, Carbon assimilation response to temperature has a different, generally lower, optimal temperature compared with development. Lohraseb *et al.* (2017) showed that, up to an optimum, the rate of any developmental process increases more rapidly with temperature than that of CO_2 assimilation. This creates a discrepancy in carbon production and needs, leading to a decrease of biomass production and yield with high temperature (Porter and Semenov, 2005; Zhao *et al.*, 2017).

Working with different temperatures thus differently modifies the rate of development and carbon assimilation. The risk is to confound the effect of temperature on one and another. To study the effect of temperature on a specific plant processes, it is then important to consider this discrepancy. In this study, we discuss this issue and propose a way to adjust our protocol according to the targeted question.

Strategy & Objectives

The need of improving crop production to face the on-going climate change and the demographical issues is not to prove anymore. The resent progresses in including genetic parameters in crop models lead to a new developing form of varietal selection, built on ideotypes, but crop models predictions are not perfect. Some of the most needed improvements are to face multiple stresses or climate variation at short time-scales.

The European project ModCarboStress of the FACCE-JPI, regrouping seven European research groups, aimed to improve crop models by improving ecophysiological representation of target plant processes and their parametrization, based on new available field data and on experiments carried out by the project partners. This thesis is a worked resulting from this project.

The initial hypothesis of this work was that model predictions could be improved by considering explicitly the effect of the thermal history of plants on key processes such as development rate and photosynthesis.

A common protocol was built to develop a data set from growth chamber experiments that could highlight tracks to improve consideration of multiple stresses and photosynthetic acclimation into growth models. The protocol included a temperature swap, with or without water deficit, on a panel of 10 spring wheat cultivars. Planned measurements included leaf expansion and development, photosynthetic capacity measurements and A/C_i and A/T curves. Facing the multiple questions related to photosynthesis response to thermal history, we chose to focus our work on this direction by multiplying the temperature change scenarios and the monitoring of assimilation in response to this change to study the dynamic of photosynthesis acclimation.

A preliminary experiment was set to assess the chosen cultivars behavior in four combinations of growth temperature and day length. This experiment revealed interesting results about the interaction of daily temperature and cumulated light quantity on wheat leaf appearance rate. The first question of this work then emerged: is there an existing relation between plant carbon content and the rate of leaf appearance? This hypothesis was develop and answered by a series of experiments in controlled conditions, resulting in a new ecophysiological model. This work constitutes the first chapter of this thesis.

The second part of this work focusses on the impact of thermal history of the plant on photosynthesis. Numerous questions can be formulated when studying this subject, for example, regarding the effect of the amplitude, frequency or sense of temperature variations. The study of previous works carried out on the subject revealed a lack of data on temperature change scenarios. The methodology previously used is also to question since studies monitoring photosynthesis before and after the change are almost non-existant. We then chose to study the response of wheat photosynthesis to a change of temperature by the monitoring of gas exchange before and after the change of growth conditions. These gas exchange measurements considered here were the carbon assimilation at saturating light, ambient temperature and atmospheric CO_2 (later referred as A_{sat}), attesting for the assimilation capacity, and then the A_{sat} response to temperature (later referred as A/T), where leaf temperature is changed at a minute scale. This last measurement described the response of photosynthesis to temperature at a short time scale, reflecting the direct response of photosynthesis metabolism to temperature.

Choosing to work on a few general measurements restricted the number of questions that could be answered but it also allowed multiplying the number of studied scenarios. The experiments carried out in this second part thus stayed at a descriptive level. Here, the objectives were first to construct a large data set of photosynthesis response to a change of temperature, then to highlight general behavior of photosynthesis acclimation to temperature, without going deeper into the mechanisms involves in the observed responses. However, our results allowed new hypotheses regarding the implication of the metabolism and the stomatal regulation on photosynthesis acclimation to temperature. These hypotheses were tested in the third chapter with a modeling approach. I used a coupled photosynthesis-stomatal conductance model (Evers *et al.*, 2010; Yin and Struik, 2010) to uncorrelate the hidden effects of temperature on photosynthesis.

Understanding the implication of these two photosynthesis regulations on its acclimation to temperature could bring new understanding of how acclimation works. This could be a good base to include thermal history effects in crop models and thus improve their predictions. The third chapter then explored photosynthesis regulation under fluctuating temperatures.

This study is thus articulated around three chapters:

1. Experimental and modelling evidences of a carbon regulated leaf appearance rate in wheat.
2. Wheat photosynthesis responses to temperature at different time scale rely on a dual regulation from the metabolism and the stomata.
3. Improving current photosynthesis model by accounting for thermal history and stomatal regulation.

Chapter 1: Experimental and modeling evidences of carbon-limited leaf appearance rate for spring and winter wheat

Experimental and modeling evidences of carbon-limited leaf appearance rate for spring and winter wheat.

Maeva Baumont[1], Boris Parent[1], Loïc Manceau[1], Hamish Brown[2], Steven M. Driever[3], Bertrand Muller[1], Pierre Martre[1]

[1] LEPSE, Université Montpellier, INRA, Montpellier SupAgro, 34060 Montpellier, France.

[2] The New Zealand Institute for Plant & Food Research Limited, Private Bag 4704, Christchurch, New Zealand.

[3] Centre for Crop Systems Analysis, Department of Plant Sciences, Wageningen University, PO Box 430, 6700 AK Wageningen, The Netherlands.

This chapter present a study submitted to the Journal of Experimental Botany on August 22th, 2018. It has currently been accepted under minor corrections.

Combining experimental results and a modelling approach, I demonstrate here that carbon availability in wheat can account for effect of environment on leaf appearance rate. This study results in an efficient ecophysiological model that predict leaf appearance rate in contrasted experimental conditions.

I. Abstract

Accurate predictions of the timing of physiological stages and the development rate are crucial for predicting crop performance under field conditions. Plant development is controlled by the leaf appearance rate (LAR) and our understanding of how LAR responds to environmental factors is still limited. Here, we tested the hypothesis that carbon availability may account for the effects of irradiance, photoperiod, atmospheric CO_2 concentration, and ontogeny on LAR. We conducted three experiments in growth chambers to quantify and disentangle these effects for both winter and spring wheat cultivars. Variations of LAR observed between environmental scenarios were well explained by the supply/demand ratio for carbon, quantified using the photothermal quotient. We therefore developed an ecophysiological model based on the photothermal quotient that accounts for the effects of temperature, irradiance, photoperiod, and ontogeny on LAR. Comparisons of observed leaf stages and LAR with simulations from our model, from a linear thermal-time model, and from a segmented linear thermal-time model corrected for sowing date showed that our model can simulate the observed changes in LAR in the field with the lowest error. Our findings demonstrate that a hypothesis-driven approach that incorpores more physiology in specific processes of crop models can increase their predictive power under variable environments.

Key words: Carbon, Crop Model, Daylength, Leaf appearance rate, Photoperiod, Photothermal quotient, Phyllochron, SiriusQuality, Temperature, Wheat.

II. Introduction

The rate at which plants develop strongly affects canopy and root structure, radiation interception, and, through the cumulative effects of these factors, biomass production, partitioning, and yield. It is therefore essential to understand how this rate is determined and how it can be modeled in order to accurately predict crop responses to their environment in the field. A widely used metric to quantify plant development rate is the phyllochron, i.e. the time-interval between successive organs at the same stage (Wilhelm and McMaster, 1995), or its reciprocal, the leaf appearance rate (LAR). Both are often expressed in (or per) thermal-time unit (i.e. in cumulative temperature above a base temperature, classically expressed in degree-days, °Cd). The phyllochron has been used for decades in the plant science community and many growth simulation models use it to model both vegetative and reproductive development (Rickman and Klepper, 1995; Fournier *et al.*, 2005; Evers *et al.*, 2006).

The success of the phyllochron as a straightforward concept relies on the linear relationship between LAR and temperature, and therefore its constancy when expressed in thermal time. However, in many situations, irregular or non-linear relationships between leaf appearance and temperature limit its value to predict development. In several grasses, including wheat, LAR increases with photoperiod (Baker *et al.*, 1980; Cao and Moss, 1989a; Masle *et al.*, 1989; Slafer *et al.*, 1994), irradiance (Rickman *et al.*, 1985; Volk and Bugbee, 1991; Bos and Neuteboom, 1998; Birch *et al.*, 1998), and atmospheric CO_2 concentration (Boone *et al.*, 1990; McMaster *et al.*, 1999), whilst it decreases with plant density (Abichou *et al.*, 2018), red/far-red ratio and blue light (Gautier and Varlet-Grancher, 1996), and nitrogen or water deficit (Longnecker and Robson, 1994).

LAR is also often reported to change with ontogeny. Indeed, the relationship between the number of visible leaves and thermal time appears as either bilinear or non-linear, both under fluctuating field conditions (Baker *et al.*, 1986; Hay and Delécolle, 1989) and under constant controlled conditions (Cao and Moss, 1991; Slafer and Rawson, 1997; Miralles and Richards, 2000). Changes in LAR with ontogeny could be related to an increase in the time taken by successive leaves to extend above the whorl of previous leaves (Miglietta, 1991; Skinner and Nelson, 1995; Streck *et al.*, 2003). However, LAR for wheat increases and decreases with leaf rank for late and early sowing, respectively, independently of sheath length (Hay and Delécolle, 1989; Abichou *et al.*, 2018). An alternative hypothesis is that the phyllochron changes with specific developmental stages. In wheat, ontogenic changes in LAR coincide with the initiation of the flag-leaf primordium

(Abichou *et al.*, 2018) or first-ridge formation (Boone *et al.*, 1990). However, in other cases, ontogenic changes in LAR occur around the time of appearance of a given leaf, independently of final leaf number and of the state of the apex (Slafer and Rawson, 1997), which suggests that ontogenic changes in LAR are not associated with any particular growth stage. Finally, it has been suggested that, at least in some conditions, apparent ontogenic changes in LAR might be due to the use of an incorrect base temperature (Hay and Delécolle, 1989).

Several models accounting for the effects of temperature and photoperiod on LAR have been proposed and compared with each other (Miglietta, 1991; Kirby, 1995; Bindi *et al.*, 1995; McMaster and Wilhelm, 1995). However, with the exception of Miglietta (1991), these models do not consider changes in LAR with ontogeny. Surprisingly, none of these LAR models have been incorporated into crop growth models, where LAR is modeled predominantly as a linear response to temperature, without any effects of photoperiod or plant age (Muchow and Carberry, 1990; Amir and Sinclair, 1991; Lizaso *et al.*, 2011). Only a few crop growth models consider photoperiod or plant age effects on LAR. For instance, the wheat model Sirius uses three different constant LAR values depending on leaf rank (Jamieson *et al*., 1995, 1998), and the photoperiod effect is modeled using an empirical relationship between sowing date and LAR (He *et al.*, 2012). A similar approach is used in the APSIM-NWheat model, where the phyllochron is empirically corrected at a fixed date after sowing (Bassu *et al.*, 2009). A recently updated version of APSIM wheat (Brown *et al.*, 2018) models phyllochron as a function of leaf rank and a photoperiod adjustment factor.

In this study, we tested the hypothesis that carbon availability could account for the effects of temperature, irradiance, photoperiod, air CO_2 concentration, and ontogeny on LAR. This hypothesis fits well with most of the effects noted above, such as the positive effect on LAR of the photoperiod or of elevated CO_2, as well as the negative effect of elevated temperature, which decreases the amount of fixed carbon per unit thermal time. Changes in LAR with ontogeny could be related to the strong alterations of source–sink relationships that take place during development (Dingkuhn *et al.*, 2005). Moreover, carbon status, in particular in the lower range, is often reported as driving shoot development (Masle, 2000; Stitt and Zeeman, 2012). Finally, carbon status is often reported to alter LAR in woody species (e.g. Davidson *et al.*, 2016).

We conducted three experiments in growth chambers in order to quantify and disentangle the effects of temperature, light intensity, photoperiod, air CO_2 concentration, and ontogeny for both winter and spring wheat cultivars. The photothermal quotient (PTQ, mol m^{-2} °Cd^{-1}), defined as the

Table 1.1. Layout and environmental conditions for the three experiments carried out in this study. Details of the 17 cultivars are given in Supplementary Table S1. Initial leaf appearance rates (LAR_i) are given for the spring wheat cv. Paragon that was grown in all experiments and treatments. LAR_i data are mean ± 1 s.d. for *n* = 4 to 6 independent replicates.

Experiment / Cultivar[a]	Treatment Name	Set point day/night air temperature (°C)	Set point PAR (µmol m^{-2} s^{-1})	Photoperiod (h)	Set point day/night air VPD (kPa)	Air CO_2 Concentration (ppm)	Average daily PAR (mol m^{-2} d^{-1})	Average daily thermal time (°C)	PTQ (mol m^{-2} °Cd)	Average day/night leaf-air VPD (kPa)	LARi (x 10^{-3} leaf °Cd^{-1})
Experiment 1 – Photothermal effect											
Paragon, <u>*Renan*</u>, <u>Récital</u>	HT.SD.320	28/24	320	8	1.5/1.0	400	9.4	24.5	0.38	1.7 /1.1	6.61 (± 0.37)
	HT.LD.170	28/24	170	16	1.5/1.0	400	9.6	26.2	0.37	1.6 /1.0	6.63 (± 0.47)
	HT.LD.280	28/24	280	16	1.5/1.0	400	16.5	26.2	0.63	1.5/0.9	7.94 (± 0.22)
	LT.LD.280	18/14	280	16	1.5/10.	400	15.9	10.3	1.54	0.8/0.6	10.84 (± 0.52)
	HT.MD.450[b]	28/24	450	14	1.5/1.0	400	22.5	26.4	0.85	1.7 /1.1	7.75 (± 0.83)
	LT.MD.320[b]	18/14	320	14	1.5/1.0	400	15.7	10.5	1.50	1.12/0.8	9.17 (± 0.71)
	280–>170[c]	28/24	280–>170	16	1.5/1.0	400	16.5–>9.6	26.2–>26.2	0.63–> 0.37	1.5/0.9–>1.6 /1.0	7.80 (± 0.52)
	170–>280[c]	28/24	170–>280	16	1.5/1.0	400	9.6–>16.5	26.2–>26.2	0.37–>0.63	1.6 /1.0–>1.5/0.9	6.49 (± 0.43)
Experiment 2 – CO_2 x temperature effect											
Paragon, Gladius, Yecora Rojo	HT.aCO_2	28/24	600	14	1.0/1.0	400	31.6	27.2	1.16	1.1 /1.0	10.8 (± 0.56)
	HT.eCO_2	28/24	600	14	1.0/1.0	800	30.0	27.2	1.10	1.1 /1.0	11.9 (± 0.64)
	LT.aCO_2	18/14	600	14	1.0/1.0	400	32.3	10.6	3.04	1.0 /0.9	11.2 (± 1.19)
	LT.eCO_2	18/14	600	14	1.0/1.0	800	28.3	10.6	2.67	1.1/1.1	15.8 (± 0.83)
Experiment 3 – Genetic variability											
Apache-sp, *Arche*, Baviacora M92, *Cadenza*, Chinese Spring, *Courtot*, Drysdale, Feeling, Gladius, *Paragon*, Récital-sp, Seri M82, *Specifik*, Yecora Rojo, Yitpi	HT.SD	28/24	190	8	1.5/1.0	400	4.9	25.5	0.20	1.48/0.84	5.00 (± 0.39)
	HT.LD	28/24	190	16	1.5/1.0	400	11.1	26.7	0.42	1.52/0.91	6.62 (± 0.54)
	LT.SD	18/14	190	8	1.3/0.9	400	5.7	8.9	0.64	1.57/0.92	6.58 (± 0.42)
	LT.LD	18/14	190	16	1.3/0.9	400	10.6	10.1	1.05	1.43/0.87	8.40 (± 0.59)

[a] Italic, photoperiod sensitive cultivars; underlined, winter wheat cultivars.

[b] Treatments were only applied to the spring wheat cv. Paragon.

[c] Treatments were only applied to the winter wheat cv. Récital.

ratio between daily photosynthetically active radiation (PAR, mol m^{-2} d^{-1}) and mean daily thermal time, was used to quantify the (potential) supply of carbon per unit of development time. Because our experimental results showed good agreement with our hypothesis, we developed a simple ecophysiological model that accounts for temperature, light, and photoperiod effects, as well as the effects of ontogeny on LAR. This model was integrated in the wheat model *SiriusQuality* (Martre *et al.*, 2006; He *et al.*, 2012; Wang *et al.*, 2017). Comparisons of leaf stages simulated with our model or with either a simple linear model or the current LAR model of *SiriusQulity* against field data with a very large range of daily mean temperatures and photoperiods showed that our proposed model accurately simulated the observed changes in LAR with sowing date (photoperiod), temperature, and ontogeny.

III. Material and methods

1. Plant material and growth condition

Three independent experiments were carried out on wheat (*Triticum aestivum*) under controlled environment conditions using winter and spring cultivars (Table 1.1, Supplementary Table S1.1). The first experiment studied the response of leaf appearance rate (LAR) to different combinations of temperature, irradiance, and photoperiod; the second studied the response of LAR to elevated CO_2 at two temperatures; and the third studied the genetic variability of the response of LAR to the photothermal quotient (PTQ, mol m^{-1} °Cd^{-2} d^{-1}).

In all experiments, seeds were imbibed for 24 h at 4 °C on wet filter paper in Petri dishes, then placed at room temperature (22 °C) for 24 h, and transferred back to 4 °C until the radicles were 5 mm long. In Experiments 1 and 3, uniform-sized seedlings were then transplanted into 1.7-L plastic pots (one plant per pot) filled with a 30:70 (v:v) mixture of soil and organic compost. Pots were placed in controlled environment growth chambers with different conditions but with a day/night air vapor-pressure deficit of 1.5/1.0 kPa set as common to all experiments and treatments. Each growth chamber was associated with one treatment, representing a combination of temperature, light intensity, and photoperiod, as detailed in Table 1.1. In Experiment 1, treatments 280→170 and 170→280 consisted of a swap between growth conditions when plants had 3.5 visible leaves. Six independent replicates were used in each treatment and the genotypes were randomized in

the growth chambers. Plants were watered daily and no nutrients were applied as the potting substrate provided enough to the plants for the duration of the experiments.

In Experiment 2, uniform-sized seedlings were transplanted to 3-l plastic pots (one plant per pot) filled with soil. Fifteen plants of each cultivar per growth temperature were placed in a five-block design in two walk-in growth chambers. In both chambers, the air vapor-pressure deficit was maintained constant at 1.0 kPa. Plants were watered daily and additional nutrients were supplied by watering with 300–500 ml of Hoagland solution (Hoagland, 1950) three times per week, from 3 weeks after transplanting.

In all experiments, leaf (T_{leaf}) and apex (T_{apex}) temperatures (°C) were measured with thermocouples secured on the lower surface of leaf blades or inserted vertically between leaf sheaths down to the base of the leaves, respectively.

2. Determination of leaf appearance rate

Main stem leaf stages were determined every 2–3 d from the ligulation of the second leaf to the appearance of the flag-leaf ligule for the spring cultivars or to the ligulation of leaf 10 for the winter cultivars. The Haun stage (Haun, 1973) was calculated as the ratio of the length of the youngest visible (expanding) leaf blade to the length of the blade of the youngest ligulated (mature) leaf. The initial LAR (LARi) was calculated as the slope of the relationship between the Haun stage and thermal time calculated using the apex temperature for Haun stage ≤5 to avoid confounding effects due to the increase in final leaf length after leaf 5 (Martre and Dambreville, 2018). To assess the changes in LAR over plant development, a spline function was fitted to Haun stage versus thermal time and LAR was calculated by taking the first derivative of the fitted spline equations.

The daily thermal time (ΔT_t, °Cd) was calculated as:

$$\Delta T_t = \sum_{i=1}^{n} \frac{1}{144} \sum_{i=1}^{n=144} T_{opt} \times f(T) \quad (1.1)$$

With,

$$f(T) = \max(0, \frac{2(T_{apex}-T_{min})^{\alpha}(T_{opt}-T_{min})^{\alpha}-(T_{apex}-T_{min})^{2\alpha}}{(T_{opt}-T_{min})^{2\alpha}} \quad ; \quad \alpha = \frac{\ln 2}{\ln(\frac{T_{max}-T_{min}}{T_{opt}-T_{min}})} \quad (1.2)$$

where $f(T)$ (dimensionless) is the non-linear temperature response of leaf initiation and growth (Wang et al., 2017), T_{apex} is the 10-min mean apex temperature, and T_{min}, T_{opt}, and T_{max} are the minimum, optimum, and maximum temperatures, respectively. Values of 0, 27.5, and 40 °C were used for T_{min}, T_{opt}, and T_{max}, respectively (Parent and Tardieu, 2012; Wang et al., 2017). The photothermal quotient (mol m^{-2} °Cd^{-1}) was calculated as the ratio of daily PAR to T*t* (Nix, 1976).

3. Gas exchange measurement

In Experiment 1, net carbon assimilation (A_{net}, µmol CO2 m−2 s−1) was measured for cv. Paragon on leaf 3 the day after its ligulation using a CIRAS-2 portable photosynthesis system (PP sytems, Amesbury, MA, USA) equipped with a 25×7-mm bead plate. Measurements were carried out under ambient temperature (leaf temperature set equal to ambient air temperature), light intensity (provided by red-white LEDs), and air CO_2 concentration (400 ppm). The cuvette relative humidity was set to maintain the ambient air vapor-pressure deficit. Daily carbon assimilation (A_{day}, mol CO_2 m^{-2} °Cd^{-1}) was calculated by integrating A_{net} over the diurnal period.

In Experiment 2, assimilation at saturating light intensity (PAR=1600 µmol m^{-2} s^{-1}; A_{sat}) was measured instead of Anet on leaf 4 with a LI-6400XT portable photosynthesis system (LI-COR, Lincoln NE, USA) fitted with a 6400–40 Leaf Chamber Fluorometer. Light was provided by a red-blue LED light source (10% blue light), leaf temperature was maintained near growth temperature (18 or 24 ±1 °C), the CO_2 concentration of the air was maintained near growth CO_2 (400 or 800 ppm), and the air–leaf vapor-pressure deficit was maintained below 1.5 kPa.

4. Soluble carbohydrate and starch assays

In Experiment 1, whole shoots of the cultivars Paragon, Renan, and Récital were sampled in treatments HT.SD.320, HT.LD.170, HT.LD.280, and LT.LD.280 (see Table 1.1) at Haun stage 3.5 at the end of the light and of dark periods for measurements of soluble sugars (glucose, fructose, and sucrose) and starch (soluble sugars and starch hereafter collectively referred to as carbohydrates). Six plants of each cultivar were sampled per treatment. Plants were immediately frozen in liquid nitrogen and stored at –80°C prior to analysis. Plants were ground in liquid nitrogen using a mixer mill (MM 200, Retsch). Soluble sugars and starch were extracted and quantified by enzymatic assays following the procedure described by Hummel et al. (2010). Night consumption of

carbohydrate (CCnight, mg g^{-1} °Cd^{-1}) was calculated as the difference in carbohydrate concentration between the measurements at the end of the day and the end of the night divided by the thermal time cumulated during the night.

5. Modeling leaf appearance rate

Our newly developed LAR model (see Results) was implemented in the wheat phenology model described by He et al. (2012). This new phenology model was developed as an independent executable component in the BioMA software framework (http://bioma.jrc.ec.europa.eu/). The BioMA component was integrated in the wheat model SiriusQuality (Martre et al., 2006; Martre and Dambreville, 2018). The source code and the documentation of the BioMA component of the LAR model (Manceau and Martre, 2018) and the source code binaries of SiriusQuality and associated BioMA components (https://github.com/SiriusQuality/Release) are available under the MIT (X11) free and open-source software license.

Our model of LAR (hereafter referred to as model M3) was compared with two other models. The first one (referred to as model M1) is a simple model where LAR expressed in thermal time unit is constant. The second one (referred to as model M2) is the LAR model used in the wheat model Sirius (Jamieson et al., 2008) and described in detail by He et al. (2012). In model M2, leaf production follows a segmented linear model in thermal time. The first three leaves appear more rapidly than the next five, and LAR slows for the subsequent leaves independently of the total number of leaves produced. As a surrogate for the apex–air temperature correction for winter sowing (day of the year 1–90 for the Northern hemisphere), the phyllochron decreases linearly with the sowing date until reaching a minimum in mid-July for the Northern hemisphere (Jamieson et al., 2008; He et al., 2012). In the three LAR models, thermal time was calculated using Eq 1 with the apex temperature assumed to be similar to soil temperature near its surface until Haun stage 4 and thereafter similar to the canopy temperature (Jamieson et al., 1995). Soil and canopy temperatures were calculated from air temperature and the energy balances of soil surface and canopy, respectively (Jamieson et al., 1995; Martre, 2013).

6. Field experiences for model evaluation

Predictions from the three LAR models were compared against two field experiments with several sowing dates. The first one was the Hot Serial Cereal (HSC) experiment conducted in Maricopa (33°4ˈN, 111°58ˈW, 358 m elevation), AZ, USA, where the spring wheat cultivar Yecora Rojo was sown about every 6 weeks for 2 years (Wall et al., 2011; White et al., 2012). The data of the HSC experiment were obtained from Kimball et al. (2018). This experiment provides a very large range of temperature (average temperature between crop emergence and appearance of the flag-leaf = 9.6–22.3 °C) and photoperiod (10.1–13.9 h), with mean daily PTQ ranging from 1.2–3.8 mol m^{-2} °Cd^{-1}. Only one year (height sowings) was used here as the results were very similar for the two years. The two summer sowings were not used as the crops died before they reached the flag-leaf ligule stage.

The second experiment (hereafter referred to as NZ2020) was conducted over three consecutive winter growing seasons (2013–2014 to 2015–2016) in Canterbury, New Zealand, near Leeston (43°45ˈS, 172°15ˈE, 18 m elevation). Each year, the winter wheat cultivar Wakanui was sown at a density of 150 seeds m−2 at three (2013) or four dates (2014 and 2015) between late-February and late-April. Fertilizer, irrigation, insecticide, herbicide, and growth regulators were applied based on local practices. Four plots (replicates) were considered per treatment. Air temperature and relative humidity were recorded in a ventilated screen at 1.6 m height with a Campbell Scientific CS500 temperature and relative humidity probe. Solar radiation was measured in the field in 2013 and 2014 and correlated very closely with solar radiation measured at an automated weather station located at 65 km from the experimental site, so daily solar radiation data from the latter station were used for subsequent years. Following emergence, five plants were marked per plot and the number of ligules that appeared were recorded at 7–14 d intervals until flag-leaf ligule appearance. Plants produced 13–18 main-stem leaves and had a protracted tillering phase, so markers were moved up the stem to a recorded position following each measurement to keep an accurate record of the number of leaves that appeared.

7. Estimation of LAR model parameters

LAR for models M1 and M2, and LAR_{min} for model M3 were estimated using the January 2009 sowing for the HSC experiment (Supplementary Fig. S1.1) and the second sowing date in 2014 and 2015 for the NZ200 experiment (Supplementary Fig. S1.2). In model M3, LAR_{min} and PTQ_{hf} were

estimated using Eq 3 (below) and the data we obtained from our experiments (see Results). α was estimated using the January 2009 sowing of the HSC experiment and the same value was used for both field experiments (Supplementary Table S1.2). The values of all parameters for the three models are given in Supplementary Table S1.2. Parameter values were estimated by minimizing the relative root-mean-squared relative error (RMSRE; Eq. 1.3) for Haun stage >1.0 using a covariance matrix adaptation–evolutionary strategy (Hansen and Ostermeier, 2001) implemented in the *SiriusQuality* software.

$$RMSRE = \sqrt{\frac{1}{n}\sum_{i=1}^{n}\left(\frac{y_i-\hat{y}_i}{y_i}\right)^2} \quad (1.3)$$

8. Data analysis and statistics

All data analyses and graphs were performed using the R statistical software version 3.4.1 (www.r-project.org). Differences in LARi between treatments and genotypes were determined using ANOVA. Genetic differences in the intercept and slope of the linear relationship between LARi and PTQ were analyzed by reduced major-axis regression with the R package smatr3 (Warton et al., 2012). All statistical differences were judged at $P < 0.05$.

Depending on the range of PTQ, data for LARi versus PTQ were fitted using either a linear equation or a three-parameter asymptotic equation given as

$$LARi = LAR_{min} + \frac{(LAR_{max}-LAR_{min})\times PTQ}{PTQ_{hf}+PTQ} \quad (1.4)$$

where, LAR_{min} (leaf °Cd^{-1}) is the minimum LAR when PTQ equals zero, LAR_{max} (leaf °Cd^{-1}) is the maximum LAR when PTQ tends to infinite, and PTQ_{hf} (mol PAR m^{-2}°Cd^{-1}) is the PTQ at which LAR is half LAR_{max} + LAR_{min}.

To assess the quality of the LAR models in the wheat model *SiriusQuality* measured (y_i) and simulated ($\hat{y}_i$) Haun stage were compared using ordinary least square regression and the mean squared error (MSE):

$$MSE = \frac{1}{n}\sum_{i=1}^{n}(y_i - \hat{y}_i)^2 \quad (1.5)$$

To get a better understanding of the model errors we decomposed the MSE in non-unity slope (NU), squared bias (SB) and lack of correlation (LC; Gauch et al., 2003):

$$NU = (1 - b^2)(\frac{(\sum_{i=1}^{n} y_i)^2}{n}) \quad (1.6)$$

$$SB = \overline{(y_i} - \overline{\widehat{y_i)}}^2 \quad (1.7)$$

$$LC = (1 - r^2)(\frac{(\sum_{i=1}^{n} \hat{y}_i)^2}{n}) \quad (1.8)$$

Where, b is the slope of the regression of $\hat{y}_i$ on y_i and r_2 is the coefficient of correlation.

The three components of the MSE, which add up to give MSE, represent different aspects of the overall deviation of the model simulations and have simple geometrical interpretations. NU reflects the rotation, SB the translation, and LC the scattering (random error) around the 1:1 line. This analysis was used in complement of the classical least square linear regression. Finally to assess the model skill the Nash–Sutcliffe modeling efficiency (EF; Nash–Sutcliffe,1970) was calculated:

$$EF = 1 - \frac{\sum_{i=1}^{n}(y_i - \hat{y}_i)^2}{\sum_{i=1}^{n}(y_i - \bar{y})^2} = 1 - \frac{MSE}{MSE_{\bar{y}}} \quad (1.9)$$

Where, $\bar{y}$ is the average over the y_i and $MSE_{\bar{y}}$ is the MSE for the model that uses $\bar{y}$ as estimator in all cases. EF is a skill measure that compares model MSE with the MSE of using the average of measured values as an estimator. Therefore, EF is useful for making statements about the skill of a model relative to this simple reference estimator. For a model that simulates perfectly, EF = 1, and for a model that has the same squared error of simulation as the mean of the measurements, EF = 0. EF is negative for a model that has a larger squared error than the mean of the measurements.

To avoid confounding effects of leaf development and growth, and auto-correlation in the data, linear regression and MSE, skill (EF) analyses were performed using the observed Haun stage value closest to five in all treatments. The root mean squared relative error (RMSRE, see Eq. 1.3) was calculated to compare the models at different leaf stages. RMSRE was calculated using all observed Haun stage values > 1.0.

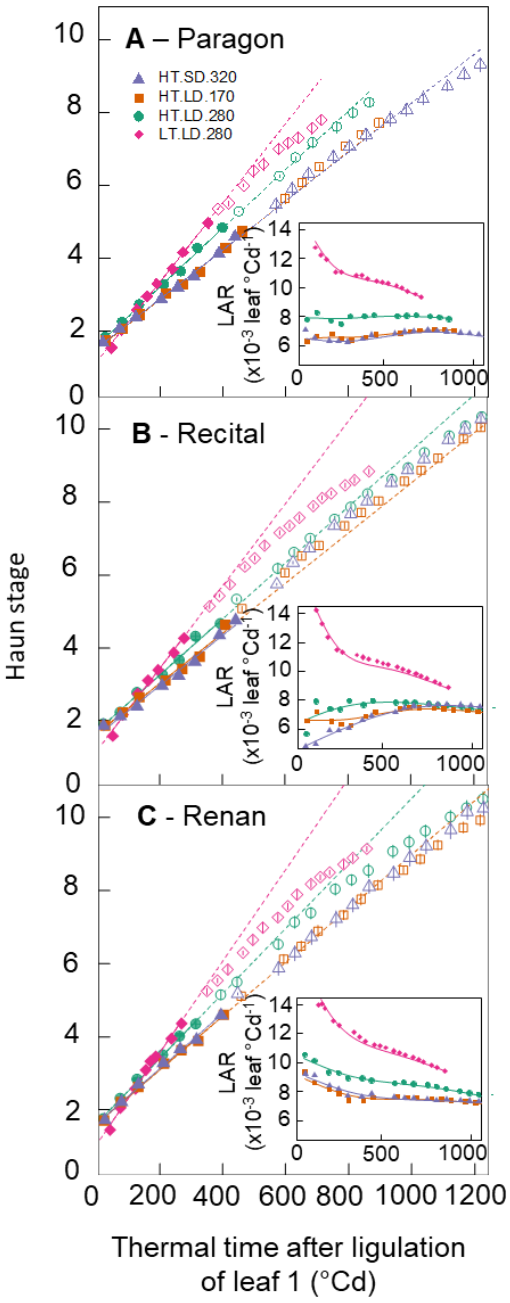

Figure 1.1. Relationship between Haun stage and thermal time after ligulation of leaf 1 for three wheat (*Triticum aestivum* L.) cultivars grown in controlled conditions with different temperatures, irradiances, and photoperiods. The photoperiod insensitive spring wheat cultivar Paragon (A), the photoperiod insensitive winter wheat cultivar Récital (B) and the photoperiod sensitive winter cultivar Renan (B) where grown in growth chambers with 28/24°C (HT.SD.320, HT. LD.170, HT.LD.280) or 18/14°C (LT.LD.280) day/night air temperature, 8 h (HT.SD.320) or 16 h (HT. LD.170, HT.LD.280, LT.LD.280) photoperiod, and 170 (HT. LD.170), 280 (HT.LD.280, LT.LD.280) or 320 (HT.SD.320) µmol m^{-2} s^{-1} PAR. Treatments are detailed in Table 1.1. Lines are linear regressions calculated for Haun stage 1.5 to 5 (closed symbols). Insets show the leaf appearance rate versus thermal time after ligulation of leaf 1. Lines are non-parametric spline curves fitted to the data. The thermal time was calculated using apex temperature and Eq. (1.1). Data are mean ± 1 s.d. for *n* = 6 independent replicates.

IV. Results

1. Leaf appearance rate depends on temperature, irradiance, photoperiod and leaf stage

The dynamics of leaf appearance was first analyzed for three contrasting cultivars (Fig. 1.1), Paragon (a photoperiod-insensitive spring wheat), Récital (a photoperiod-insensitive winter wheat), and Renan (a photoperiod-sensitive winter wheat), grown in four treatments with stable environmental conditions differing in temperature, photoperiod, and light intensity (Experiment 1; Table 1) in such a way that we could compare treatments differing in temperature only (LT.LD.280 versus HT.LD.280), irradiance only (HT.LD.280 versus HT.LD.170), or both irradiance and photoperiod but with a similar daily irradiance (HT.SD.170 versus HT.LD.170).

The initial leaf appearance rate (LARi, calculated for leaves 1–5) differed significantly between treatments for the three cultivars (Fig. 1.1, Supplementary Table S3), although they had a similar response of LARi to the treatments (i.e. there were no significant treatment × cultivar interactions). The highest values of LARi were observed for the treatments with longer photoperiods and higher irradiance (LT.LD.280, HT.LD.280). For plants grown at high temperature, decreasing either the photoperiod (HT.SD.320) or the irradiance (HT.LD.280) decreased LARi (Fig. 1.1). Remarkably, changing both photoperiod and light intensity for a similar daily radiation and PTQ resulted in similar values of LAR (HT.SD.320 versus HT.LD.170).

In treatment LT.LD.280 (which showed the highest LARi), LAR decreased with plant age for the three cultivars (insets in Fig. 1.1), including the winter cultivars (Fig. 1.1B, C), which stayed in the vegetative stage during the whole experiment. Therefore, the decrease of LAR with plant age in this treatment was related neither to floral transition nor to the development and formation of the spike. In the other treatments, LAR was either stable (for Paragon), increased (for Récital), or decreased (for Renan) with plant age. Overall, the LAR of all cultivar/treatment combinations converged towards the same value as the plants aged.

2. Changes in leaf appearance rate with environmental conditions is a dynamic process

We analyzed the dynamic changes in LAR with changes in irradiance. Plants from the two high-temperature plus long-photoperiod treatments were swapped between irradiance conditions at

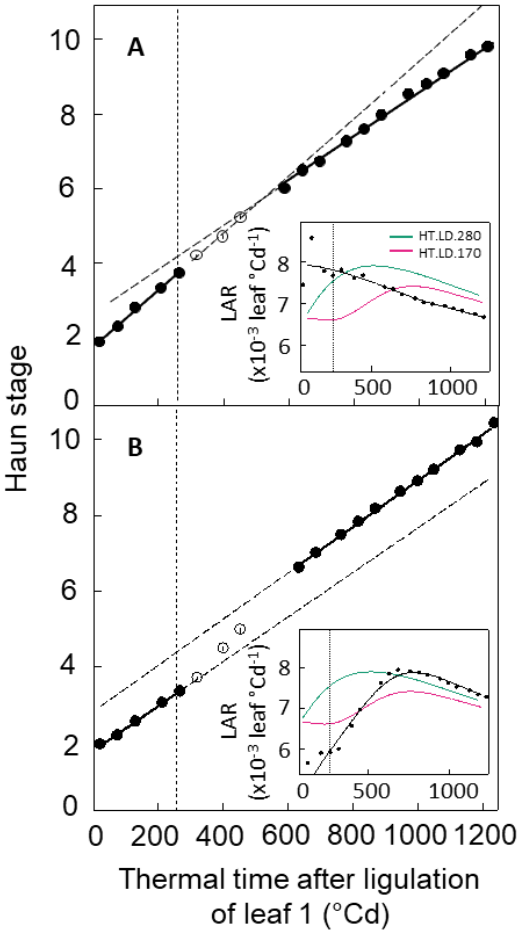

Figure 1.2. Relationship between Haun stage and thermal time after ligulation of leaf 1 for the photoperiod insensitive winter wheat cultivar Récital grown in controlled conditions with different irradiance. The plants were grown from planting to 270 °Cd after ligulation of leaf 1 at 28/24°C day/night air temperature and 16 h photoperiod and either 280 (A) or 170 (B) µmol m^{-2} s^{-1} PAR. At 270 °Cd after ligulation of leaf 1, plants were transferred from low to high PAR (A, 170→280) or from high to low PAR (B, 280→170). Solid symbols are data used to fit linear regression before and after the change in irradiance. Insets show leaf appearance rate versus thermal time after ligulation of leaf 1. Lines are non-parametric spline curves fitted to the data. Curves for treatments HT.LD.280 (green lines) and HT.LD.170 (pink lines) are from Figure 1 and are shown for comparison. The thermal time was calculated using apex temperature and Eq. (1). Data are mean ± 1 s.d. for *n* = 6 independent replicates.

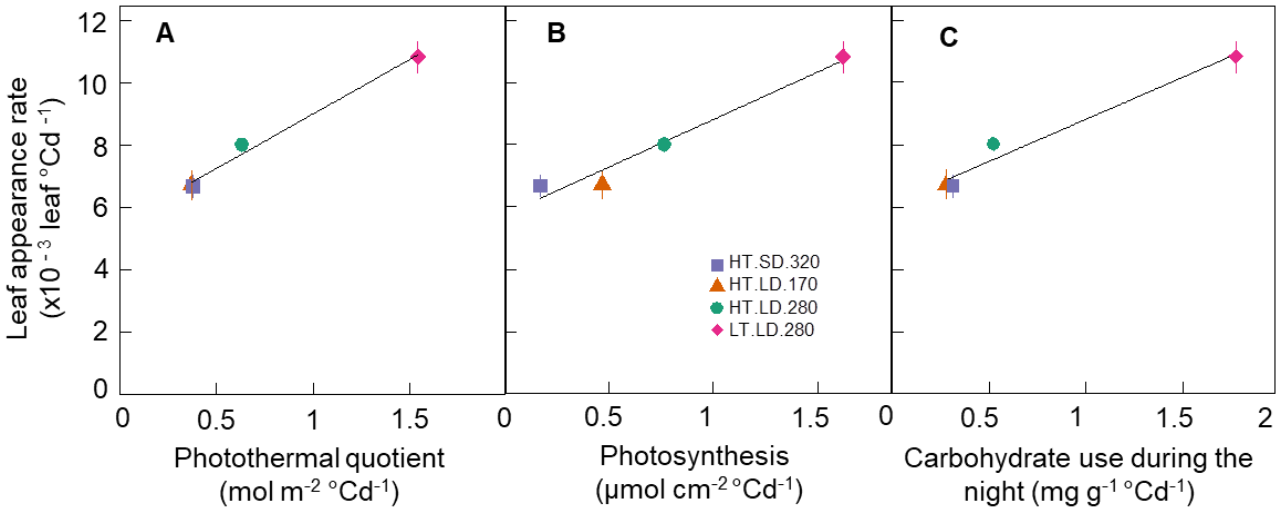

Figure 1.3. Relationship between initial leaf appearance rate (calculated for Haun stage ≤ 5) and photothermal quotient (A), net photosynthesis (B), and carbohydrate use during the night (C) for the photoperiod insensitive spring wheat cv. Paragon grown in controlled conditions with different combinations of temperature, irradiance, and photoperiod. Treatments are as in Figure 1. Data are mean ± 1 s.d. for *n* = 6 independent replicates. The thermal time was calculated using apex temperature and Eq. (1.1).

270 °Cd after ligulation of leaf 1 (treatments 280→170 and 280→170). The environmental conditions before and after the irradiance swap were similar to treatments HT.LD.170 and HT.LD.280 in Fig. 1.1, in order to compare LARs at similar thermal time and to avoid confounding effects of plant age. Moreover, the winter wheat cultivar Récital was used to avoid confounding effects due to floral transition or spike development because it stayed in the vegetative stage during the whole experiment. The LAR of plants transferred from 280 µmol m^{-2} s^{-1} to 170 µmol m^{-2} s^{-1} PAR started to decrease about 250 °Cd (i.e. ~1.3 phyllochrons) after transfer to low irradiance, and the mean LAR after the transfer was 23% lower than before (Fig. 1.2A). The opposite behavior was observed when plants were transferred from 170 µmol m^{-2} s^{-1} to 280 µmol m^{-2} s^{-1} PAR, but LAR responded more rapidly to the change in irradiance (Fig. 1.2B). LAR increased within less than 140 °Cd (i.e. ~0.8 phyllochrons) after the transfer and the mean LAR was 12% higher than before.

3. Leaf appearance rate is correlated with photoperiod quotient, net daily photosynthesis and carbohydrate turnover during the night

LAR was modified by temperature (even when expressed per unit thermal time), photoperiod, and instantaneous irradiance. To test if whether these effects could be accounted for by the average mean radiation per thermal- time unit, we calculated the photothermal quotient (PTQ) for all treatments in the three experiments, under ambient air CO_2 concentration. The variation of LARi for cv. Paragon in Experiment 1 was well explained by a unique linear relationship linking LARi to PTQ independently of the cause of variation of PTQ (r^2=0.965, P=0.018; Fig. 1.3A). A similar correlation was found between LARi and either daily net photosynthesis (r=0.982, P=0.0179; Fig. 3B) or carbohydrate consumption during the night (r=0.985, P=0.0147; Fig. 1.3C, Supplementary Fig. S1.1, S1.3), supporting the hypothesis that LAR is at least partly limited by carbon availability in the plant.

The highest PTQ value tested in our experiments was 1.5 mol m^{-2} °Cd^{-1}, while the range of PTQ sensed by plants in field conditions could reached up to 4 mol m^{-2} °Cd^{-1} in our database of wheat field trials. The relationship between LAR and PTQ was therefore further tested on a larger range of PTQ values using data from the literature where the response of LAR to either temperature (Cao and Moss, 1989b, 1989c; Bos and Neuteboom, 1998), photoperiod (Cao and Moss, 1989a, 1989c), or irradiance (Rickman et al., 1985; Bos and Neuteboom, 1998) was studied for plants

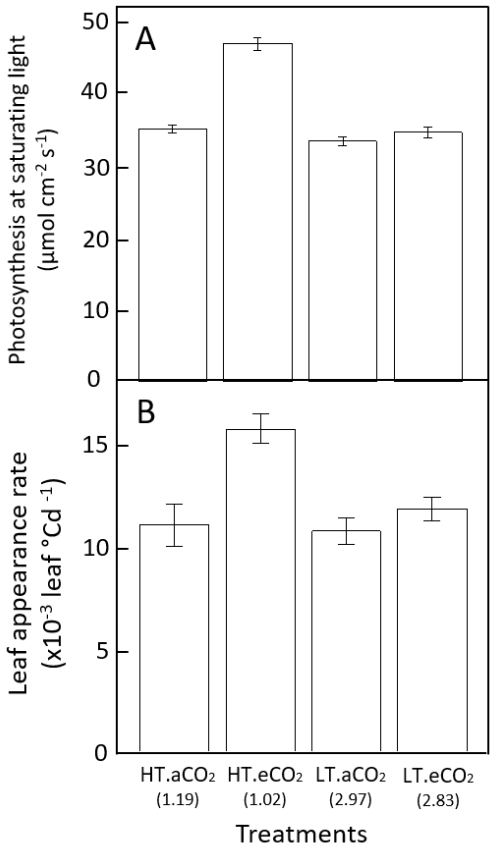

Figure 1.5. Photosynthesis at saturating light (A) and initial leaf appearance rate (calculated for Haun stage ≤ 5) (B) for Paragon grown in controlled conditions at 18/14°C (LT.aCO_2 and LT.eCO_2) or 28/24°C (HT.aCO_2 and HT.eCO_2) day/night air temperature and ambient (LT.aCO_2 and HT.aCO_2) or elevated (HT.eCO_2 and HT.eCO_2) air CO_2 concentration. Numbers in parenthesis below the treatment names are photothermal quotient (mol m^{-2} °Cd^{-1}). Details of the cultivars are given in Supplementary Table S1. Data are mean ± 1 s.d. for *n* = 5 (A) or *n* = 3 (B) independent replicates.

grown in growth chambers or green houses (Supplementary Table S1.5, S1.4). These data provide a very large range of variation of PTQ (up to 15 mol m^{-2} °Cd^{-1}) and when our data and those from the literature were considered together the relationship between LAR and PTQ was well described well by Eq. (1.4) (Fig. 1.4), Supplementary Table S1.5).

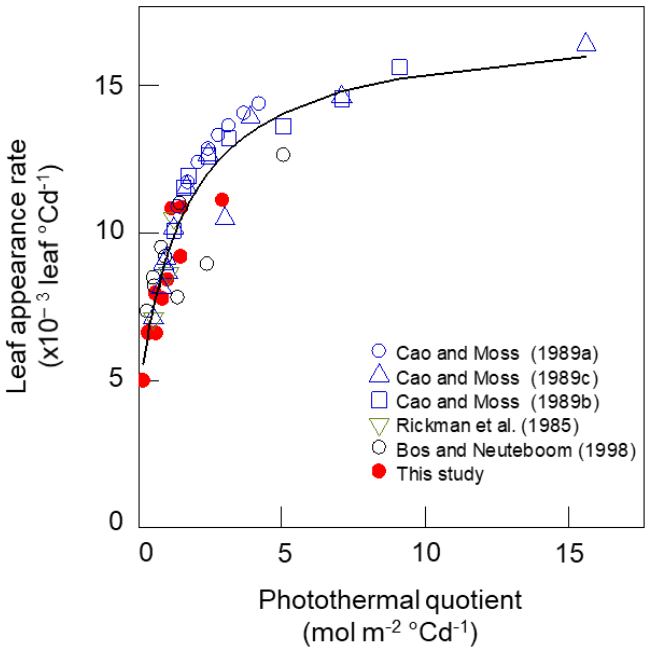

Figure 1.7. Relationship between leaf appearance rate and photothermal quotient for several wheat cultivars grown in controlled conditions with different combinations of temperature, irradiance, and photoperiod. Closed symbols are all treatments from experiment 1 to 3 at ambient air CO2 concentration (Table 1.1). Open symbols are data from the literature (Supplementary Table S2), solid line is Eq. 1.4 fitted to all data points (LAR = 0.004996 [± 0.000731] + ((0.002364 [± 0.0007] – 0.04996 [± 0.000731]) × PTQ) / (1.9807 [± 0.5803] + PTQ).

4. Elevated CO2 increases leaf appearance rate at high temperature

In order to strengthen our hypothesis of carbon limitation for LAR, we tested the effect of elevated air CO_2 concentration on LARi (Experiment 2, Table 1.1). Plants of cv. Paragon were grown under two temperature regimes (18/14 °C and 28/24 °C, day/night) and two atmospheric CO_2 concentrations (400 ppm and 800 ppm). At 18/14 °C, photosynthesis under saturating light was not significantly different (P=0.064) between the two CO_2 treatments (Fig. 5A), while at 28/24 °C it was 33.7% higher under elevated CO_2 compared with ambient CO_2 ($P=7.3\times10^{-4}$). Similarly, LARi was not significantly different between the CO_2 treatments at 18/14 °C (P=0.019) but was 29.6% lower at 400 ppm than 800 ppm CO_2 at 28/24 °C ($P=1.54\times10^{-3}$; Fig. 5B).

5. Genetic variability of the response of leaf appearance rate to photothermal quotient

We assessed the genetic variability of the response of LARi to PTQ for 15 spring wheat cultivars grown under two temperature regimes (18/14 °C and 28/24 °C, day/night) and two photoperiod treatments (8 h or 16 h) in factorial combination (Experiment 3, Table 1). The effect of PTQ on LARi was highly significant, while the effect of cultivar and the interaction between PTQ and cultivar

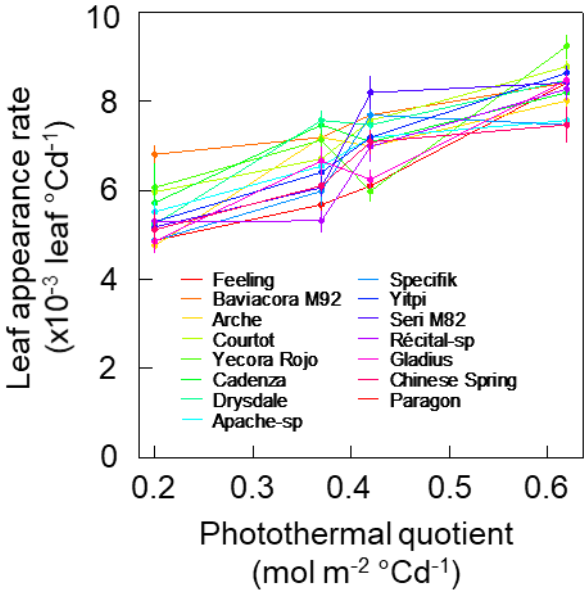

Figure 1.6. Relationship between initial leaf appearance rate (calculated for Haun stage ≤ 5) and photothermal quotient for 15 spring wheat cultivars grown in controlled conditions with different combinations of temperature and photoperiod. Details of the cultivars are given in Supplementary Table S1. Data are mean ± 1 s.d. for *n* = 4 independent replicates.

were not significant (Fig. 1.6; Supplementary Table S1.6). The response of LARi to PTQ was analyzed by linear regression (Supplementary Table S1.7). The slope of the LARi–PTQ relationship was not significantly different among cultivars (P=0.77) and was on average 7.83 leaves m^2 mol^{-1} PAR (95% confidence interval [CI] 6.90–8.90). However, the intercept of the relationship was significantly different among cultivars (P = 0.02) and ranged from 2.74×10^{-3} leaves $°Cd^{-1}$ (CI 0.02–5.47) for cv. Feeling to 4.69×10^{-3} leaves $°Cd^{-1}$ (CI 1.98–7.40) for cv. Cadenza.

6. A model of carbon limitation of leaf appearance rate

We showed that differences in LARi due to temperature, light intensity, and photoperiod can be explained by a unique curvilinear relationship between LAR and PTQ (Fig. 1.4). PTQ reflects the balance between the incident irradiance available for growth and the potential growth of sinks driven by temperature. The demand for carbon for respiration scales with plant size and can be approximated by the green area index [GAI, m^{-2} (leaf) m^{-2} (ground)]. The demand for carbohydrates for leaf growth increases between leaf 3 and terminal spikelet because of the regular formation and development of axillary tillers and associated roots (Kirby et al., 1985; Abichou et al., 2018). After terminal spikelet, growing leaves also compete for carbohydrates with fast-growing internodes and spikes. These changes in the source–sink balance during the plant growth cycle are at least partially compensated for by the increase in leaf area index. The decrease in LAR with ontogeny observed in our experiments (Fig. 1.1), as well as in many other studies (see Introduction), may reflect the decrease of the source–sink ratio with ontogeny.

We propose a simple model of LAR that summarizes the results above, in which (1) LAR depends on the supply-to-demand ratio for soluble carbohydrate, estimated by the ratio of intercepted light to thermal time; (2) the demand for soluble carbohydrate is proportional to plant size and this proportionality can be approximated by the green area index; (3) soluble carbohydrates in the plant provide a buffering capacity to fluctuating environments in the field; and (4) leaves are able to maintain a minimum rate of development. The model is given as:

$$LAR(d) = \frac{LAR_{min} + \left(\frac{(LAR_{max} - LAR_{min}) \times \overline{I_{int}}(d) / \overline{T_t}(d)}{PTQ_{hf}}\right)}{S_{C/GAI} \times \overline{GAI_{eff}}(d)} \quad (1.10)$$

where, $\overline{I_{int}}(d)$ [MJ PAR m^{-2} (ground)] is the cumulative PAR intercepted by the canopy during the period *d*, $\overline{T_t}(d)$ (°Cd) is the thermal time accumulated during the period *d*, $\overline{GAI_{eff}}(d)$ [m^{-2} (leaf)

m^{-2} (ground)] is the mean green area fraction over the period *d*, *d* (°Cd) is the thermal time over which intercepted irradiance and thermal time are integrated, and $S_{C/GAI}$ [m^2 (ground) m^{-2} (leaf)] is an empirical parameter that scales carbon demand to GAI. In Eqn 1.10, LAR tends to infinite when GAI tends to 0. Therefore, a minimum value of $\overline{GAI_{eff}}$ was considered as the potential GAI when Haun stage = 3.5, just after the first tiller appears on the main stem. $\overline{GAI_{eff}}$ is given as:

$$\overline{GAI}_{eff}(d) = \begin{cases} LN_{eff} \times A_{L_{juv}}^{pot} \times PD, & LN < LN_{eff} \\ \overline{GAI}_{max}(d), & LN \geq LN_{eff} \end{cases} \quad (1.11)$$

where, $A_{L_{juv}}^{pot}$ (cm^2) is the potential surface area of juvenile leaves, as defined in the *SiriusQuality* leaf growth model (Martre and Dambreville, 2018), PD (plant m^{-2}) is the plant density, LN (leaf main $stem^{-1}$), is the number of main stem emerged leaves, and LNeff (leaf), the number of main stem leaves above which the demand for respiration increases relative to sink formation and $\overline{GAI}_{max}(d)$ is the maximum green area index fraction averaged over the period *d* since emergence. The maximum value of $\overline{GAI}(d)$ is taken so that $\overline{GAI}_{eff}$ does not decrease if the rate of senescence of the oldest leaves is higher than the expansion of the growing leaves.

In Eq. 1.10, environmental variables are averaged over several days to account for the buffering effect of stored soluble carbohydrates. The parameter *d* was set equal to 70 °Cd (Rickman et al., 1985; Lattanzi et al., 2005). The fraction of light intercepted by the crop during the period d is calculated from its exponential relationship with GAI (Monsi and Saeki, 2005).

7. Prediction of leaf stage and leaf appearance rate for different sowing date in the field

The three LAR models (M1, M2, and M3) were evaluated against two field experiments conducted in contrasting environments (HSC and NZ2020). In both experiments, LARi varied significantly with sowing dates. In the HSC experiment, LARi was constant and maximum for winter and spring sowings (between January and March, averaging 11.86×10^{-3} leaves $°Cd^{-1}$) and decreased by 27% for the late-autumn sowing. In the NZ2020 experiment, crops were sown between late-summer and mid-autumn and LARi was constant and maximum for the first three sowings (averaging 10.45×10^{-3} leaves $°Cd^{-1}$) but decreased on average by 25% for the latest sowing. The final number of leaves on the main stem was very different for the two experiments: 7.0–9.3 leaves $main\ stem^{-1}$ for HSC and 17.7–12.8 leaves main stem−1 for NZ2020.

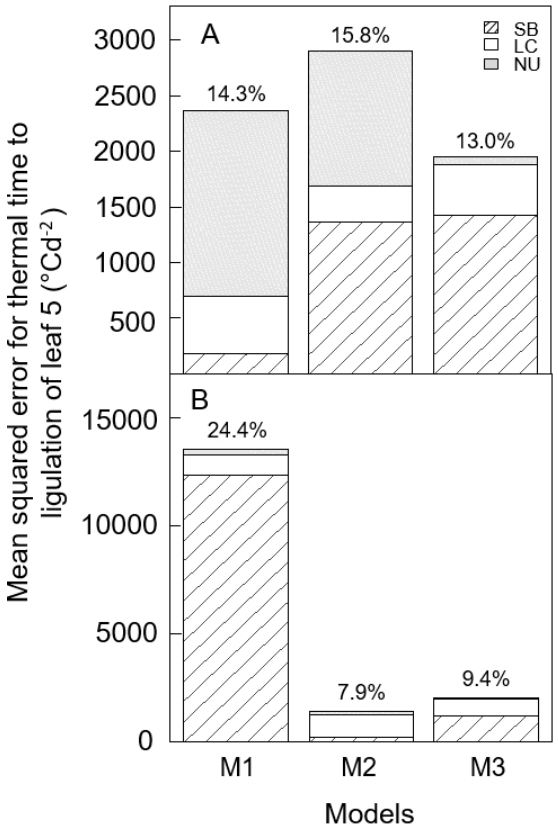

Figure 1.7. Mean squared error (MSE) for thermal time to ligulation of leaf 5 (Haun stage 5) estimated using three alternative models of leaf appearance rate for (A) the photoperiod insensitive spring wheat cultivar Yecora Rojo sown every about six weeks between March 2007 and January 2009 in the field at Maricopa, USA, and (B) for the winter wheat cultivar Wakanui sown in the field in late February, March, and April for three consecutive years at Leeston, New Zeland. MSE was decomposed in squared bias (SB), lack of correlation (LC), and non-unity slope (NU). MSE was calculated for the observed HS closest to 5 to avoid confounding effects between leaf development and growth and autocorrelation in the data. Model M1, constant LAR; model M2, Sirius LAR model; model M3, LAR model proposed in this study.

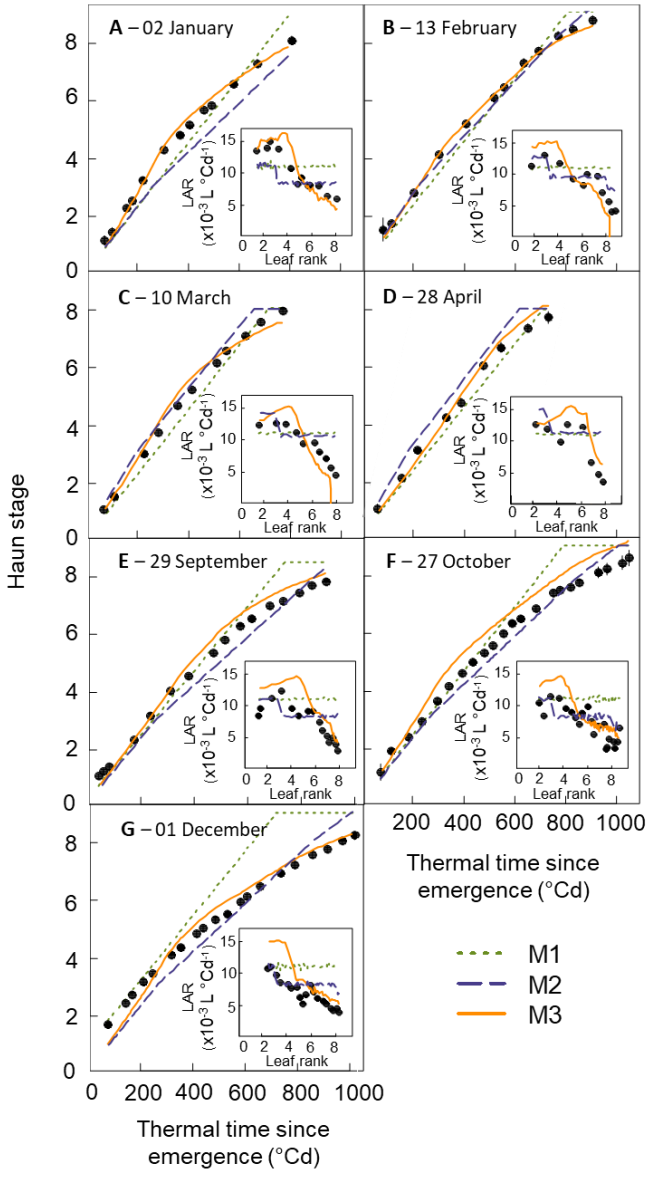

Figure 1.8. Relationship between observed (close circle) and simulated (lines) Haun stage and thermal time after emergence for the spring wheat cultivar Yecora Rojo grown in field at Maricopa, Arizona US. Crops were sown about every six weeks between early January and early December 2008 as indicated in the figure. Lines are simulations obtained with the wheat model *SiriusQuality* and using either a constant phyllochron (Model M1, dotted green lines), a segmented linear model in thermal time corrected for the sowing date (Model M2, dashed blue lines) or Eq. (4) (Model M3, solid orange lines). Insets show observed (closed circles) and simulated (lines) leaf appearance rate versus leaf rank. The thermal time was calculated using apex temperature and Eq. (1) for the observed values and canopy temperature for the simulated data (see Material and Method). Data are mean ± 1 s.d. for n = 3 independent replicates.

In the HSC experiment, the error (MSE) of M3 for thermal time to Haun stage 5 was only 82% and 67% of that of M1 and M2, respectively (Fig. 1.7A). Lack of correlation (LC) contributed to 73% of the total error of M3, while the error of M1 was dominated by non-unity slope (NU) and that of M2 by squared bias (SB) and NU. In the NZ2020 experiment, the error for thermal time to Haun stage 5 was 85% lower for M3 than for M1 but was 41% higher for M3 than for M2 (Fig. 1.7). Squared bias and LC contributed nearly two-thirds and one-third of the total error of M3, respectively. Therefore, M3 had a much lower error than M1 for both data sets and outperformed M2 in Arizona, but in New Zealand both models had comparable and small errors (RRMSE<9.5%).

In the HSC experiment, M3, which is based on biological hypotheses, provided a good simulation of the dynamics of leaf appearance and the observed changes of LAR with sowing date and plant ontogeny (Fig. 1.8). Compared with M1 and M2, the relative error (RMSRE) for Haun stage was reduced by 17% and 22%, respectively (Supplementary Table S1.8). M3 also simulated the dynamics of leaf appearance in the NZ2020 experiment reasonably well (Fig. 1.9) but the relative error for Haun stage was 10% higher for M3 than for M2 (Supplementary Table S1.8). Combining the two experiments, the overall RMSRE for Haun stage was 46% and 13% lower for M3 than for M1 and M2, respectively.

V. Discussion

In this study, we investigated the effects of temperature, photoperiod, irradiance, CO_2 concentration, and cultivars on wheat LAR. We showed that initial LAR (LARi) changed significantly with all the factors studied excluding genotype (Fig. 1.1 and 1.5). We also showed that the response of LARi to environmental factors could be accounted for by the photothermal quotient (PTQ) (Fig. 1.4). LARi was also correlated with net photosynthesis and carbohydrate use at night3. Our results thus supported our hypothesis that LAR in wheat is carbon-limited. Based on our results, we developed and evaluated under field conditions a new model of LAR (Eq. 1.10) that accounts for both environmental and ontogenic changes in LAR (Fig. 1.8 and 1.9). The simulation results supported the modelling hypothesis that changes of LAR with ontogeny are due to changes in the carbon supply–demand ratio.

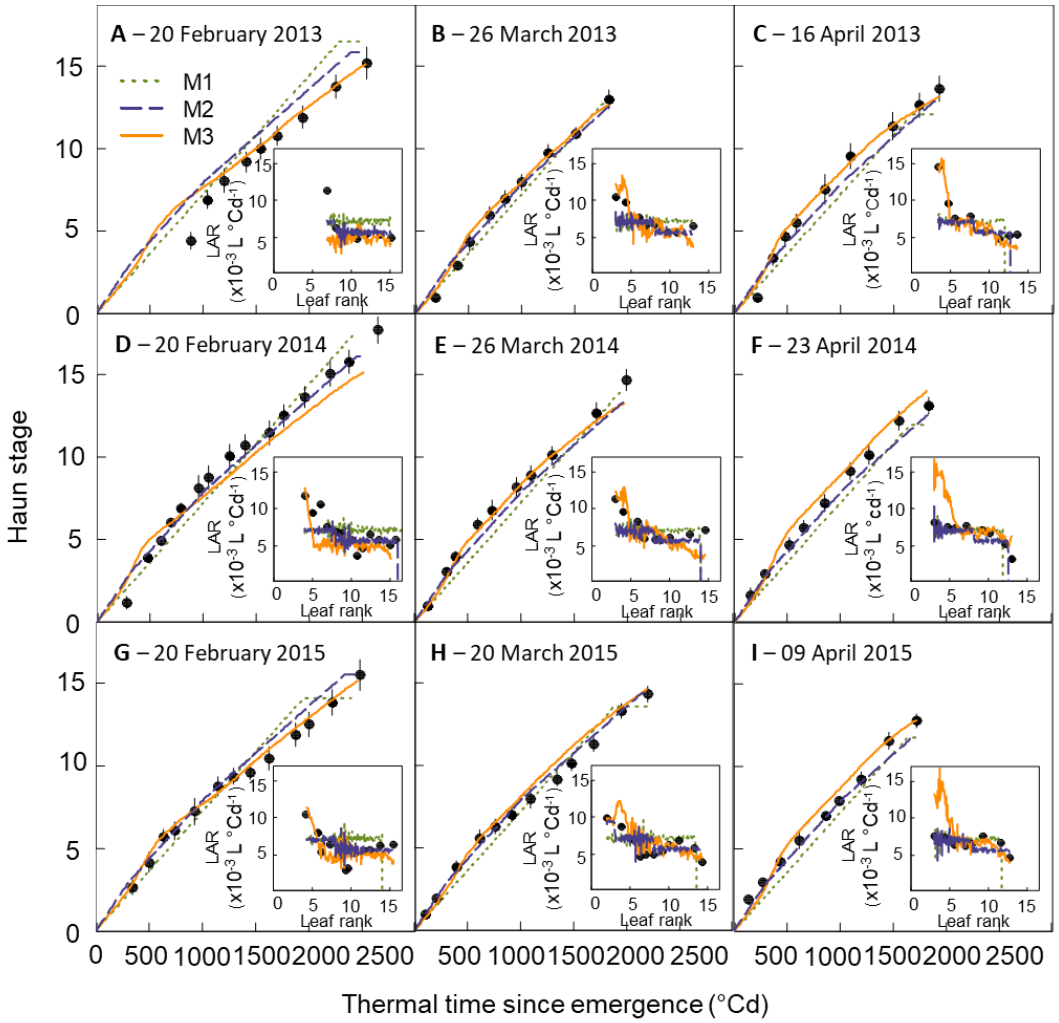

Figure 1.9. Relationship between observed (close circle) and simulated (lines) Haun stage and thermal time after emergence for the spring wheat cultivar Wakanui grown in field at Leeston, New Zeland. Crops were sown from 2013 to 2015 in the end of February, March and April (11 sowings). Lines are simulations obtained with the wheat model *SiriusQuality* and using either a constant phyllochron (Model M1, dotted green lines), a segmented linear model in thermal time corrected for the sowing date (Model M2, dashed blue lines) or Eq. (4) (Model M3, solid orange lines). Insets show observed (closed circles) and simulated (lines) leaf appearance rate versus leaf rank. The thermal time was calculated using canopy temperature and Eq. (1) for the observed values and canopy temperature for the simulated data (see Material and Method). Data are mean ± 1 s.d. for *n* = 15 independent replicates.

1. Leaf appearance rate in wheat is carbon-driven

Relationships between temperature, irradiance, photoperiod, and LAR have been observed in a range of plant species, including cereals such as maize (Birch et al., 1998), rice (Yin and Kropff, 1996), wheat and barley (Cao and Moss, 1989c; Volk and Bugbee, 1991; Bos and Neuteboom, 1998), and dicots such as quinoa (Bertero, 2001), lucerne (alfalfa, Brown et al., 2005; Teixeira et al., 2011), and lettuce (Kitaya et al., 1998). However, no physiological explanation for the observed variations of LAR in relation to environmental factors has yet been proposed. Here, we found a unique relationship between LAR and PTQ for a large range of environmental conditions (Fig. 4). The fact that the photoperiod effect could be accounted for by a unique source–sink relationship for both photoperiod-insensitive and -sensitive spring and winter wheat cultivars was not expected. The treatments in our experiments allowed us to disentangle the effect of photoperiod per se and irradiance, and the results strongly suggested that the effect of photoperiod on LAR was mainly due to the increase of daily irradiance with longer photoperiods. An additional effect of photoperiod per se is not incompatible with our results, but this effect would be smaller compared to the effect of irradiance and would bring its own physiological determinisms and genetic variability. The correlation between LAR and net daily photosynthesis and carbon use during the night (Fig. 1.3), as well as the increase of LAR at elevated CO_2 (Fig. 1.5), also supported the hypothesis that LAR in wheat is carbon-limited. In good agreement with our results, (McMaster et al. (1999) found that wheat plants grown under elevated CO_2 (725 ppm) had values of LAR that were 10–15% higher than under ambient CO_2 (360 ppm), and leaf photosynthesis and carbohydrate concentration were positively correlated with LAR.

Leaf appearance rate results from three processes: (1) cell division in the apical meristem of the expanding leaf primordium; (2) cell division of the intercalary meristem of the expanding leaf primordium; and (3) expansion of cells derived from the meristem in the leaf lamina and sheath. Christ and Körner (1995) showed that step-changes in CO_2 concentration, and thus in carbon supply, have no effect on leaf elongation rate. This was most likely due to the fact that, in contrast to our current study, the leaves measured were initiated several plastochrons before the air CO_2 concentration was increased. The effect of CO_2 on wheat leaf growth acts mainly through an increased number of dividing cells at the base of expanding leaves, which is determined in the apical meristem before leaf appearance (Masle, 2000). The lack of correlation between soluble carbohydrate concentration in the elongation zone and leaf expansion rate after their emergence

suggests that after leaves have emerged above the whorl of subtending leaves, their elongation rate is not limited by carbon availability (Kemp and Blacklow, 1980). This also agrees with studies showing that the control of leaf growth switches from a metabolic limitation to hydraulic and mechanical control during the course of leaf ontogeny (Pantin et al., 2011).

2. Changes of LAR with plant age reflect changes in sink-source relationship

LAR decreases with plant age both in controlled conditions and in the field for wheat (Calderini et al., 1996; Slafer and Rawson, 1997; Streck et al., 2003; Ochagavía et al., 2017) and also for other grass species such as sugarcane (Inman-Bamber, 1994) and tall fescue (Skinner and Nelson, 1995). But to date it has only been included in crop growth models through an empirical effect of leaf rank on LAR (Jamieson et al., 1995) or through an effect of the distance from the meristem to the whorl (Streck et al., 2003). In our results, the decrease of LAR with plant age depended on environmental conditions (Fig. 1.1 and 1.2), which was incompatible with a unique relationship linking LAR and Haun Stage (Streck et al., 2003).

As LAR depends on plant carbon availability, it is tempting to hypothesize that the decrease of LAR with plant age is associated with changes in plant source–sink balance and with a lower availability of carbon. As the wheat plant develops, the formation and development of new tillers increases the demand for carbon, and after the terminal spikelet stage expanding leaves also compete for carbon with the growing internodes and spikes. In tall fescue, LAR decreases rapidly after the appearance of leaf 7, and this can be suppressed if new tillers are trimmed (Skinner and Nelson, 1995). In that study, the decrease in LAR with leaf number was due both to an increase of the duration of the leaf elongation through the whorl of subtending leaves and to a decrease of the interval between the initiation of successive leaves, and both may be due to the slowing down of leaf elongation rate (Skinner and Nelson, 1995). Slafer and Rawson (1997) reported that LAR after leaf 6 is more sensitive to photoperiod than that of leaves appearing before. This is in good agreement with a carbon-limitation of LAR, and the results of (Skinner and Nelson, 1995) in tall fescue.

3. Considering the carbon-limitation of leaf appearance rate improves the prediction of leaf stages in the field

Many crop growth models calculate leaf appearance assuming a constant LAR and do not consider the effects of photoperiod, light intensity, or plant age. Where there have been attempts to model the response of LAR to photoperiod, these have been empirical models (Jamieson et al., 2008; Abichou et al., 2018; Brown et al., 2018) and they are probably limited in the range of environmental conditions in which they can be used. Moreover, these models have a large number of parameters. Here, we present an ecophysiological model (Eq. 1.10) that can easily be integrated into crop growth models and has 40% fewer parameters than the Sirius LAR model. Our model was able to simulate the changes in LAR with both sowing date and plant age in two contrasting environments.

Several crop growth models do not use leaf stages and leaf number to simulate heading or anthesis date, but instead use a more empirical approach based on the thermal-time requirement between phenological phases and modifications of thermal time by vernalization and photoperiod (e.g. Ritchie, 1991; Stöckle et al., 2003; Brisson et al., 2009). One of the reasons such phenology models are used in crop growth models is that the error in leaf-stage prediction with the leaf-number approach may lead to large errors in the prediction of anthesis date. Although these two types of approaches may provide very similar results (Jamieson et al., 2007), models based on leaf number allow for separation of the effect of temperature on development and vernalization (Allard et al., 2012) and better represent biological processes, and thus can more directly be related to physiological processes or even genes, for instance those controlling flowering time (Brown et al., 2013; Sanna et al., 2014). A phenology model based on leaf number also allows the linking of phenology with leaf growth (Lawless et al., 2005; Martre and Dambreville, 2018). The improvement of leaf-stage modeling provided by our model is thus an important step to improve models based on leaf number and to introduce more physiological insights into crop growth models.

VI. Supplementary data:

Content:

Table S1. Details of the cultivars used in this study.

Table S2. Parameters of the LAR models compared in this study.

Table S3. Analysis of variance for the response of LARi to PTQ and cultivar.

Table S4. Environmental conditions and LARi from the literature.

Table S5. Analysis of variance for the response of initial leaf appearance rate to temperature, CO2 and cultivar.

Table S6. Analysis of variance for the response of LARi to PTQ and cultivar shown in Figure 5

Table S7. Summary statistics of the linear regression analysis of LARi versus PTQ for 15 spring wheat cultivars.

Table S8. Model errors for leaf stage.

Figure S1. Relationship between observed and simulated Haun stage and thermal time since emergence for January 2009 HSC sowing.

Figure S2. Relationship between observed and simulated Haun stage and thermal time since emergence for early March 2014 and 2015 NZ sowing.

Figure S3. Photosynthesis at saturating light for the spring wheat cv. Paragon grown in controlled conditions at two temperature regimes and two air-CO_2 concentration.

Table S1. Name, country of origin, registration year, growth habit, and photoperiod sensitivity and genotype at the Vrn and Ppd loci of the 17 wheat genotypes (herein referred as cultivars) used in this study.

Name	Status	Country of origin*	Registration year*	Growth habit*	Vernalization genes£				Photoperiod sensitivity	Photoperiod sensitivity genes#		
					Vrn-A1$	Vrn-B1$	Vrn-D1$	VRN-B3¥		Ppd-A1$	Ppd-B1$	Ppd-D1$
Apache-sp[1]	Near isogenic line	France	NA	Spring	***5***	1	1	NA	Insensitive	NA	b	***a***
Arche[2]	Cultivar	France	1989	Spring	***5***	1	1	2	Sensitive	b	b	b
Baviacora M92	Cultivar	Mexico	1992	Spring	v	v	***a***	NA	Insensitive	b	***a***	***a***
Cadenza[2]	Cultivar	England	1993	Spring	***a***	***2***	1	2	Sensitive	c	b	b
Chinese spring[2]	Landrace	China	NA	Spring	***2***	1	2	2	Insensitive	b	a	b
Courtot[2]	Cultivar	France	1974	Spring	***5***	***2***	1	2	Sensitive	NA	b	b
Drysdale[3]	Cultivar	Australia	2001	Spring	v	***a***	***a***	NA	Insensitive	NA	***a***	***a***
Feeling	Cultivar	France	2015	Spring	NA	NA	NA	NA	NA	NA	NA	NA
Gladius[3]	Cultivar	Australia	2007	Spring	***a***	***a***	v	NA	Sensitive	NA	***a***	b
Paragon	Cultivar	England	1998	Spring	***a***	NA	NA	NA	Sensitive	b	b	b
Récital[2]	Cultivar	France	1986	Winter	2	1	1	2	Insensitive	a	***a***	***a***
Récital-sp[1]	Near isogenic line	France	NA	Spring	***a***	***a***	***a***	NA	Insensitive	NA	***a***	***a***
Renan	Cultivar	France	1989	Winter	2	1	1	2	Sensitive	b	b	c
Seri M82[3]	Cultivar	Mexico	1982	Spring	v	***a***	***a***	NA	Insensitive	a	***a***	***a***
Specifik	Cultivar	France	2010	Spring	NA	**2**	1	NA	Sensible	NA	NA	b
Yecora Rojo	Cultivar	USA	1975	Spring	2-3	**2**	1	NA	Insensitive	b	b	**a**
Yitpi[3]	Cultivar	Australia	2000	Spring	***a***	***a***	v	NA	Insensitive	NA	**a**	d

[1] Isogenic line of the winter wheat cultivar Récital and Apache introgressed with the Vrn-A1pr-5 spring allele (Rousset el al, 2011) of Arche.
[2] Vernalization and photoperiod genes information given by Rousset et al. (2011).
[3] Vernalization and photoperiod genes information given by Zheng et al. (2011).
* Source: http://www.wheatpedigree.net/
$ The Vrn spring alleles and Ppd photoperiod insensitive alleles are in bold italic type.
£ Mutant (spring type) is semi-dominant. Mutation of one homeologous gene is sufficient to give a spring growth habit.
¥ Mutant (spring type) is semi-dominant.
Relative potency of the reduction in flowering time for the photoperiod insensitive variants: Ppd-D1a=Ppd-A1a>Ppd-B1a.

Table S2. Name, definition, value and unit of the parameters of the leaf appearance rate (LAR) models compared in this study. Model M1, constant LAR; model M2, segmented linear model in thermal time corrected for the sowing date (He *et al*., 2012); model M3, LAR model proposed in this study (Eq. 1.10).

Name	Definition	Value		Unit
		Yecora Rojo	Wakanui	
Model M1				
LAR	Leaf appearance rate	0.0111	0.00714	leaf °Cd^{-1}
Model M2				
LAR	Leaf appearance rate	0.00833	0.00714	leaf °Cd^{-1}
L_{incr}	Haun stage above which LAR is increased by P_{incr}	8	8	leaf
L_{decr}	Haun stage up to which LAR is decreased by P_{decr}	3	3	leaf
P_{incr}	Factor increasing LAR for leaf number higher than or equal to L_{incr}	1.25	1.25	dimensionless
P_{decr}	Factor decreasing LAR for leaf number less than L_{decr}	0.75	0.75	dimensionless
R_{P}	Rate of decrease of LAR for winter sowing	0.003	0.003	°Cd d^{-1}
$SD_{\mathrm{W/S}}$	Sowing date for which LAR is maximum	90	90	day of the year
$SD_{S/A}^{nh}$	Sowing date for which LAR is minimum in the northern hemisphere	200	-	day of the year
$SD_{S/A}^{sh}$	Sowing date for which LAR is minimum in the southern hemisphere	-	151	day of the year
Model M3				
$S_{\mathrm{C/GAI}}$	Scaling coefficient of carbon demand to green area index	1.26	1.26	m^2 (ground) m^{-2} (leaf)
d	Thermal time over which intercepted irradiance and thermal time are integrated	70	70	°Cd
$\mathrm{LAR}_{\mathrm{min}}$	Leaf appearance rate for photothermal quotient equals zero	0.0138	0.005	leaf °Cd^{-1}
$\mathrm{LAR}_{\mathrm{max}}$	Maximum leaf appearance rate when photothermal quotient tends to infinite	0.0264	0.0264	leaf °Cd^{-1}
$\mathrm{PTQ}_{\mathrm{hf}}$	Photothermal quotient when leaf appearance rate is half $\mathrm{LAR}_{\mathrm{max}} + \mathrm{LAR}_{\mathrm{min}}$	0.46	0.46	MJ (PAR) m^{-2} °Cd^{-1}

Table S3. Analysis of variance for the response of initial leaf appearance rate to environmental treatment (E) and genotype (G) shown in Figure 1.

Effect	Degree of freedom	Sum of squares	Mean squares	F-value	*P*-value
E	1	4.12×10^{-5}	4.12×10^{-5}	177.38	9.65×10^{-7}
G	1	9.96×10^{-7}	9.96×10^{-7}	4.29	0.072
G x E	1	2.11×10^{-7}	2.11×10^{-7}	0.91	0.368
Residuals	8	12.360	0.281	-	-

Table S4. Environmental conditions and initial leaf appearance rate (LARi) from the literature sown in Figure 4. Average daily thermal time was calculated using Eq. 1.1.

Reference / Cultivar	Set point day/night air temperature (°C)	Set point PAR (µmol m^{-2} s^{-1})	Photoperiod (h)	Set point day/night air VPD (kPa) [a]	Average daily PAR (mol m^{-2} d^{-1})	Average daily thermal time (°C)	PTQ (mol m^{-2} °Cd)	LARi (x 10^{-3} leaf $°Cd^{-1}$)
Cao and Moss (1989a) – Growth chamber, photoperiod								
Stephens	15/15	400	8	NA	11.52	8.18	1.41	10.87
	15/15	400	10	NA	14.40	8.18	1.76	11.71
	15/15	400	12	NA	17.28	8.18	2.11	12.38
	15/15	400	14	NA	20.16	8.18	2.46	12.85
	15/15	400	16	NA	23.04	8.18	2.82	13.28
	15/15	400	18	NA	25.92	8.18	3.17	13.60
	15/15	400	21	NA	30.24	8.18	3.70	14.04
	15/15	400	24	NA	34.56	8.18	4.22	14.36
Cao and Moss (1989c) – Growth chamber, temperature								
Stephens	7.5/7.5	400	14	NA	20.16	1.29	15.63	16.38
	10/10	400	14	NA	20.16	2.84	7.10	14.61
	12.5/12.5	400	14	NA	20.16	5.14	3.92	13.91
	15/15	400	14	NA	20.16	8.18	2.46	12.64
	17.5/17.5	400	14	NA	20.16	11.88	1.70	11.54
	20/20	400	14	NA	20.16	16.04	1.26	10.15
	22.5/22.5	400	14	NA	20.16	20.34	0.99	9.15
	25/25	400	14	NA	20.16	24.35	0.83	8.15
Cao and Moss (1989b) – Growth chamber, photoperiod x temperature interactions								
Stephens	20/20	400	6	NA	8.64	16.04	0.54	7.1
	15/15	400	6	NA	8.64	8.18	1.06	8.63
	10/10	400	6	NA	8.64	2.84	3.04	10.49
	20/20	400	10	NA	14.40	16.04	0.90	8.95

Table S4. Continued.

Stephens	15/15	400	10	NA	14.40	8.18	1.76	11.91
	10/10	400	10	NA	14.40	2.84	5.07	13.60
	20/20	400	14	NA	20.16	16.04	1.26	10.08
	15/15	400	14	NA	20.16	8.18	2.46	12.61
	10/10	400	14	NA	20.16	2.84	7.10	14.52
	20/20	400	18	NA	25.92	16.04	1.62	11.53
	15/15	400	18	NA	25.92	8.18	3.17	13.19
	10/10	400	18	NA	25.92	2.84	9.13	15.61
Rickman et al., (1985) – Green house, irradiance								
Stephens	17/17	500	12	0.82 / 0.82	10.8	11.10	1.95	7.10
	17/17	275	12	0.82 / 0.82	5.94	11.10	1.07	8.63
	17/17	140	12	0.82 / 0.82	3.02	11.10	0.54	10.49
Bos and Neuteboom (1998) – Growth chamber, irradiance x temperature interactions								
Minaret	18/13	111	14	0.61 / 0.45	5.59	9.76	0.57	8.20
	18/13	191	14	0.61 / 0.45	9.63	9.76	0.99	9.17
	18/13	286	14	0.61 / 0.45	14.41	9.76	1.48	10.99
	23/18	111	14	0.84 / 0.61	5.59	17.64	0.32	7.35
	23/18	191	14	0.84 / 0.61	9.63	17.64	0.55	8.47
	23/18	286	14	0.84 / 0.61	14.41	17.64	0.82	9.52
	13/8	111	14	0.45 / 0.32	5.59	3.96	1.41	7.81
	13/8	191	14	0.45 / 0.32	9.63	3.96	2.43	8.93
	13/8	286	14	0.45 / 0.32	20.16	3.96	5.09	12.61

[a] NA, not available.

Table S5. Analysis of variance for the response of initial leaf appearance rate to temperature (T), air CO_2 concentration (CO_2) and genotype (G) effects shown in Figure 4.

Effect	Degree of freedom	Sum of squares	Mean squares	*F*-value	*P*-value
CO2	1	1.11×10^{-04}	1.11×10^{-04}	246.7	$< 2.00 \times 10^{-16}$
T	1	1.41×10^{-05}	1.41×10^{-05}	31.4	1.14×10^{-06}
G	2	6.17×10^{-05}	3.08×10^{-05}	68.7	1.53×10^{-14}
CO_2 x T	1	2.73×10^{-05}	2.73×10^{-05}	60.9	5.80×10^{-10}
CO_2 x G	2	2.35×10^{-05}	1.17×10^{-05}	26.2	2.59×10^{-08}
T x G	2	1.27×10^{-05}	6.37×10^{-06}	14.2	1.59×10^{-05}
CO_2 x T x G	2	3.16×10^{-06}	1.58×10^{-06}	3.5	0.0378
Residuals	46	2.07×10^{-05}	4.50×10^{-07}	-	-

Table S6. Analysis of variance for the response of initial leaf appearance rate to photothermal quotient (PTQ) and genotype (G) shown in Figure 6.

Effect	Degree of freedom	Sum of squares	Mean squares	F-value	*P*-value
PTQ	1	63.24	63.24	225.14	$< 2.00 \times 10^{-16}$
G	14	7.05	0.50	1.49	0.17
PTQ x G	14	2.21	0.16	0.47	0.93
Residuals	30	10.15	0.33	-	-

Table S7. Summary statistics of the linear regression analysis of initial leaf appearance rate versus photothermal quotient for 15 spring wheat cultivars grown in controlled conditions with different temperature and photoperiod (Experiment 3, Table 1). CI, confidence intervals.

Cultivar	r^2	*P*-value	Slope (leaf m^2 mol^{-1} PAR)		Intercept (× 10^{-3} leaf °Cd^{-1})	
			Estimated	95% CI	Estimated	95% CI
Apache-sp	0.902	0.050	5.13	2.20 - 12.10	4.62	2.49 - 6.74
Arche	0.852	0.076	8.02	2.96 - 21.69	3.51	-0.52 - 7.54
Baviacora M92	0.960	0.020	3.99	2.24 - 7.09	5.92	4.87 - 6.95
Cadenza	0.881	0.061	6.02	2.41 - 15.01	4.69	1.98 - 7.40
Chinese Spring	0.879	0.063	6.07	2.41 - 15.29	4.00	1.22 - 2.77
Courtot	0.965	0.017	7.00	4.09 - 11.99	4.43	2.73 - 6.13
Drysdale	0.872	0.066	7.96	3.11 - 20.42	3.98	0.26 - 7.71
Feeling	0.943	0.029	8.74	4.46 - 17.14	2.74	0.02 - 5.47
Gladius	0.946	0.027	8.63	4.46 - 16.67	3.09	0.46 - 5.71
Paragon	0.994	0.003	6.71	5.32 - 8.45	4.07	3.39 - 4.74
Recital-sp	0.819	0.094	8.32	2.84 - 24.33	3.12	-1.51 - 7.74
Seri M82	0.772	0.121	9.19	2.86 - 29.54	3.26	-2.49 - 9.01
Specifik	0.704	0.161	7.64	2.13 - 27.42	3.43	-2.03 - 8.89
Yecora Rojo	0.692	0.167	8.73	2.39 - 31.87	3.58	-2.78 - 9.95
Yitpi	0.987	0.006	8.09	5.77 - 11.34	3.62	2.42 - 4.81
Overall	0.765	$< 2 \times 10^{-16}$	6.86	6.90 - 8.90	4.07	3.24 - 4.11

Table S8. Root mean squared relative error (RMSRE) calculated

for Haun stage > 1.0 for the HSC and NZ2020 experiments, and for both experiments together (overall). Model M1, constant LAR; model M2, Sirius LAR model; model M3, LAR model proposed in this study.

Model	RMSRE (%)		
	HSC	NZ2020	Overall
M1	15.04	25.32	20.58
M2	15.77	8.39	12.80
M3	12.49	9.26	11.08

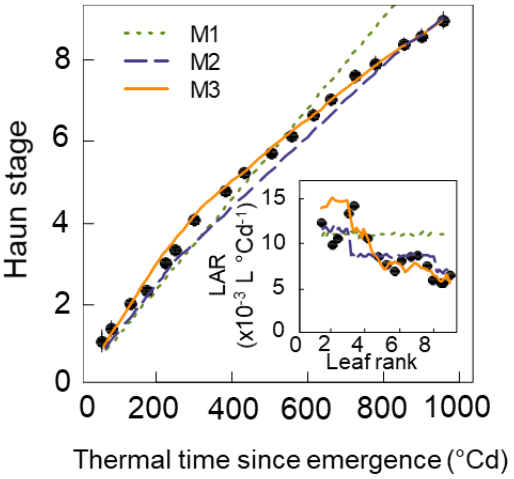

Figure S1. Relationship between observed (close circle) and simulated (lines) Haun stage and thermal time after emergence for the spring wheat cultivar Yecora Rojo sown in the field at Maricopa, Arizona US on 12 January 2009. Lines are simulations obtained with the wheat model *SiriusQuality* and using either a constant phyllochron (model M1, dotted green lines), a segmented linear model in thermal time corrected for the sowing date (model M2, dashed blue lines) or our new model (model M3, solid orange lines). Inset shows observed (closed circles) and simulated (lines) leaf appearance rate versus leaf rank. The thermal time was calculated using apex temperature and Eq. (1.1) for the observation and using simulated near-surface soil or canopy temperature and Eq. (1.1) for the simulated data (see Material and Methods). Data are mean ± 1 s.d. for *n* = 3 independent replicates.

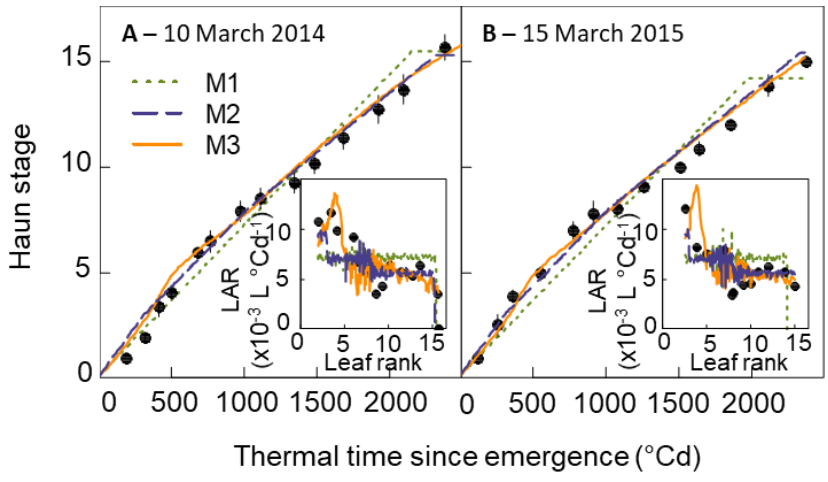

Figure S2. Relationship between observed (close circle) and simulated (lines) Haun stage and thermal time after emergence for the spring wheat cultivar Wakanui sown in the field at Leeston, New Zeland. Lines are simulations obtained with the wheat model *SiriusQuality* and using either a constant phyllochron (model M1, dotted green lines), a segmented linear model in thermal time corrected for the sowing date (model M2, dashed blue lines) or our new model (model M3, solid orange lines). Inset shows observed (closed circles) and simulated (lines) leaf appearance rate versus leaf rank. The thermal time was calculated using apex temperature and Eq. (1.1) for the observation and using simulated near-surface soil or canopy temperature and Eq. (1.1) for the simulated data (see Material and Methods). Data are mean ± 1 s.d. for *n* = 15 independent replicates.

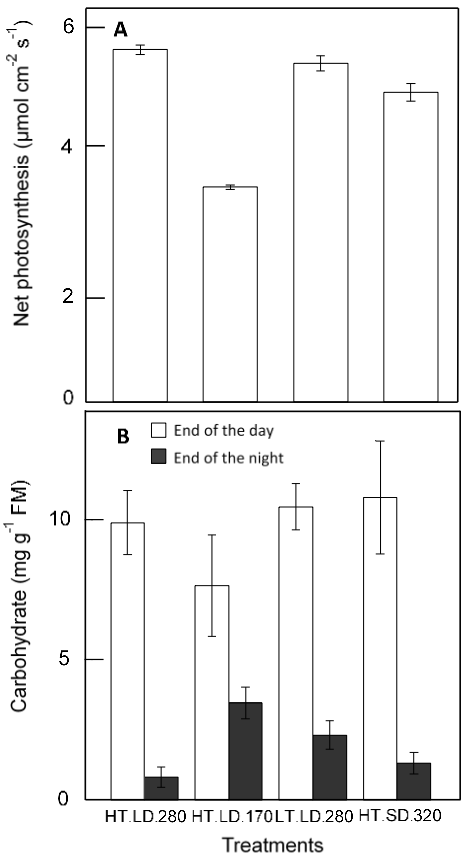

Figure S3. Net photosynthesis (A) and carbohydrate concentration (B) for the spring wheat cv. Paragon grown in controlled conditions with different combinations of temperature, irradiance, and photoperiod. Treatments are as in Figure 1. Data are mean ± 1 s.d. for n = 6 independent replicates.

Chapter 2: Rapid acclimation of CO_2 assimilation capacity mediated by stomatal conductance and carboxylation rate.

Rapid acclimation of CO_2 assimilation capacity mediated by stomatal conductance and carboxylation rate.

Maeva Baumont[1], Boris Parent[1], Bernard Genty[2], Bertrand Muller[1], Pierre Martre[1]

[1] LEPSE, Université Montpellier, INRA, Montpellier SupAgro, 34060 Montpellier, France

[2] BVME, CNRS, CEA, Aix-Marseille University, Saint-Paul-lez-Durance, France

---

This chapter will be coupled with Chapter 3 in view of latter submittion.

I. Abstract

Under a constantly-changing environment, with temperature fluctuating up to 20°C within one day, plants are able to optimize processes such as photosynthesis in the new growth conditions. However, very few crop models consider an explicit acclimation of photosynthesis to temperature, probably due to the lack of ecophysiological studies on the dynamics of photosynthesis as it acclimates to changes of temperature. In this study, we aim at characterizing and quantifying the temporal aspects of acclimation of photosynthesis in wheat, in view of improving models of photosynthesis in crop models. We considered a large number of scenarios of temperature changes, differing in the range of temperature; the amplitude of temperature variations; and the direction of temperature variations. The influence of stomatal conductance as putative driver of such responses was particularly analyzed. Results on fully-acclimated plants showed an ontogenic effect on leaf assimilation rate and changes of temperature responses of photosynthesis that did not support the hypothesis that acclimated plants reach their maximum assimilation capacity at growth temperature. Time courses of assimilation rate for plant subject to changes of growth temperature showed a rapid acclimation of photosynthesis in all cases. This acclimation was driven by stomatal conductance and metabolism depending on the direction of temperature change. Overall, our quantitative description of timing and magnitude of acclimation of wheat photosynthesis to changes of growth temperature provides a solid basis for photosynthesis model improvement in crop models.

Keywords: Acclimation, Photosynthesis, Temperature, Wheat.

II. Introduction

Plants are subject to rapid changes of temperature, which can reach up to 20°C of amplitude within a single day (Rondadini et al., 2006) and affect most plant processes. These variations are superimposed to temperature differences between days and seasons, which together built the thermal history of the plant. These variations are likely to rise in a near future with higher frequency of extreme events such as heat waves due to global changes (Trnka *et al.*, 2014). To ensure their growth and/or survival under this constantly changing environment, plants are able to acclimate to changes in temperature, optimizing processes such as photosynthesis in the new growth conditions (J Berry and Bjorkman, 1980; Yamori et al., 2013). This has been an important research area in the last decades (e.g. Way and Oren, 2010 for trees; Bunce, 2000 for herbaceous; Boese and Huner, 1990 for dicots). These studies highlight different acclimation potentials between species, generally related to their climatic origin (Slayter and Morrow, 1977; Yamori et al., 2010, 2013).

Photosynthesis responds to temperature following a bell-shaped curve, defined by a minimum temperature (T_{min}) at which photosynthesis starts to occur, an optimal temperature (T_{opt}) at which photosynthesis is at its maximum rate, and a maximum temperature (T_{max}) beyond which no photosynthesis is possible. The ascending phase between T_{min} and T_{opt} is characterized by the increase of enzyme activity with temperature (Daniel *et al.*, 2008), while the decreasing phase between T_{opt} and T_{max} is generally associated first with the rise of photorespiration and then with the loss of integrity for molecules and membranes at high temperature (Kim and Portis, 2005; Upchurch, 2008). Most plants show abilities to adjust their carbon assimilation to their growth temperature (T_{growth}). This acclimation is characterized by a shift of cardinal temperatures, especially T_{opt}, and of assimilation capacity, ensuring a better efficiency to face their new growth condition (Way and Yamori, 2014; Zaka *et al.*, 2016). Photosynthesis acclimation can be due to a change in biochemical factors such as intracellular CO_2 concentration, closely related to stomatal conductance, maximum rate of Rubisco carboxylation ($V_{C_{\max}}$) or maximum rate of photosynthesis electron transport ($J_{\max}$) but the implication of each of these factors in acclimation is still unclear (Medlyn *et al.*, 2002; Perdomo *et al.*, 2016). Bunce (2000) showed that the temperature dependency of $J_{\max}$ is close to that of the assimilation rate at saturating light (A_{sat}) for several species from diverse environments and Yamasaki et al. (2002) demonstrated the high plasticity of electron transport in winter wheat when facing a temperature change. Others reported a close

correlation between assimilation rate at saturating light (A_{sat}) acclimation and Vc_{max} (Law and Crafts-Brandner, 1999; Yamori *et al.*, 2005; Hikosaka *et al.*, 2006). Some authors suggested that acclimation of photosynthesis to warmer temperature improves the most limiting biochemical process which differs between plant types and growth conditions (Sage and Kubien, 2007; Smith and Dukes, 2017) but the underlying physiological limitation is often unclear. High temperature in natural conditions often comes with a rise of the air-leaf vapor pressure deficit ($VPD_{air\text{-}leaf}$) triggering a closure of stomata in order to maintain plant water status (Osonubi and Davies, 1980; Tardieu and Simonneau, 1998).

In parallel to photosynthesis, stomatal conductance (g_s) changes with temperature. Since stomatal opening controls gas exchange potential, assimilation and g_s are known to be closely related (Farquhar and Sharkey, 1982). It is difficult to determinate which one drives the other in a given condition and underlying limitations could emerge from this correlation especially at high temperature (Flexas *et al.*, 2014). Assessing the impact of temperature on photosynthesis would require a constant stomatal conductance (g_s) to ensure measurement of assimilation capacities only. However, this is often not the case because of the difficulties to control $VPD_{air\text{-}leaf}$ at a constant value over a large range of temperatures in the cuvette of a gas exchange measurement system. Overall, this correlation and potential limitation of stomatal conductanceon photosynthesis needs to be considered if one aims at better understanding the assimilation response to temperature and its acclimation to the thermal history of the plant.

While this consensus that photosynthesis can acclimate to a new thermal environment, there are very few studies on the dynamics of the response of photosynthesis as it acclimates to changes of temperature. Such quantitative and dynamic studies are however needed in view of improving models of photosynthesis. Model simulations under the predicted future climate reveal that temperature changes would have the bigger negative impact on crop yield (Asseng *et al.*, 2011; Bassu *et al.*, 2014). However, these models do not consider the impact of thermal history on plant processes. Acclimation to temperature is not considered in crop models and could make a large avenue for their improvement (Smith and Dukes, 2013; Li *et al.*, 2015).

To model biomass production, crop models use either a photosynthesis-respiration model (e.g. Wang and Engel, 1998; Yin and van Laar, 2005) or a simpler approach based on the concept of light used efficiency (LUE) (Monteith, 1977). LUE-based models use simple response curves of LUE to temperature, valid in most conditions, without considering the thermal history of the plant.

However, by considering much “flatter” responses than a response of photosynthesis observed in one environmental scenario (Parent and Tardieu, 2014), they consider implicitly that acclimation of photosynthesis is total and instantaneous in a large range of temperature. Similarly, crop model that use a photosynthesis-respiration model consider a unique response of photosynthesis parameters to temperature such as it could be observed under an average condition, and therefore consider implicitly that there is no effect of the thermal history of the plant, and no acclimation.

There are only few studies on physiological modelling of acclimation to temperature in the literature (Bauerle *et al.*, 2007; Kattge and Knorr, 2007; Perdomo *et al.*, 2016; Smith and Dukes, 2017). Kattge and Knorr (2007) highlighted the importance of taking into account the responses to growth temperature (T_{growth}) to model photosynthesis. Their results show that including T_{growth} effect on Vc_{max} and $J_{max.}$ in a Farquhar-based model (Farquhar *et al.*, 1980) of photosynthesis modifies assimilation responses to leaf temperature (T_{leaf}). However, their model only considers steady states and does not include the time response of photosynthesis acclimation to temperature. Dewar et al. (1999) proposed a simple model of temperature acclimation of the ratio of photosynthesis to respiration. This model considered the temporal aspect of the acclimation process but there is no possibility to uncouple respiration and photosynthesis, which can limit its use.

Here, we aimed at characterizing and quantifying the temporal aspects of acclimation of photosynthesis in wheat, in view of improving models of photosynthesis in crop models. We considered three sources of variation, which could affect the time course of photosynthesis acclimation to a change T_{growth}: (i) the considered range of temperature; (ii) the amplitude of temperature variations; and (iii) the direction of temperature variation. A large number of temperature change scenarios was settle to cover the factorial of these variations, with daily temperature ranging from 8°C to 33°C and with increasing and decreasing temperatures. The influence of stomatal conductance as putative driver of such responses was particularly analyzed.

Overall, our results drive the discussion toward the implication of g_s in photosynthesis acclimation to temperature. Our quantitative description of timing and magnitude of acclimation of wheat photosynthesis to changes of T_{growth} provides a solid basis for crop model improvement by considering the effect of thermal history on plant performances.

Table 2.1: Layout and environmental conditions for the three experiments carried out in this study. PAR, photosynthetic active radiation; PTQ, photothermal quotient; A_{sat}, leaf carbon assimilation rate at saturating light, T_{leaf}, leaf temperature; and T_{growth}, growth temperature.

Treatment Name	Set point day/night air temperature (°C)	Set point PAR (µmol m^{-2} s^{-1})	Average daily PAR (mol m^{-2} d-1)	Average daily thermal time (°C)	Average daily PTQ (mol m^{-2} °Cd)	Measured variable	
						A_{sat}	A_{sat}/T_{leaf}
Experiment 1 - Effect of T_{growth} on A_{sat} and acclimation of A_{sat} to an increase of T_{growth}							
T8	8/4	125	6.27	7.20	0.87	X	
T13	13/9	250	11.53	11.65	0.99	X	
T18	18/14	320	16.32	16.05	1.02	X	
T23	23/19	415	20.65	20.24	1.02	X	
T28	28/24	450	22.92	25.33	0.90	X	
T33	33/29	610	30.91	31.60	0.98	X	
T8-> T18	8/4->18/14	125 -> 320	6.27 -> 16.32	7.20 -> 16.05	0.87 -> 1.02	X	
T13-> T23	13/9->23/19	250 -> 415	11.53 -> 20.65	11.65 -> 20.24	0.99 -> 1.02	X	
T18-> T28	18/14->28/24	320 -> 450	16.32 -> 21.92	16.05 -> 25.33	1.02 -> 0.90	X	
T23-> T33	23/19->33/29	415 -> 610	20.65 -> 30.91	20.24 -> 31.60	1.02 -> 0.98	X	
Experiment 2 – Acclimation of A_{sat} and its response to temperature in response to an increase or a decrease of T_{growth}							
C	18/14	320	15.33	16.45	0.93	X	X
W	28/24	450	21.48	26.23	0.82	X	X
CW	18/14->28/24	320 -> 450	16.33 -> 21.48	16.45 -> 26.23	0.93 -> 0.82	X	X
WC	28/24->18/14	450 -> 320	21.48 -> 16.33	26.23 -> 16.45	0.82 -> 0.93	X	X
Experiment 3 - Light x T_{growth} interactions							
T13.LL	13/9	250	11.39	11.82	0.96	X	X
T23.HL	23/19	400	20.56	21.27	0.97	X	X
T23.LL	23/19	250	12.85	21.30	0.60	X	X
T13.LL-> T23.HL	13/9->23/19	250 -> 400	12.49 -> 20.56	11.26 -> 21.27	0.96 -> 0.97	X	X
T13.LL-> T23.LL	13/9->23/19	250 -> 250	12.49 -> 12.85	11.26 -> 21.30	0.96 -> 0.60	X	X
T23.HL-> T13.LL	23/19->13/9	400 -> 250	20.56 -> 12.49	21.27 -> 11.26	0.97 -> 0.96	X	

III. Material and Methods

1. Plant material and growth conditions

Three independent experiments were carried out in controlled conditions with the spring wheat (*Triticum aestivum* L.) cultivar Paragon grown under either stable environmental conditions, or switching between temperature regimes depending on treatment and experiments. Table 2.1 summarizes the environmental conditions of all treatments of the three experiments carried out in this study. In the first experiment (hereafter Exp. 1), we studied the effect of growth temperature (T_{growth}) on leaf carbon assimilation and stomatal conductance and their acclimation to a change in T_{growth} in the microcosm platform of the CNRS European Ecotron at Montpellier, France that comprises 12 identical and independent 2 m^3 growth chambers (working area of 1 m^2). In the second experiment (Exp. 2) carried out in the growth chambers facilities of INRA LEPSE comprising four 17 m^3 chambers (working area of 1m^2), we studied the temperature response of leaf carbon assimilation and stomatal conductance to an increase or a decrease in T_{growth}. In the third experiment (Exp. 3) carried out at Cadarache CNRS center in 1m^3 growth chambers (working area of 1m^2), we also studied the interaction between irradiance and T_{growth} on leaf carbon assimilation and stomata conductance at a finer time resolution and with control of CO_2.

In all experiments, seeds were imbibed for 24 h at 4°C on a wet filter paper in Petri dishes, then placed at room temperature (22°C) for 24 h and transferred back to 4°C until the radicles reached 5-mm long. Seedlings were then transplanted in 1.7 L plastic pots filled with a 30:70 (v:v) mixture of soil and organic compost. Pots were placed in growth chambers with different temperatures and irradiances but a day/night air vapor pressure deficit (VPD_{air}) set at 1.3/1.0 kPa in all experiments and treatments. Plant density was identical in all experiments with 60 plants m^{-2}. Each growth chamber was associated with one growth temperature, with night temperature 4°C lower than day temperature, and one irradiance, representing one stable treatment. Temperatures were chosen to represent the range undergone by wheat during its growing season without triggering injury. In the treatments with changing conditions, half of the plants were transferred between growth chambers when they reached 3.5 visible leaves (that is, Haun stage [Haun, 1973] 3.5). This stage was chosen for the transfer because it insures that leaves already present in the seed were fully developed and that plants were still at vegetative stage. In all experiments, the irradiance was adjusted to ensure a similar photothermal quotient between treatments, and therefore similar development rate (see Chapter 1).

Table 2.2: Lamina length and maximum width and sheath length for mature leaf 4 of the spring wheat cultivar Paragon in the three experiments carried out in this study.

Experiment	Lamina length (cm)		Lamina width (cm)		Sheath length (cm)	
	23/19°C	28/24°C	23/19°C	28/24°C	23/19°C	28/24°C
Exp. 1	31.5 ± 1.8	32.8 ± 2.0	0.86 ± 0.05	0.88 ± 0.03	8.3 ± 0.5	9.8 ± 0.7
Exp 2	-	34.7 ± 2.9	-	0.92 ± 0.06	-	9.7 ± 1.0
Exp 3	29.4 ± 1.6	-	0.82 ± 0.06	-	7.9 ± 0.7	-

Length and width of leaf 4 together with phyllochron were measured in all treatments and compared between equivalent treatments of each experiment (see Table 2.2). They indicate that the different growth chambers had no impact on wheat development. Air CO_2 concentration was not controlled, except in Exp. 3 were it was controlled at 400 ppm. A minimum of five independent replicates were used in each treatment. Plants were watered daily to maintain the soil water content near field capacity.

2. Gas exchange measurements

All gas exchange measurements were performed with CIRAS-2 (PP sytems, Amesbury, MA, USA) portable photosynthesis systems equipped with a 25 x 7 mm bead plate. Gas exchange measurement device consists in a block, inside which the incoming air is modified to stick to the set points (CO_2 concentration, humidity level, temperature), connected to a clamp sheltering measurement cuvette in which the leaf is placed through tubes. In the CIRAS-2, the infrared gas analyzers (two for CO_2, and two for H_2O placed before and after the leaf cuvette) are located in the block, so the air out-coming the cuvette pass through the tubes before being measured, which increases the difficulties to control VPD when the difference between the cuvette temperature and the external temperature (surrounding the tube) is important since condensation can be formed. They CIRAS-2 systems were calibrated before each measurement campaign by comparing carbon assimilation and stomatal conductance in similar climate conditions (temperature, humidity and light intensity) for at least two different leaves of three wheat plants. A coefficient was applied to measurements of each device to correct for any differences. For all measurements, the device clamp was placed inside the growth chamber while the connected block was outside, under constant environmental conditions.

In all experiments, leaf carbon assimilation (A_{sat}, µmol CO_2 m^{-2} s^{-1}) and stomatal conductance (g_s, µmol H_2O m^{-2} s^{-1}) were measured at saturating light and ambient temperature and atmospheric CO_2 concentration. Measurements were performed on the youngest ligulated leaf between Haun stage 3 and 5.

The response of A_{sat} to leaf temperature (T_{leaf}; hereafter A/T) was measured in experiments 2 and 3. Plants were maintained at their growth temperature while the temperature in the leaf cuvette was changed from 8°C to 38°C by steps of 5°C. Relative humidity in the leaf cuvette was changed to maintain a target air-leaf VPD ($VPD_{air\text{-}leaf}$) of 1.5 kPa. Because of the apparatus limitations, all

T_{leaf} could not be reached for all treatments and measured $VPD_{air\text{-}leaf}$ ranged from 0.5 kPa at 8°C to 6.4 kPa at 38°C in experiment 1 and from 0.5 kPa at 8°C to 3.2 kPa at 38°C in experiments 2 and 3. Preliminary measurements showed no hysteresis when temperature was increased or decreased between 8°C and 38°C (data not shown). Preliminary measurements also showed that A_{sat} and g_s reached a constant value in less than 7 mn after a change in T_{leaf}. Data were therefore recorded every 10 s during 90 s starting 7 min after T_{leaf} reached the set value. Response curves were obtained by fitting the data to a three parameters beta function (Wang and Engel, 1998):

$$A_{\mathrm{sat}}(T) = \frac{f(T)}{T_{\mathrm{leaf}}} \tag{2.1}$$

with,

$$f(T) = max\left(0, \frac{2(T-T_{\min})^{\alpha}(T_{\mathrm{opt}}-T_{\min})^{\alpha}-(T-T_{\min})^{2\alpha}}{(T_{\mathrm{opt}}-T_{\min})^{2\alpha}}\right);\ \alpha = \frac{\ln 2}{\ln\left(\frac{T_{\max}-T_{\min}}{T_{\mathrm{opt}}-T_{\min}}\right)} \tag{2.2}$$

where T (°C) is T_{leaf} measured in the leaf cuvette, and $T_{\min}$, T_{opt}, and $T_{\max}$ are the fitted minimum, optimum, and maximum temperatures, respectively.

3. Measurements of leaf and apex temperature and thermal time calculation

In all growth chambers, T_{leaf} and apex temperature (T_{apex}, °C) were measured with thermocouples secured on the lower surface of leaf blades or inserted vertically between leaf sheaths down to the base of the leaves, respectively. The daily thermal time was calculated as:

$$\Delta T_{\mathrm{t}} = \sum_{i=1}^{n} \frac{1}{144} \sum_{i=1}^{n=144} T_{\mathrm{opt}} \times f(T) \tag{2.3}$$

where $f(T)$ (dimensionless) is the nonlinear temperature response of leaf initiation and growth given by Eq. (2.2), where T is the 10 min average T_{leaf}. Values of 0, 27.5 and 40°C were used for $T_{\min}$, T_{opt}, and $T_{\max}$, respectively (Parent and Tardieu, 2012).

4. Data analysis and statistics

All data analyses and graphs were made using the R statistical software version 3.4.1 (R Core Team, 2017).

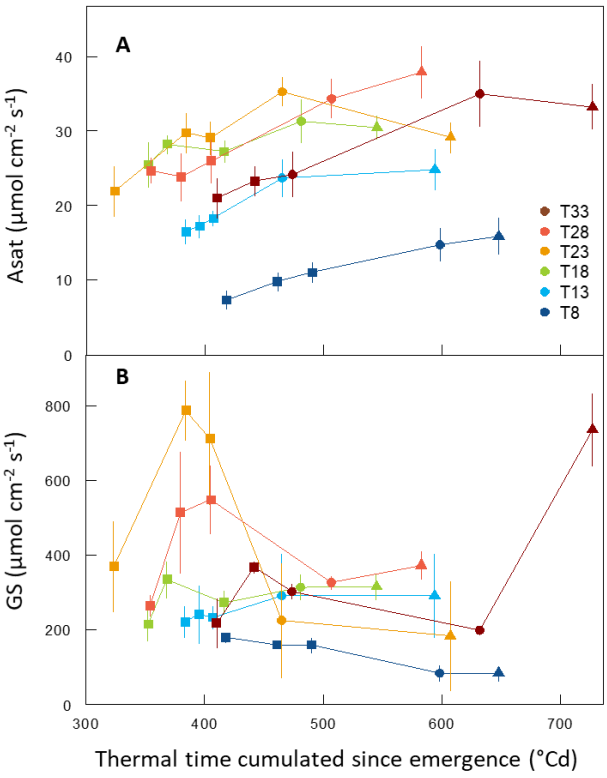

Figure 2.1. Ontogenic changes in carbon assimilation and stomatal conductance at saturating light for the spring wheat (*Triticun aestivum* L.) cultivar Paragon grown in controlled conditions at different temperatures. (**A**) Leaf assimilation rate at saturating light (A_{sat}) versus thermal time after plant emergence. (**B**) Stomatal conductance (g_s) versus thermal time after plant emergence. Measurements were taken on the youngest ligulated leaf (squares, leaf 3; circles, leaf 4; and triangles, leaf 5). Treatments are detailed in Table 1 (Experiment 1). Data are mean ± 1 s.d. for *n* = 5 independent replicates.

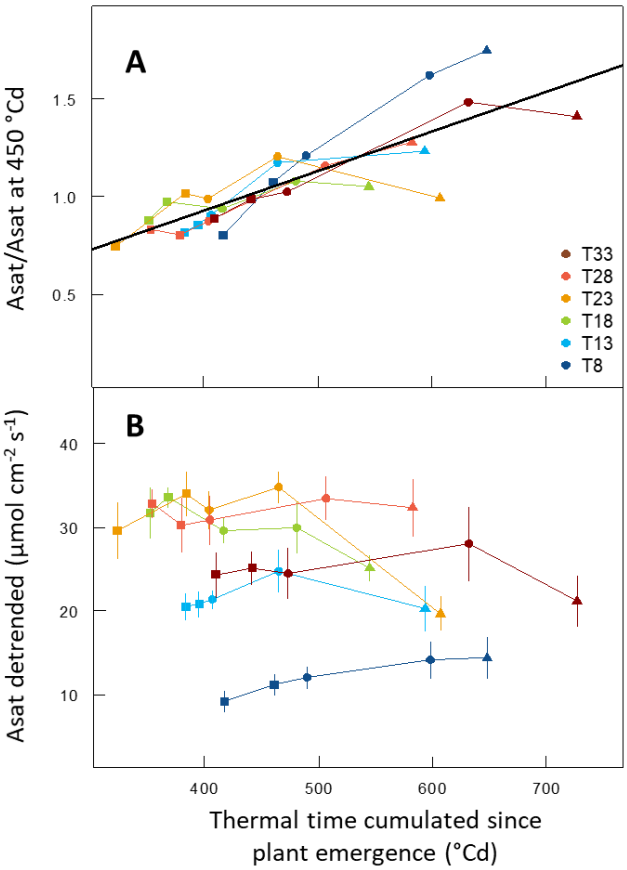

Figure 2.2. Leaf assimilation rate at saturating light (A_{sat}) versus thermal time after plant emergence. (**A**) A_{sat} normalized by A_{sat} at 450°Cd after emergence. The solid line is the linear regression calculated for all treatment. (**B**) A_{sat} detrended using the linear regression shown in (A). Treatments are detailed in Table 1 (Experiment 1). Measurements were taken on the last ligulated leaf (squares, leaf 3; circles, leaf 4; and triangles, leaf 5). Data are mean ± 1 s.d. for *n = 5* independent replicates

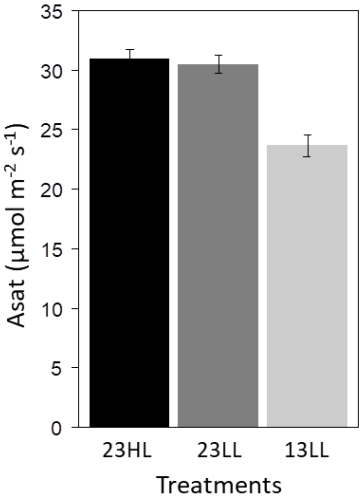

Figure 2.3. Leaf assimilation rate at saturating light (A_{sat}) for the spring wheat (*Triticun aestivum* L.) cultivar Paragon grown in controlled conditions at two irradiances (LL, 250 µmol m^{-2} s^{-1}; HM, 400 µmol m^{-2} s^{-1}) and two temperatures (13, 13/9 °C day/night; 23, 23/19°C). A_{sat} is the average of A_{sat} measured several time on leaf 4 from its ligulation to the ligulation of leaf 5. Environmental conditions are detailed in Table 1 (Experiment 3). Data are mean ± 1 s.d. for *n = 5* independent replicates.

IV. Results

1. Leaf carbon assimilation capacity depends on growth temperature and changes with ontogeny

A_{sat} measured on the youngest ligulated leaf differed between stable thermal treatments from 8°C to 33°C, but increased during plant development in all thermal scenarios (Fig. 2.1A). A similar trend of A_{sat} was found when focusing on measurements carried out on the same leaf (e.g. leaf 3 in Fig.2.1A) and when it was measured on different leaves, which suggested that the increase in A_{sat} was related to plant age rather than to leaf age (Fig.2.1.A). Similar differences at a given time after emergence were observed on g_s between thermal scenarios. However, the increasing trend with plant age was not observed on g_s (Fig.2.1B). Indeed, g_s was stable when comparing values measured on different leaves just after their appearance, while a bell-shaped trend was observed on leaf 3 over time, suggesting an effect of leaf age rather than plant age (Fig. 2.1B).

As g_s did not show a trend similar to that of A_{sat}, the increase of A_{sat} with plant age might indicate an increase in photosynthetic capacity with plant age. *This will be discussed when nitrogen leaf-content will be available.* The ontogenic trend of A_{sat} was similar for all temperature treatments and was well represented by a linear relationship between A_{sat} normalized by A_{sat} at 450°Cd for each treatment and thermal time after plant emergence (r^2 = 0.72; P = 3.54 x10^{-9}; Fig. 2.2A). In the results presented hereafter, the slope of this relationship (1.69 x10^{-3} µmol m^{-2} s^{-1} °Cd^{-1}) was used to detrend A_{sat}, so that A_{sat} of plants of different ages could be compared (Fig. 2.2B).A_{sat} increased as T_{growth} changed from 8°C/4°C to 23°C/19°C and decreased for T_{growth} higher than 23°C/19°C (Fig. 2.1A and Fig. 2.2B). Because the irradiance was adjusted at each T_{growth} to have a similar photothermal quotient (see Chapter 1), it avoided confounding effects of development when analyzing the response of A_{sat} to temperature. We checked that changes in A_{sat} with T_{growth} were not due to differences in irradiance, by growing plants at similar temperatures (23°C/19°C) and contrasted light (250 and 400 µom m^{-2} s^{-1} , treatments 23LL and 23HL, respectively). A_{sat} was not modified by irradiance (Fig. 2.3) and so A_{sat} could be compared at similar values of photothermal quotient.

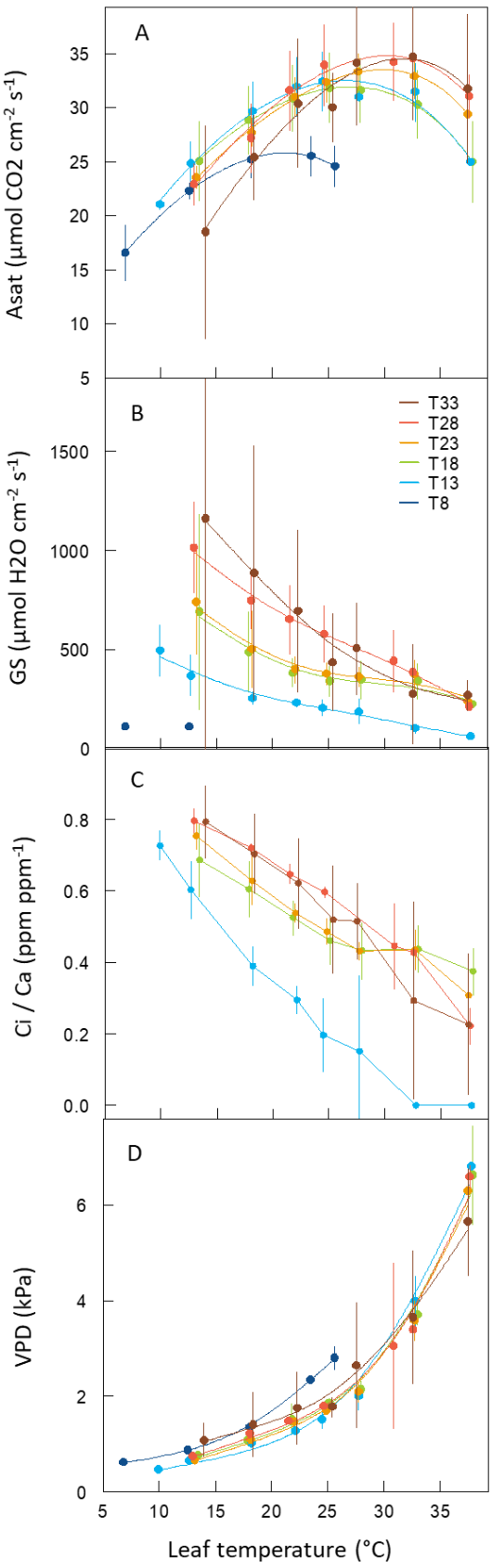

Figure 2.4. Effect of temperature on carbon assimilation, stomatal conductance, leaf intern CO2 concentration ratio to external CO2 concentration (Ci/Ca) and VPD at saturating light for the spring wheat cultivar Paragon grown in controlled conditions at different temperatures. (**A**) Leaf assimilation rate at saturating light (A_{sat}) versus T_{leaf}. (**B**) Stomatal conductance (g_s) versus T_{leaf}. (**C**) Ci to Ca ratio versus T_{leaf}. (**D**) VPD versus T_{leaf}. Treatments are detailed in Table 1 (Experiment 1). Lines in (A) are non-linear curves fitted to the data using Eq. 2. Values of the fitted parameters are given in Table 2.3. Lines in (B) and (D) are non-parametric spline curves fitted to the data. Measurements were taken on leaf 5 15°Cd to 50°Cd after its ligulation. Data are mean ± 1 s.d. for *n* = 3 independent replicates.

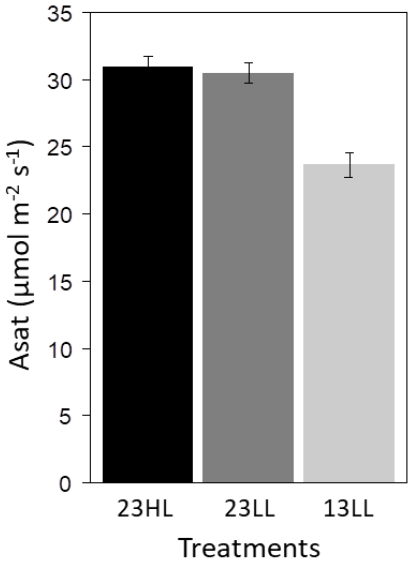

Figure 2.3. Leaf assimilation rate at saturating light (A_{sat}) for the spring wheat (*Triticun aestivum* L.) cultivar Paragon grown in controlled conditions at two irradiances (LL, 250 µmol m^{-2} s^{-1}; HM, 400 µmol m^{-2} s^{-1}) and two temperatures (13, 13/9 °C day/night; 23, 23/19°C). A_{sat} is the average of A_{sat} measured several time on leaf 4 from its ligulation to the ligulation of leaf 5. Environmental conditions are detailed in Table 1 (Experiment 3). Data are mean ± 1 s.d. for *n = 5* independent replicates.

2. Optimal temperature of leaf carbon assimilation rate and maximal assimilation capacities depend on growth temperature

The effects of T_{leaf} on A_{sat} showed a similar bell-shaped pattern in all treatments with stable thermal conditions (Fig.2.4.A), but values differed between treatments (Table 2.3).

Table 2.3: Values of the parameters of the A_{sat} / T_{leaf} modeled with Eq. 2.2. Measurements were made on leaf 5 of stable treatments of Exp. 1 (see table 2.1).

Treatment	T_{opt} (°C)	T_{min} (°C)	T_{max} (°C)	A_{sat}^{opt} (µmol cm² s^{-1})
T8	21.1 ± 0.2	- 4.1 ± 0.8	36.1 ± 3.4	25.7 ± 0.1
T13	26.5 ± 0.1	- 3.2 ± 2.8	45.3 ± 5.0	32.5 ± 0.5
T18	27.0 ± 0.3	- 4.9 ± 1.4	44.4 ± 1.4	31.9 ± 0.1
T23	29.9 ± 0.4	- 4.2 ± 1.5	43.0 ± 1.6	33.5 ± 0.2
T28	30.3 ± 0.9	-1.4 ± 3.3	44.8 ± 5.6	34.8 ± 0.6
T33	31.8 ± 1.3	3.8 ± 3.6	44.9 ± 11.0	34.5 ± 1.2

A_{sat} measured at T_{growth} increased with T_{growth} (Fig. 2.6A), reaching at 33°C/29°C twice the value measured at 8°C/4°C. To the opposite, stomatal conductance decreased for above 25°C (Fig. 2.6A).

The temperature at which A_{sat} was maximum (T_{opt}), calculated from curve fitting, differed between treatments and increased with T_{growth}. Indeed, T_{opt} was maximum in the warmest thermal scenarios (33°C/29°C), with T_{opt} value very close to the growth temperature. T_{opt} decreased at lower growth temperature but stayed higher than T_{growth} so that the difference between T_{opt} and T_{growth} increased at lower temperature (Fig.2.6.B).

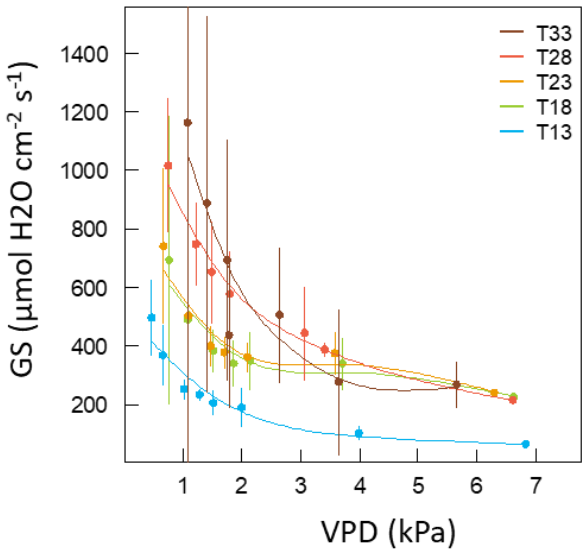

Figure 2.5. Stomatal conductance (g_s) versus air-leaf vapor pressure deficit ($VPD_{air\text{-}leaf}$) in the leaf cuvette of the gas exchange measurement system for the spring wheat cultivar Paragon grown at six different growth temperatures. Treatments are detailed in Table 1 (Experiment 1). Measurements were taken on leaf 5 15°Cd to 50°Cd °Cd after its ligulation. Data are mean ± 1 s.d. for *n = 3* independent replicates.

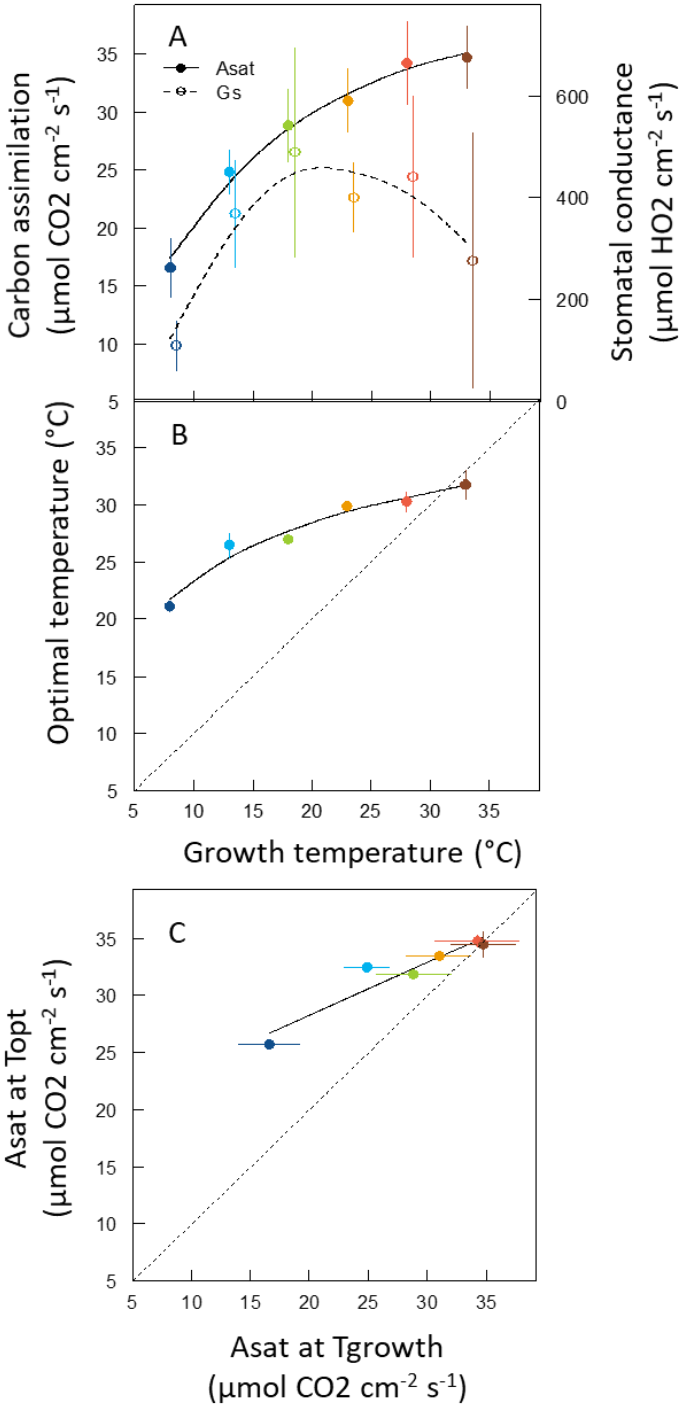

Figure 2.6. Effect of growth temperature on carbon assimilation, stomatal conductance, and carbon assimilation at optimum temperature measured at saturating light for the spring wheat cultivar Paragon grown at different temperatures. (**A**) Leaf assimilation rate and stomatal conductance at saturating light (A_{sat}) at growth temperature (T_{growth}) versus T_{growth}. (**B**) Optimum temperature of A_{sat} (T_{opt}) versus T_{growth}. (**C**) Leaf assimilation at saturating light at T_{opt} versus leaf assimilation at saturating light at T_{growth}. T_{opt} and assimilation at T_{opt} were estimated by fitting A_{sat}/T_{leaf} data using Eq. 2. Treatments are detailed in Table 1 (Experiment 1). Measurements were taken on leaf 5 15°Cd to 50°Cd after its ligulation (Fig. 2.2B). Solid lines in (A) and (B) are non-parametric spline curves fitted to the data. Solid line in (C) is linear fitted to the data. Dotted lines in (B) and (C) are the 1:1 line. Data are mean ± 1 s.d. for *n* = 3 independent replicates.

The value of A_{sat} at T_{opt} (here after termed A_{sat}^{opt}) increased when T_{growth} increased (Fig. 2.4A, Table 2.3) but less than the increase of A_{sat} with T_{growth}. It resulted that the distance between assimilation that plant actually does at its T_{growth} (A_{sat}^{growth}) and maximal assimilation that plants are capable of (A_{sat}^{opt}) with the same machinery is smaller with higher T_{growth} (Fig 2.6C). Therefore, plants seemed to limit their carbon assimilation at low T_{growth}, probably because of a lower sink demand. The relation between A_{sat}^{opt} and T_{opt} was well represented by a linear regression (r^2 = 0.85; P = 9.38 x10^{-3}; Fig 2.7A).

By contrast, g_s decreased almost linearly when T_{leaf} increased (Fig 2.4B). This response of g_s to T_{leaf} could be due to the increase in $VPD_{air-leaf}$ in the leaf cuvette (Fig. 2.5). However, the response of $VPD_{air-leaf}$ to T_{leaf} was independent of T_{growth} (Fig. 2.4D). C_i/C_a (intern to extern CO_2 concentration) also shows a decrease with T_{leaf}, proving that g_s could limit the assimilation rate a high T_{leaf} (Fig 2.4C). Again, this decrease is independent from T_{growth}, suggesting that the increase of T_{opt} and A_{sat}^{opt} with T_{growth} are not due to g_s.

3. A change in growth temperature results in an acclimation of the short-term response of photosynthesis to temperature

The response of A_{sat} to T_{leaf} was determined before and after changes of T_{growth} for plants transferred from 13°C/9°C to 23°C/19°C (Fig 2.8A; treatment 13LL.23HL) or from 18°C/14°C to 28°C/24°C (Fig 2.8B, Treatment CW). Response curves were measured before transfer and 100°Cd after transfer and compared to that of plants grown under stable growth conditions. A_{sat} of plants transferred from 13°C/9°C to 23°C/19°C reached the same values as plant growing at 23°C/19°C from emergence (Fig. 2.9A). Similarly, T_{opt} calculated from curves of A_{sat} vs T_{leaf} (Figure 2.8) for plants transferred from 13°C/9°C to 23°C/19°C reached similar values as plant grown at 23°C/19°C (Fig 2.9A). The same behavior was observed for plants transferred from 18°C/14°C to 28°C/24°C. We observed this acclimation after 100 °Cd and on leaf produced at the new T_{growth}.

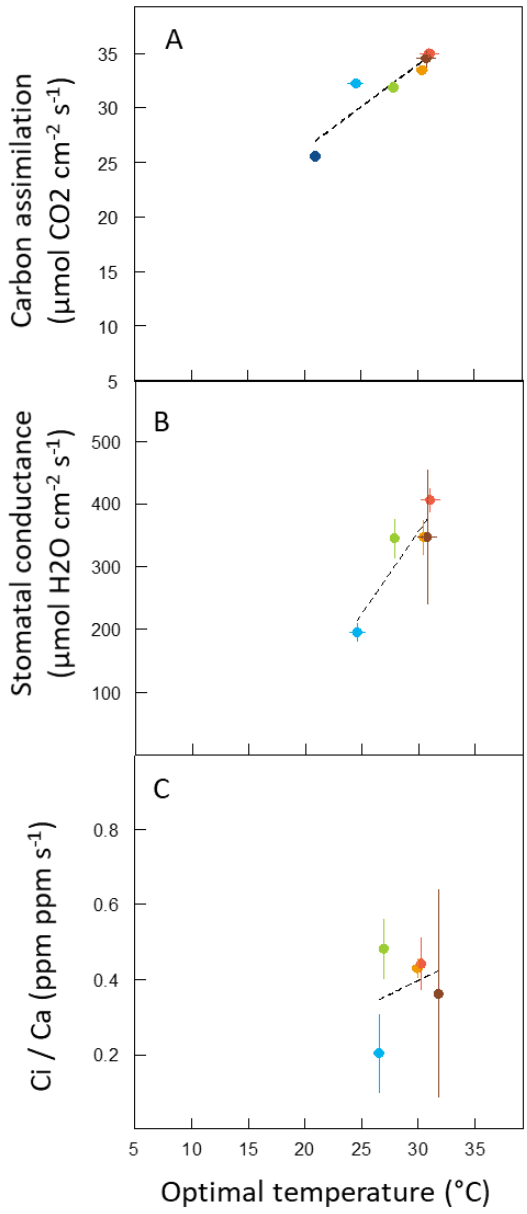

Figure 2.7. Relation between carbon assimilation, stomatal conductance and Ci/Ca ratio and carbon assimilation optimum temperature at saturating light for the spring wheat cultivar Paragon grown at different temperatures. (**A**) Leaf assimilation rate at saturating light (A_{sat}) at T_{opt} versus T_{opt}. (**B**) Stomatal conductance at T_{opt} versus $T_{opt.}$ (**C**) *Ci/Ca* at T_{opt} versus T_{opt}. T_{opt} was estimated by fitting A_{sat}/T_{leaf} data using Eq. 2. Treatments are detailed in Table 1 (Experiment 1). Measurements were taken on leaf 5 15°Cd to 50°Cd after its ligulation (Fig. 2.2B). Dashed lines are linear regressions fitted to the data. Data are mean ± 1 s.d. for n = 3 independent replicates.

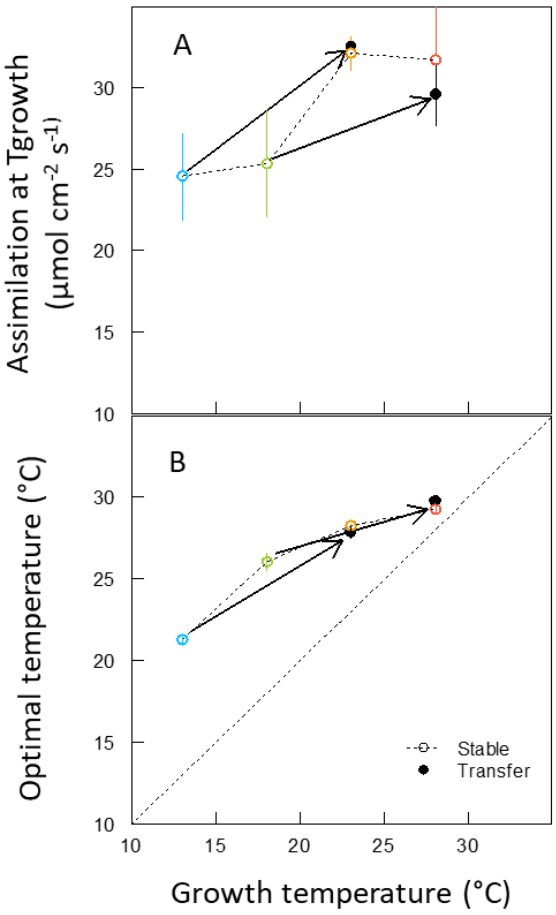

Figure 2.9. Effect of growth temperature on leaf carbon assimilation at saturating light and its optimal temperature for the spring wheat cultivar Paragon grown in controlled conditions. **(A)** Leaf assimilation rate at saturating light (A_{sat}) at growth temperature (T_{growth}) versus T_{growth}. (**B**) Optimum temperature of A_{sat} (T_{opt}) versus T_{growth}. Treatments are detailed in Table 1 (Experiments 2 and 3). T_{opt} was estimated by fitting A_{sat}/T_{leaf} data using Eq. 2. Open circles are treatments without temperature transfer and closed circles are treatments with temperature transfer at Haun stage 3.5. The treatments with temperature transfer (13LL.23HL and CW) measurements were taken 100°Cd to 150°Cd after transfer. Arrows indicate changes in A_{sat} at T_{growth} or

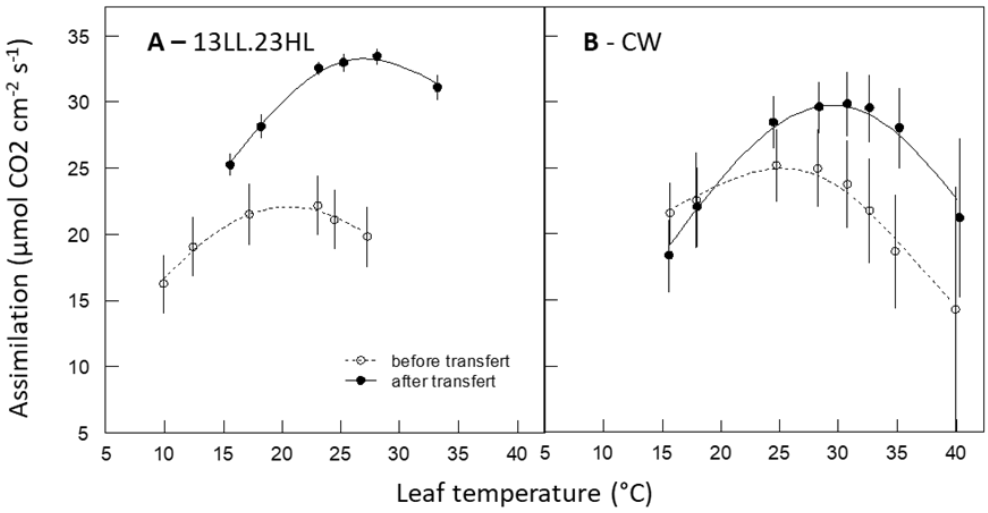

Figure 2.8. Leaf assimilation rate at saturating light (A_{sat}, A and B) and stomatal conductance (g_s, C and D) versus leaf temperature (T_{leaf}) for the spring wheat cultivar Paragon grown in controlled conditions at different temperatures and irradiances. Plants were transferred from 13°C/9°C (day/night) to 23°C/19°C (treatment 13LL.23HL, A) or from 18°C/14°C to 28°C/24°C (treatment CW, B). Treatment detailed are given in Table 2.1 (experiments 2 and 3). Measurements were taken on leaf 3 the day before (open circles, dashed lines) or on leaf 5 between 150°Cd and 250°Cd after (closed circles, solid lines) the change in temperature. In (A) and (B) lines are non-linear regression fitted to data using Eq. 2Data are mean ± 1 s.d. for n = 3 independent replicates.

The change of T_{growth} was accompanied by a change of growth irradiance as the photothermal quotient was kept constant. The effect of this change of irradiance was investigated by comparing A_{sat} of plants growing at 23/19°C under two different irradiances (Fig.2.10) and for plants transferred from 13°C/9°C to 23°C/19°C at these two irradiances. In all cases (stable treatment vs after transfer to low vs high irradiance) A_{sat} reached similar values (Fig.2.10). Therefore, acclimation observed in Figure 2.8 and 2.9 were not due to changes in irradiance.

4. Assimilation capacities change rapidly with a change of growth temperature

The dynamic of the response of A_{sat} to changes in T_{growth} was first investigated by monitoring the time course of A_{sat} after increasing T_{growth} by 10°C starting from four different T_{growth} (Fig.2.11). In all treatments A_{sat} changed resulting in a new A_{sat} similar to the one of plants grown from emergence in the new condition but the time to reach this new value depended on the treatment

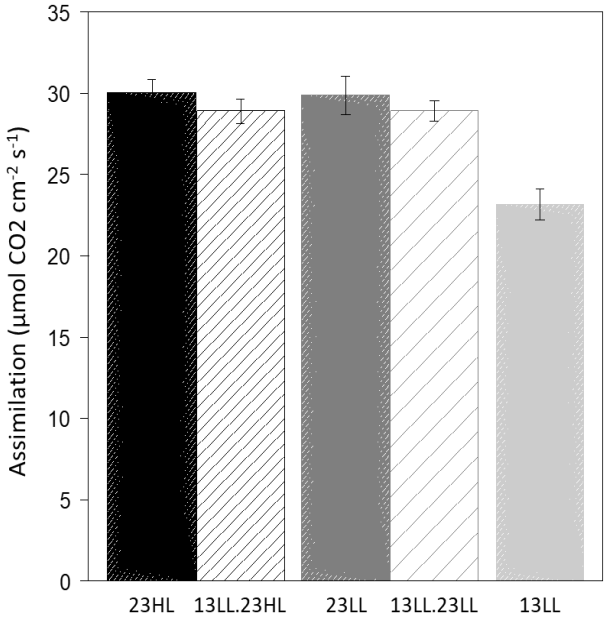

Figure 2.10. Leaf assimilation rate at saturating light (A_{sat}) for the spring wheat cultivar Paragon grown in controlled conditions with two irradiance (LL, 250 µmol m^{-2} s^{-1}; HM, 400 µmol m^{-2} s^{-1}) and two temperatures (13, 13/9 °C day/night; 23, 23/19°C). In treatments 23HL, 23LL and 13LL plants experienced the same growth conditions during the whole experiment while in treatments 13LL->23HL and 13LL->23LL plants were transferred from treatment 13LL to 23HL and from 13LL to 23LL at Haun stage 3.5. Treatment detailed are given in Table 1 (experiment 1). A_{sat} here is the average of A_{sat} measured several times on leaf 4 from its ligulation to the ligulation of leaf 5. Data are mean ± 1 s.d. for *n = 5* independent replicates

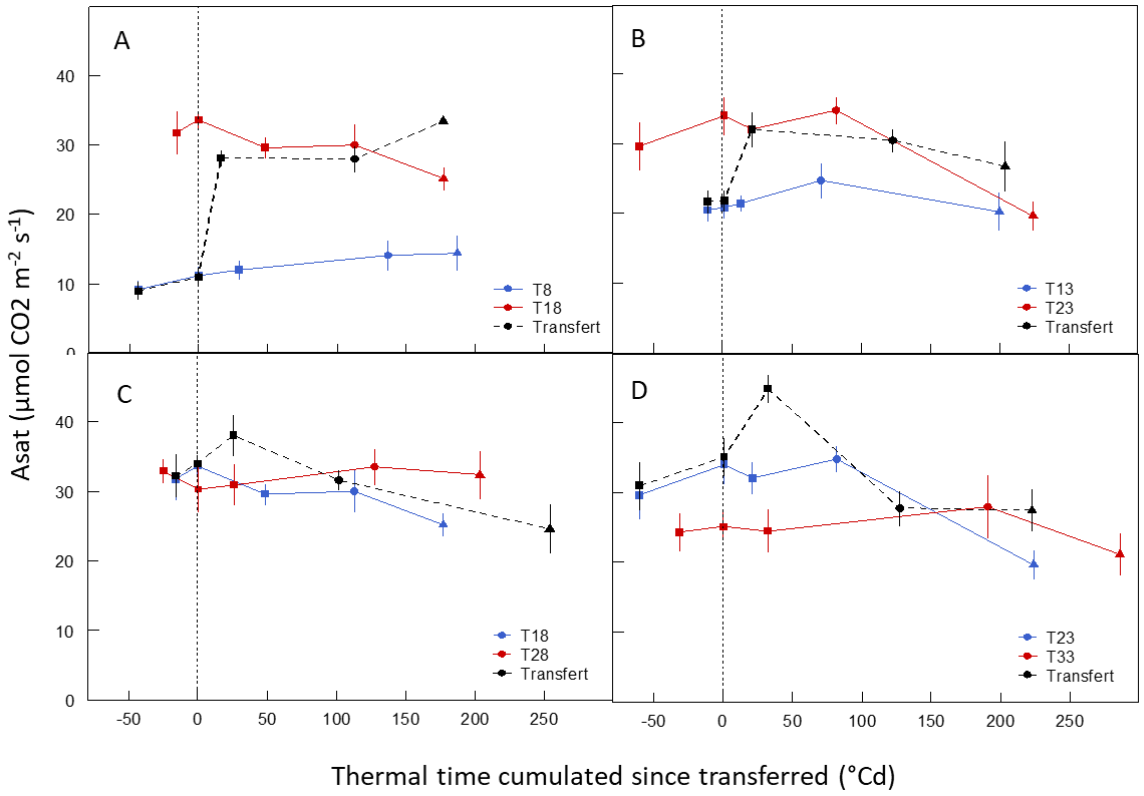

Figure 2.11. Time course of leaf carbon assimilation and stomatal conductance at saturating light before and after changes in growth temperature for the spring wheat cultivar Paragon grown in controlled conditions. Plants were transferred at Haun stage 3.5 from 8°C/4°C (day/night) to 18°C/14°C (A and E); from 13°C/9°C to 23°C/19°C (B and F), from 18°C/14°C to 28°C/24°C (C and G); or from 23°C/19°C to 33°C/29°C (D and H). Treatments are detailed in Table 1 (Experiment 1). Measurements were taken on the last ligulated leaf (squares, leaf 3; circles, leaf 4; and triangles, leaf 5). Data are mean ± 1 s.d. for *n* = 5 independent replicates.

(Fig. 2.11A to D). Because the values of acclimated A_{sat} (values of plants growing under stable temperature) were more different between T_{growth} of 8/4°C and 18/14°C than 13/9°C and 2/19°C or 18/14°C and 28/24°C (Fig.2.6), A_{sat} had to change more between 8/4°C and 18/14°C compared to between 18/14°C and 28/24°C to reach acclimated value. This could explain why the time to reach acclimated values was shorter for plants transferred from 18/14°C to 28/14°C compared to plants transferred from 8/4°C to 18/14°C.

5. Correlation between assimilation capacities and stomatal conductance varies with temperature

Because a complete acclimation of A_{sat} was observed in less than 100°Cd in these four treatments shown in Figure 2.11, the time course of acclimation of A_{sat} and g_s were recorder at higher time resolution for plants transferred from 13°C to 23°C and from 23°C to 13°C (Figure 2.12).

For plants transferred from 13/9°C to 23/19°C, acclimation of A_{sat} was almost instantaneous, increasing just after transfer, with even higher values than for plants constantly grown at 23/19°C. g_s and C_i/C_a also increased after transfer but not as fast as A_{sat}, indicating an acclimation process of A_{sat} which would be at least partly independent from g_s.

To the contrary, in plants transferred from 23/19°C to 13/9°C, A_{sat} was reduced rapidly, to values even lower than plants constantly grown at 13/9°C. g_s decreased also very rapidly to values even lower than plants constantly grown at 13/9°C and then increased again slowly. C_i/C_a decreased together with g_s and increased again when g_s increased. It indicated a possible limitation of photosynthesis by g_s.

Overall, these results seem to indicate that two mechanisms act together at different time step, depending if temperature decreases or increases.

V. Discussion

1. Are assimilation capacities adjusted during early development?

Leaf carbon assimilation capacity, determined as the leaf carbon assimilation rate at saturating light, ambient CO_2 and ambient temperature, increased with plant age in all thermal treatments

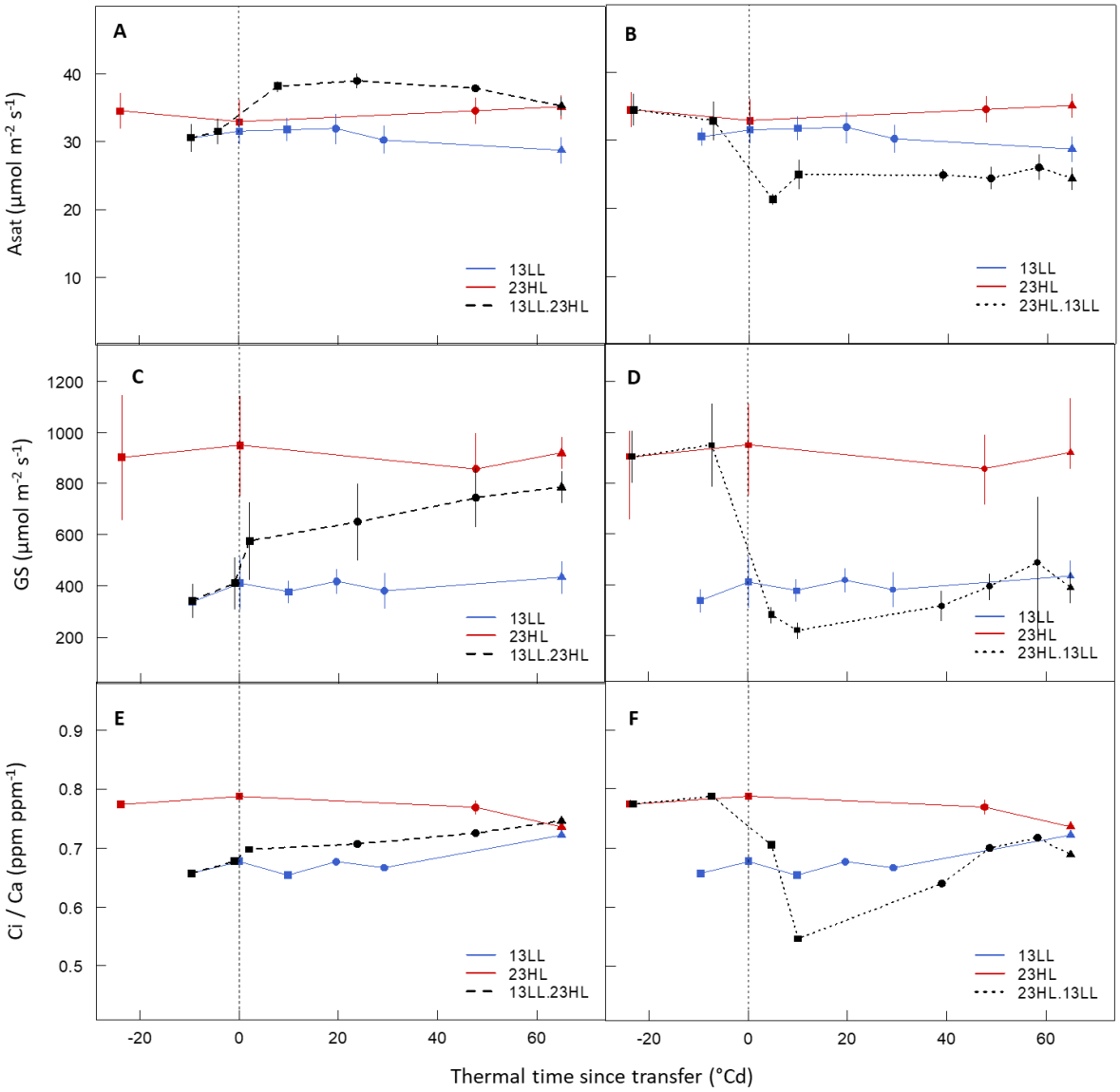

Figure 2.12. Time course of leaf carbon assimilation and stomatal conductance at saturating light for after changes in growth temperature for the spring wheat cultivar Paragon grown in controlled conditions. (**A** and **B**) Leaf assimilation rate at saturating light (A_{sat}) versus thermal time after temperature transfer. (**C** and **D**) Stomatal conductance (g_s) versus thermal time after temperature transfer. Plants were transferred at Haun stage 3.5 from 13 °C/ 9°C (day/night) to 23 °C/19X°C (A and C) or from 23°C/ 19°C to 13°C/ 9°C (B and D). Treatments are detailed in Table 1 (Experiment 3). Measurements were taken on the last ligulated leaf (squares, leaf 3; circles, leaf 4; and triangles, leaf 5). Data are mean ± 1 s.d. for *n = 5* independent replicates.

tested in this study. To our knowledge, this is the first time that this effect of ontogeny on wheat photosynthesis is observed. Sesták (1985) reported increases of photosynthetic capacities with leaf age through modification of electron transport and carboxylation rates capacities, but it was mostly happening when leaf was not fully mature yet. Here the increase of A_{sat} was observed on measurements performed on fully developed leaves after ligule appearance, and with the same effect on one leaf or successive leaves so that it is not due to leaf development but rather to plant development. At whole-plant or canopy scale, an increase of plant carbon assimilation rate with crop development has already been observed for wheat in the field (Gerbaud and André, 1980) but the increase was linked to the increasing number of photosynthetic leaves in the canopy. Overall, we found only one study on black cherry (*Prunus serotina*) reporting ontogenic effects such as those observed in our study (Horsley and Gottschalk, 1993).

This ontogenic effect could result from morphologic or metabolic adjustments to growth conditions to ensure better carbon assimilation. This could be due to some modifications of leaf cell organization (Sharkey, 1985; Oguchi *et al.*, 2005), chloroplasts number or position in the mesophyll cells, or by adjusting Rubisco activation rate (Krapp and Stitt, 1995; Salvucci and Crafts-Brandner, 2004) or isotomers (Dean *et al.*, 1985; Galili *et al.*, 1998). Such adjustments could be observed through leaf nitrogen content (Evans, 1983; Martre *et al.*, 2006). More experiments are needed to confirm or not this effect at the leaf and whole plant levels.

2. How different are the responses pf assimilation to long and short-term changes of temperature

We measured A_{sat} responses to short-term and long-term changes in temperature. In regards to the time spent by plants at the measurement temperature, the whole growth period versus a few minutes, we considered that they represent the fully acclimated and the non-acclimated responses to temperature, respectively. For both responses, A_{sat} followed a bell-shape curve. Different T_{growth} triggered an acclimation of *A*/*T* through a modification of T_{opt} and A_{sat}^{opt} as observed in the literature (Berry and Bjorkman, 1980; Yamori *et al.*, 2013; Way and Yamori, 2014), with T_{opt} between 20°C and 30°C and A_{sat}^{opt} between 25 and 35 µmol m^{-2} s^{-1} depending on T_{growth}. For A_{sat} response to T_{growth}, T_{opt} varied from 23°C to 28°C and A_{sat}^{opt} was not modified by T_{growth} and averaged 32 µmol m^{-2} s^{-1}. Overall, the *A*/*T* response curves were much closer for different T_{growth} than in previous studies (Yamasaki *et al.*, 2002; Nagai and Makino, 2009). Differencing short- and

long-term A_{sat} response to temperature would probably improve crop model predictions, but regarding our results, a unique response to temperature might be good enough to describe wheat assimilation response to temperature. Comparing simulation of a model with a unique response or with a more precise consideration of time effect on assimilation response to temperature may help understanding the impact of accounting for acclimation in crop models.

3. At low temperature fully acclimated plants do not reach their maximum assimilation capacities

In order to maximize carbon uptake, we could hypothesize that carbon assimilation is maximum under current environmental conditions when plants are fully acclimated. However, *A*/*T* curves revealed that T_{opt} for wheat could be far from T_{growth}. T_{opt} was the closest to T_{growth} for T_{growth} between 28°C/24°C and 33°C/29°C. For lower T_{growth}, T_{opt} was always higher than T_{growth}. Some studies have already shown that the relationship between T_{opt} and T_{growth} is not a 1 to 1 relation (Yamasaki *et al.*, 2002; Yamori *et al.*, 2013; Zaka *et al.*, 2016). Yamori *et al.* (2013) also highlighted a divergence between T_{opt} and T_{growth} for many C3 plants, with T_{opt} being closer to T_{growth} around 25°C and an increase in T_{opt} of 0.49 $°C^{-1}$ per degree-Celsius increase in T_{growth} on average across C3 species for T_{growth} between 5°C and 45°C. Here, the increase of T_{opt} was 0.38°C (T_{opt} = 0.38 x T_{growth} + 19.9; r^2 = 0.86) per degree-Celsius increase in T_{growth} for T_{growth} ranging from 8°C/4°C to 33°C/29°C. Overall, at low temperature, even fully acclimated wheat plants do not reach their maximum photosynthetic capacities.

4. The acclimation of short-term response of assimilation capacity to temperature in not due to a regulation through stomatal conductance

Many cross-regulations exist between g_s and A_{sat}, which makes it difficult to disentangle the regulatory mechanisms (Wong *et al.*, 1979). In our study, g_s varied with both T_{growth} and T_{leaf}, it increased when T_{growth} increased from 8°C/4°C to 28°C/24°C and decreased for higher T_{growth}. This raises the question of a stomatal-driven response of A_{sat} to T_{growth}. Overall, the values of g_s reached here were in a usual range, as well as Ci/Ca ratio (from 0.54 ppm ppm^{-1} for T8 to 0.78 for T33), showing no constraint of the stomata on *A*sat (Farquhar and Sharkey, 1982; Flexas *et al.*, 2014).

However, in the A/T curves, an increase of T_{leaf} always resulted in a decrease of g_s, probably triggered by the increase of $VPD_{air\text{-}leaf}$ (Morison and Gifford, 1983; Streck, 2003). Leaf internal CO_2 was therefore reduced, which, coupled with a temperature-enhanced metabolism, could result in a limitation of A_{sat} by g_s (Long and Bernacchi, 2003; Flexas *et al.*, 2008). The C_i/C_a ratio decreased when T_{leaf} increased, indicating a decrease of CO_2 availability (Farquhar and Sharkey, 1982). However, the C_i/C_a decrease was essentially the same among the different T_{growth}; therefore the acclimation of A/T did not result from a limitation of A_{sat} by g_s. In Chapter 3, we used a coupled photosynthesis-stomatal conductance model to analyze the impact of g_s on A/T response curves and confirm this conclusion.

5. Two process driving acclimation to temperature

Our results showed a rapid acclimation of A_{sat} to a change of T_{growth} for a wide range of temperatures and in both directions of T_{growth} variation. A_{sat} of transferred plants reached the A_{sat} of plant fully-grown in the new conditions in less than 150°Cd in all tested changes of T_{growth}. Changes of A_{sat} were observed a few hours only after the change of T_{growth} from 13°C/9°c to 23°C/19°C. The acclimation of g_s and C_i/C_a was slower and the lower C_i/C_a and g_s compared to that of wheat plants fully-grown in the new condition could highlight a transient limitation of A_{sat} by CO_2 diffusion into the leaf. We can therefore conclude that neither g_s nor CO_2 diffusion limited A_{sat} and A_{sat} acclimation in this case was probably due to assimilation metabolism.

Different patterns of changes of A_{sat}, g_s and C_i/C_a were observed in response when T_{growth} was decreased. A_{sat} of plants transferred from 23°C/19°C to 13°C/9°C reached values lower than those of plants grown at 13°C/9°C from emergence in less than 4 h. Changes in g_s and C_i/C_a paralleled those of A_{sat} to lower values than those of plant grown at 13°C/9°C from emergence and then increased. This sharp decrease of in C_i/C_a reflected a limitation of A_{sat} by CO_2 diffusion during the initial response of A_{sat} to the decrease in T_{growth}. Only 15 °Cd (20 h) after T_{growth} change, A_{sat} increased faster than g_s and C_i/C_a, indicating that assimilation was not limited by CO_2 diffusion after the initial response and an acclimation of metabolism occurred.

Metabolism-driven acclimation of photosynthesis to temperature has often been reported in the literature (Medlyn *et al.*, 2002; Mäkelä *et al.*, 2004; Hikosaka *et al.*, 2006; Kattge and Knorr, 2007; Perdomo *et al.*, 2016; Scafaro *et al.*, 2017), with altered activation state of Rubisco or carboxylation capacities. The potential role of CO_2 diffusion in the response of photosynthesis to

temperature has already been mentioned (Flexas *et al.*, 2014). However, to our knowledge, no study has highlighted its potential role in assimilation response to a change of temperature, probably because of the difficulties to uncorrelate A_{sat} and g_s.

VI. Conclusion

Our study shows that assimilation responds quickly to a change of temperature. Two processes might be implicated in the response of assimilation to short and long-term temperature changes, with a dominant effect of metabolism in response to an increased temperature, and a limitation by the CO_2 diffusion in the other case. Our quantitative description of timing and magnitude of acclimation of wheat photosynthesis to changes of growth temperature provides a solid basis for crop models improvement.

Chapter 3: Model evidence of a metabolism driven acclimation of assimilation capacities to temperature

Model evidence of a metabolism driven acclimation of assimilation capacities to temperature

Maeva Baumont[1], Boris Parent[1], Bernard Genty[2], Bertrand Muller[1], Pierre Martre[1]

[1]LEPSE, Université Montpellier, INRA, Montpellier SupAgro, 34060 Montpellier, France

[2]BVME, CNRS, CEA, Aix-Marseille University, Saint-Paul-lez-Durance, France

---

This chapter will be coupled with Chapter 2 in view of latter submission.

I. Introduction

In the previous chapter, we studied the responses of photosynthesis to long and short-term changes in temperature. We concluded in : i) an acclimation of the response to temperature (A/T) to a new growth temperature (T_{growth}), through a modification of the optimal temperature (T_{opt}) and a modification of assimilation capacities at T_{opt} (A_{sat}^{opt}); ii) a rapid acclimation of the assimilation capacities at the growth temperature (A_{sat}^{growth}) to a change of T_{growth}, independently from the temperature range and/or from the direction of temperature variations.

However, stomatal conductance (g_s) largely varied with temperature changes, possibly affecting A/T curves. If it was the case, it would mean that these responses would not be robust but could change due to any condition affecting stomatal conductance. We also observed a possible effect of g_s on A_{sat} acclimation to a change of T_{growth}. Uncoupling g_s and A_{sat} could allow to better understand the underlying mechanisms of A_{sat} acclimation to temperature, possibly linked to g_s or other metabolic processes. However, the close relation between A_{sat} and g_s makes difficult to uncorrelate one from another in experimental conditions.

A strategy could be to use a photosynthesis model to test the impact of stomatal conductance on the observed responses to temperature and their acclimation. Most photosynthesis models are derived from the Farquhar-von Caemmerer-Berry model (thereafter called the FvCB model). They are generally used to simulated carbon assimilation at leaf level at short time step. The FvCB model simulates the response of carbon assimilation to temperature through the individual responses of the different underlying processes implied in carbon assimilation. Currently, the responses of these different processes are considered as independent from growth temperature in FvCB-derived models (Bernacchi *et al.*, 2001). However, most processes response to temperature depend on growth temperature, especially the variables linked to CO_2 carboxylation (Medlyn *et al.*, 2002; Yamori *et al.*, 2005; Kattge and Knorr, 2007; Perdomo *et al.*, 2016). Successful modelling of these responses at different T_{growth} have already been achieved using sink-based models, in which the response of assimilation to temperature can be easily included (Zaka *et al.*, 2016). Another method to model the impact of T_{growth} on the response of assimilation to temperature is to modify the parameters of an empirical response of assimilation to temperature as function of T_{growth}. For example, using the response of Yan and Hunt (1999) and changing T_{opt} and T_{max} regarding T_{growth}. This approach supposes to determine the parameters of carbon

assimilation T_{opt} and T_{max} for various T_{growth}, as we have done in Chapter 2. FvCB models were preferred here because of their mechanistic approach that allows combining a diffusional model to the photosynthesis model (Yin and Struik, 2009). A combined carbon assimilation and CO_2 diffusion model presented the opportunity to uncorrellate A_{sat} from g_s in various temperature conditions, and to answer the questions raised in the previous chapter.

Here in Chapter 3, a carbon assimilation model has been used to simulate photosynthesis independently or not from g_s, allowing to test the hypothesis of g_s-dependent or independent acclimation. We used a gas exchange model derived from the Farquhar-von Caemmerer-Berry model and developed by Yin and Struik 2009. Its particularity is that two equations able to predict carbon assimilation can be used: one using the measured g_s as an input, and another in which g_s is not part of the input and is calculated afterward from the simulated A_{sat}. It was used to i) simulate the short-term and long-term temperature effect on assimilation capacities; ii) test the interaction between g_s and A_{sat}; iii) discuss the properties and limits of the existing model to deal with acclimation of assimilation to temperature.

II. Model description

In this part, I describe the Farquhar-von Caemmerer-Berry model. The specific options / parameter values / hypotheses used in this study are detailed in ***bold / italics***

1. The Farquarh-von Cammerer-Berry model (Farquhar *et al.*, 1980)

The gas exchange model used here is the one developed in the crop model GECROS (Xinyou and Laar, 2005). It is derived from the Farquhar-von Caemmerer-Berry model (here after referred as the FvCB model), which considers that photosynthesis (A) is the minimum of the Rubisco carboxylation limited assimilation rate (A_c), and the electron transport limited assimilation rate (A_j) (Farquhar *et al.*, 1980; von Caemmerer, 2000; Bernacchi *et al.*, 2013):

$$A = \min(A_c, A_j) \quad (3.1)$$

A_j and A_c are calculated as a function of J_{max} (the maximal rate of electron transport) and Vc_{max} (the maximal rate of carboxylation) with respectively:

$$A_j = \frac{(C_c - \Gamma_*)J}{4C_c + 8\Gamma_*} - R_d \quad (3.2)$$

$$A_c = \frac{(C_c - \Gamma_*)Vc_{max}}{C_c + K_{mC}(1 + {}^{O}/_{K_{mO}})} - R_d \quad (3.3)$$

Where C_c is the Rubisco-carboxylation site CO_2 concentration (ppm), K_{mC} and K_{mO} are respectively the Rubisco CO_2 and O_2 Michaelis-Menten constant, and Γ_* is the CO_2 compensation point without mitochondrial respiration (R_d). J is the electron transport rate (µmol de photons m^{-2} s^{-1}) for the incoming light intensity. ***Measurements carried out here were all obtained at saturating light, we then considered*** $\boldsymbol{J = J_{max}}$.

R_d and variables linked to the kinetic properties of Rubisco (K_{mC} and K_{mO}) depend on temperature and are estimated with an Arrhenius equation normalized in regards to their values at 25°C:

$$Parameter = Parameter_{25} \times e^{\frac{(T-25)E}{[298.R(T+273)]}} \quad (3.4)$$

Where T is the temperature expressed in °C (***here, the leaf temperature***), E is the activation energy defining the responsiveness of the target parameter to temperature, and R is the universal gas constant. J_{max} and Vc_{max} are obtained through a modified Arrhenius equation (accounting for a decrease from a given temperature T) with:

$$Parameter = Parameter_{25} \times e^{\frac{(T-25)E}{[298.R(T+273)]}} \times \frac{1 + e^{\frac{(298.S-D)}{298.R}}}{1 + e^{\frac{(T+273)S-D}{R(T+273)}}} \quad (3.5)$$

Where S is the entropy, D is the energy of deactivation, defining the responsive shape of the supra- optimal temperature range. ***The S, E, D and parameter values at 25°C used here for each parameter are given in table 3.1. The used values were the one considered constant for every C3 species, according to Bernacchi et al. (2003).***

Γ_* depends on the O_2 air concentration (O) and on the Rubisco CO_2/O_2 specificity factor ($S_{c/o}$) with:

$$\Gamma_* = \frac{0.5O}{S_{c/o}} \quad (3.6)$$

Where the factor 0.5 is the fraction of mole of released CO_2 when Rubisco catalyzes 1 mole of O_2 during photorespiration. $S_{c/o}$ also depends on temperature following equation 3.4.

Since J_{max} and Vc_{max} depends on the enzyme concentration, J_{max25} and Vc_{max25} are defined in the model through the leaf-nitrogen content (N_{leaf} in g leaf^{-1}), each one following a specific linear relationship:

$$J_{max25} = 99.38 \times N_{leaf} + 5.75 \quad (3.7)$$

$$Vc_{max25} = 30.40 \times N_{leaf} + 4.36 \quad (3.8)$$

The constant values used here are issued from Yin et al. (2009).

The A_c and A_j part of the FvCB model can be written in a common way with:

$$A = \frac{(C_c - \Gamma_*)x_1}{C_c + x_2} - R_d \quad (3.9)$$

Where, for the Rubisco-limited part:

$$x_1 = Vc_{max} \quad \text{and} \quad x_2 = K_{mc}(1 + {}^{O}/_{K_{mO}}) \quad (3.10)$$

And for the electron transport-limited part:

$$x_1 = J/4 \quad \text{and} \quad x_2 = 2\Gamma_* \quad (3.11)$$

The original FvCB model initially used the intercellular CO_2 level (C_i) in place of the C_c in equation 3.9. In the leaf, CO_2 needs to pass through several layers of resistances (these resistances are estimated with their numerical inverse, giving the conductance) to reach the site of carboxylation located in the chloroplasts in the mesophyll cells. From ambient air to the chloroplasts, there is first the boundary layer diffusional conductance (g_b), then the stomatal conductance (g_s) and the mesophyll-component conductance (g_m). The two first components give the drawdown of C_i relatively to C_a (ambient CO_2 level). g_s was for long considered as the most important component limiting CO_2 diffusion in the leaf and C_c and C_i were considered equal; but g_m is now known to be important enough to trigger a significant drawdown of C_c relative to C_i (Flexas *et al.*, 2014). G_m responds to temperature and probably to irradiance and CO_2 air concentration (Bernacchi, 2002; Terashima *et al.*, 2006; Flexas *et al.*, 2008). Because of the lack of knowledge on the two last variables (irradiance and CO_2 air concentration), g_m is estimated through temperature only with equation 3.5. C_c is then calculated according to the Fick's first law of CO_2 diffusion along the leaf layer, which indicates that the molar flux due to diffusion is proportional to the concentration gradient:

$$C_c = C_a - \frac{A}{g_s} - \frac{A}{g_m} \quad (3.12)$$

Yin and Struik, 2009 developed an analytic solution to Eq. 3.9:

$$A^3 + pA^2 + qA + r = 0 \quad (3.13)$$

Solution of this equation can be found in Yin and Struik (2009).Two solutions to this equation are possible. The first one is using g_s as an input, while the second one combined a diffusion model to the photosynthesis model, allowing a simulation of g_s without inquiring g_s.

2. Coupled modelling of photosynthesis and diffusional conductance (Yin and Struik, 2009)

The diffusional conductance model is based on the Fick's first law of diffusion, allowing calculation of the different conductance and CO_2 concentration. Combining equation 3.9 to 3.12 gives:

$$C_c = \frac{x_1.\Gamma_* + x_2(A+R_d)}{x_1 - A - R_d} \quad (3.14)$$

Where x_1 and x_2 are determined according to the limiting process (A_c or A_j). Then:

$$Ci = C_c + \frac{A}{g_m} \quad (3.15)$$

And finally:

$$g_s = g_0 + \frac{(A+R_d)\times f(VPD)}{Ci - Ci_*} \quad (3.16)$$

Where g_0 is the residual stomatal conductance at extremely low light, Ci_* is the Ci compensation point in the absence of R_d ($Ci_* = \Gamma_* - {R_d}/{g_m}$), and $f(VPD)$ is a function translating the effect of VPD on g_s. This effect of VPD on g_s is not yet fully understood and is described empirically through:

$$f(VDP) = \frac{1}{\frac{1}{a - bVPD} - 1} \quad (3.17)$$

In this Chapter, we used the FvCB model combined with the diffusional model in order to test our hypotheses of gs-limited / gs-non-limiting response of assimilation to temperature in regard to acclimation.

III. Material and Methods:

1. Growth conditions

Experimental data comes from the experimentations described in Chapter 2. We used only a few treatments among the numerous ones described in the last chapter, here reported in table 3.1.
For details of the growing conditions, gas exchange measurements and thermal time calculation, please refer to the Chapter 2 Material and Methods.

2. Model parametrization

a. Constant parameters

The parameters used in the model were all coming from previous studies of Yin XY working group. The energies of activation, deactivation and entropy terms associated to the g_m, K_{mC}, K_{mO} and Rd calculation, as well as the values of some parameters at 25°C, can be considered constant for C3-species (Bernacci et al., 2002) and these constants were therefore used here. Values of other parameters specific to the species were issued from previous studies by Yin working group on wheat (Yin *et al.*, 2009). All these constant parameters are resumed in table 3.2.

b. Nitrogen leaf content optimization

We considered that N_{leaf} acclimated to the growth temperature. N_{leaf} content was optimized so that the simulated *A* could fit A/T data measured on leaf 5 of treatments T8, T13, T18, T23, T28 and T33 (see table 3.1). N_{leaf} values for each treatment are exposed in Table 3.3. N_{leaf} was considered stable regardless of the leaf rank and the plant age.

3. Model use and evaluation

To test our hypothesis, the model was used to simulate A_{sat} in our experimental conditions. A_{sat} was either simulated with our measured variables as input (C_a, light intensity, growth and leaf temperature, VPD; as well as g_s and C_i); or without g_s and C_i as input, and they were then calculated afterward according to equation 3.14 to 3.16; or with a constant imposed g_s. The

Table 3.1: Layout and environmental conditions for the three experiments carried out in this study. PAR, photosynthetic active radiation; PTQ, photothermal quotient; A_{sat}, leaf carbon assimilation rate at saturating light, T_{leaf}, leaf temperature; and T_{growth}, growth temperature.

Treatment Name	Set point day/night air temperature (°C)	Set point PAR (µmol m^{-2} s^{-1})	Average daily PAR (mol m^{-2} d-1)	Average daily thermal time (°C)	Average daily PTQ (mol m^{-2} °Cd)	Measured variable	
						A_{sat}	A_{sat}/T_{leaf}
T8	8/4	125	6.27	7.20	0.87	X	
T13	13/9	250	11.53	11.65	0.99	X	
T18	18/14	320	16.32	16.05	1.02	X	
T23	23/19	415	20.65	20.24	1.02	X	
T28	28/24	450	22.92	25.33	0.90	X	
T33	33/29	610	30.91	31.60	0.98	X	
13LL	13/9	250	11.39	11.82	0.96	X	X
23HL	23/19	400	20.56	21.27	0.97	X	X
13LL-> 23HL	13/9->23/19	250 -> 400	12.49 -> 20.56	11.26 -> 21.27	0.96 -> 0.97	X	X
23HL-> 13LL	23/19->13/9	400 -> 250	20.56 -> 12.49	21.27 -> 11.26	0.97 -> 0.96	X	

simulated A_{sat} values were then compared to the measured A_{sat} values. The model performances were evaluated by calculating the mean squared error. If $\hat{Y}$ is a vector of n predictions generated on a data set of *n* observation, and *Y* is a vector of observed values of the variable being predicted:

$$MSE = \frac{1}{n}\sum_{i=1}^{n}(Y_i - \hat{Y}_i)^2 \qquad (3.18)$$

IV. Results:

1. The different acclimated responses to temperature observed in Chapter 2 could not be simulated by the model without including specific acclimation processes.

The responses of assimilation to temperature (A/T) for plants grown at various growth temperatures have shown different T_{opt} and A_{opt}, as well as different T_{min} and T_{max} (see chapter 2, and Fig 3.1A), indicating an acclimation of A/T to T_{growth}. We first tried to simulate these different responses of assimilation to temperature with the model, in order to test if these differences could come from different assimilation capacities trigger by different N_{leaf} only.

Simulation of these A/T curves with the model showed changes of A_{sat}^{opt} depending on growth temperature but no change of T_{opt} (Fig. 3.1B; and Fig. 3.2 A and B). The predicted T_{opt} were similar regardless of T_{growth}, resulting in over-estimated T_{opt} for all treatments excepted for plants grown at 23°C (T23), for which simulated T_{opt} was similar to the measured value (Fig. 3.2A). Simulations showed changes of A_{sat}^{opt} with T_{growth}, with an increase of A_{sat}^{opt} from T8 to T28 and then a decrease (Fig 3.1B), in the same way as observed response curves. However, the estimated A_{sat}^{opt} were always higher than observed values (Fig. 3.2B). Simulated A_{sat} at growth temperature was under-estimated for T_{growth} from 8/4°C (T8) to 23/19°C (T23), and was well predicted for T28 and T33 (Fig. 3.2C).

The predicted acclimation of A_{sat}^{opt} to growth temperature was due to the optimization of N_{leaf} in each treatment. Indeed, prediction of A/T without optimization of N_{leaf} resulted in similar response curves in all treatments (Fig. 3.1C).

Table 3.2: Parameters values used in the photosynthesis models

Parameter		Unit	Value	Comments
Vcmax	Ea	J mol^{-1}	87700	
	DEa	J mol^{-1}	203500	
	S	J K^{-1} mol^{-1}	6550	
Jmax	Ea	J mol^{-1}	87700	
	DEa	J mol^{-1}	203500	
	S	J K^{-1} mol^{-1}	6550	
Gm	Ea	J mol^{-1}	49600	
	DEa	J mol^{-1}	437400	
	S	J K^{-1} mol^{-1}	1400	
	Gm25	µmol m^{-2} s^{-1}	180	Mesophyll conductance at 25°C
Gb		µmol m^{-2} s^{-1}	1500	Combined boundary and turbulence layer conductance
O		mbar	210	Oxygen partial pressure of the air
KmC	KmC25	µbar	272.38	Values of the Michaelis-Menten constant for C at 25°C
	Ea	J mol^{-1}	80990	
KmO	KmO25	µbar	165.82	Values of the Michaelis-Menten constant for C at 25°C
	Ea	J mol^{-1}	23720	
Sco25		µbar $µbar^{-1}$	2.8	Relative CO2/O2 specific factor for Rubisco at 25°C
f(VPD)	a	-	0.85	
	b	kPa^{-1}	0.14	

Table 3.3: Optimized leaf nitrogen conten for each growth temperature

Treatment	Leaf nitrogen content (mg g^{-1})
T8	2.72
T13	2.72
T18	2.49
T23	2.62
T28	2.73
T33	2.38

Overall, the model was not able to predict the observed acclimation of T_{opt} and A_{sat}^{opt} to T_{growth} indicating that acclimation was not due to the changes of Vc_{max25} only (trigger in the model through changes in N_{leaf}), tested here by optimizing N_{leaf}.

2. The model indicated that the observed responses to temperature were not due to a limiting stomatal conductance

The model was used to simulate the response of A_{sat} to leaf temperature (A/T) for wheat plants grown at 28/24°C (treatment T28, see Table 3.1) either using the measured g_s as an input, or g_s calculated afterward (see Model description). Both equations resulted in similar response curves (Fig 3.3A). Despite a slight underestimation of A_{sat} for the lower and higher T_{leaf}, both models were able to simulate the observed pattern for this treatment.

The measured g_s showed values up to 1000 µmol m^{-2} s^{-1}, and the calculated g_s values were almost always lower (Fig 3.3B). This indicates that for such range of values, stomatal conductance did not influence the assimilation response to temperature observed at this T_{growth}.

This result was verified in the other thermal treatments. We simulated A/T curves with or without the measured g_s as input, for wheat plants grown at several T_{growth}; 13/9°C (T13), 23/19°C (T23) or 33/29°C (T33). These data showed large variations of g_s. However, the predicted A/T did not describe well the experimental responses for all T_{growth} (Fig 3.4A to C). For T33, the model fitted well the experimental observations with only an underestimation of A_{sat} at the higher T_{leaf} (Fig 3.4C). For T23, the model also underestimated A_{sat} at the lower and higher T_{leaf}, and over-estimated assimilation at optimal temperature (A_{sat}^{opt}) (Fig. 3.4B). For T13, A_{sat}^{opt} was also over-estimated and predicted values at low T_{leaf} were underestimated, but the higher discrepancy between simulated and observed values was the over-estimation of T_{opt} (Fig 3.4A).

For all growth temperatures, the predictions using or not the measured g_s as an input did not differ. Even for larger range of measured stomatal conductance (from 50 µmol m^{-2} s^{-1} in T13 to more than 1000 µmol m^{-2} s^{-1} in T28) (Fig 3.4D and 3.3B), the model predicted that stomata did not limit the assimilation responses to temperature. Calculated g_s response to temperature followed a bell shape curve for every T_{growth}, similarly to the responses of assimilation. The calculated g_s was always lower than the measured values for all treatments at low T_{leaf}, but reached the observed

values for T23 and T33 at higher T_{leaf} (Fig 3.4 E to F). At T13, Simulated g_s values were largely above the measured values at higher T_{leaf} (Fig 3.4 D).

Overall, the fact that the predicted A_{sat} values did not differ between the two options, despite this large difference between calculated and measured g_s indicated that gs was probably not limiting in these conditions.

3. The model does not simulate the rise of assimilation capacities with plant development

Assimilation capacities increased with plant development in all tested environmental conditions (see chapter 2). We compared the observations of A_{sat} for treatment 23HL (T_{growth} = 23/19°C) with simulations of the model. N_{leaf} was optimized for each T_{growth} based on the response of A_{sat} of leaf 5 to temperature and was considered constant regardless of leaf number or plant age. The model predicted a constant A_{sat} regardless of plant age and was therefore not able to describe the ontogenic changes of A_{sat} (Fig 3.5).

It resulted that simulated A_{sat} values were closer to the detrended A_{sat} values (see chapter 2 for more detail) than to the raw values (Fig. 3.5). Hereafter, for comparing simulated and observed time courses of assimilation, we use therefore the detrended A_{sat} values.

4. The current model is able to simulate the quick change of assimilation capacities to a rapid change of growth temperature but not the long term acclimation to growth temperature.

Results from Chapter 2 highlighted a quick acclimation of A_{sat} to a change of T_{growth}, regardless the considered change of temperature, from 8/4°C to 33/29°C, and the direction of variation. We tested if the model was able to simulate these observed rapid changes. Here, we used only the results from the third experiment presented in Chapter 2 since it presented the most important number of measurements over time, with the two directions of temperature variation. In this experiment, plants were grown at either 13/9°C (treatment 13LL) or 23/19°C (23HL). Half of the plants of each treatment were swapped between the two T_{growth} at Haun Stage = 3.5 (leaf 4

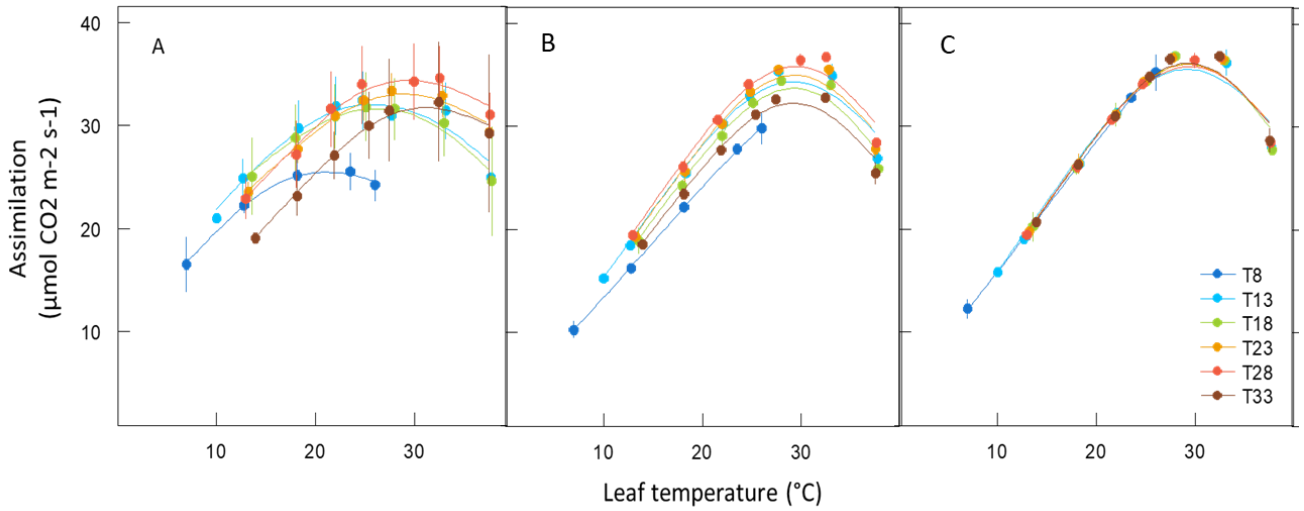

Figure 3.1: Assimilation at saturating light measured (A), simulated with leaf-nitrogen content dependent optimized for each growth temperature (B) or simulated with an identical leaf-nitrogen content (C) response to leaf temperature. Observed data were measured for the spring wheat cultivar Paragon grown at several temperature. Data are mean ± 1 s.d for *n* = 3 independent replicates.

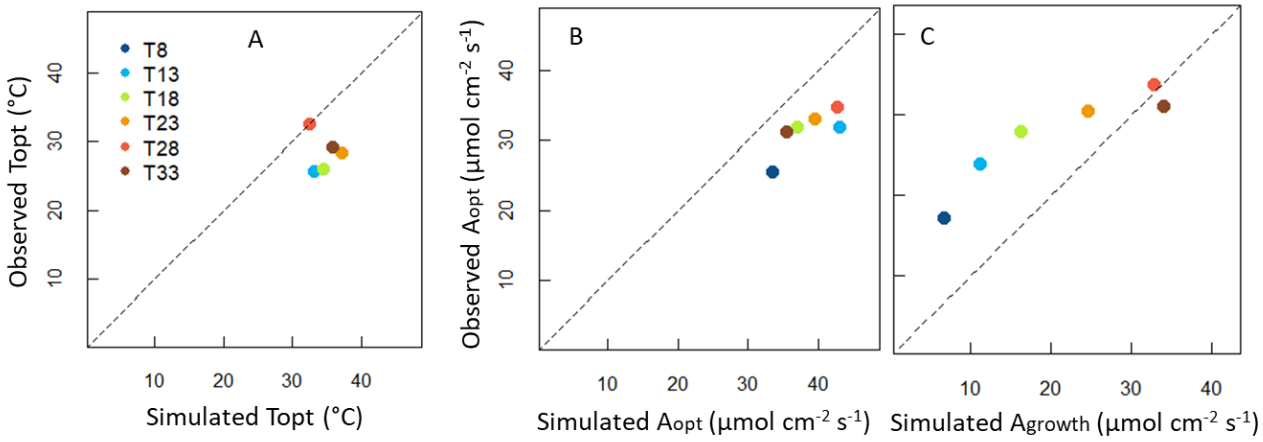

Figure 3.2: Relation between observed and simulated optimal temperature (Topt) of the assimilation response to leaf temperature (A), assimilation capacities at the Topt (B), and assimilation capacities at the growth temperature (C) for spring wheat cultivar Paragon grown at 6 different growth temperature. Simulations were made with the measured g_s as an input. Dotted lines are the 1:1 linear relation. Data are mean ± 1 s.d for *n* = 3 independent replicates.

reaching half of the length of the leaf 3), resulting in treatment 13LL.23HL and 23HL.13LL. We hypothesized that N_{leaf} acclimated to T_{growth} for leaf at least partially developed at the new T_{growth}. Therefore, for simulations, N_{leaf} values of transferred plants were considered unchanged for leaf 3 (*i.e* the value was the one optimized for the T_{growth} before the transfer). For leaf 4 and 5, the considered N_{leaf} was the one optimized for the new T_{growth}.

The observed values of A_{sat} acclimated in less than a few hours, regardless the direction of variation. The model was able to predict this quick change of A_{sat}, with A_{sat} immediately reaching A_{sat} predicted for plants fully grown in the new T_{growth} (Fig. 3.6A and B). However, as seen in figure 3.2C, the simulated A_{sat} at T_{growth} was under-estimated, especially for T_{growth} = 13/9°C. Thus, the model was predicting a quick acclimation of A_{sat}, but values diverged from observed A_{sat} values (Fig. 3.6A and B).

Overall, the model simulated a rapid change of assimilation capacity with a change of temperature, as that observed in Chapter 2. Since no effect of T_{growth} is accounted in the used model except through N_{leaf}, and considering that the quick change was predicted immediately after the change (so when N_{leaf} was still considered unchanged), we can say that this quick change of assimilation was due to the direct effect of temperature on metabolism and was not due to acclimation. But long-term predicted values were far from those observed. As observed with A/T curves at different T_{growth}, this model is not able to simulate the real acclimation process, i.e, a long-term change in A_{sat} due to new growth temperature. The model simulate the quick change of assimilation, but do not simulate acclimation to long-term temperature.

5. Simulation of assimilation capacities shows that stomatal conductance does not drive the acclimation of assimilation capacities to a change of growth temperature

Our measured data also showed different responses of g_s to a change of T_{growth}, with g_s of plants transferred from cold to warm slowly acclimating to reach the value of plant fully grown in the new growth condition (more than 100°Cd) (Fig 3.6C), while g_s of plants transferred from warm to cold immediately dropped to a lower value than plants fully grown in the new growth condition (Fig 3.6D). We hypothesized that two processes drive the changes of A_{sat} with a change of T_{growth};

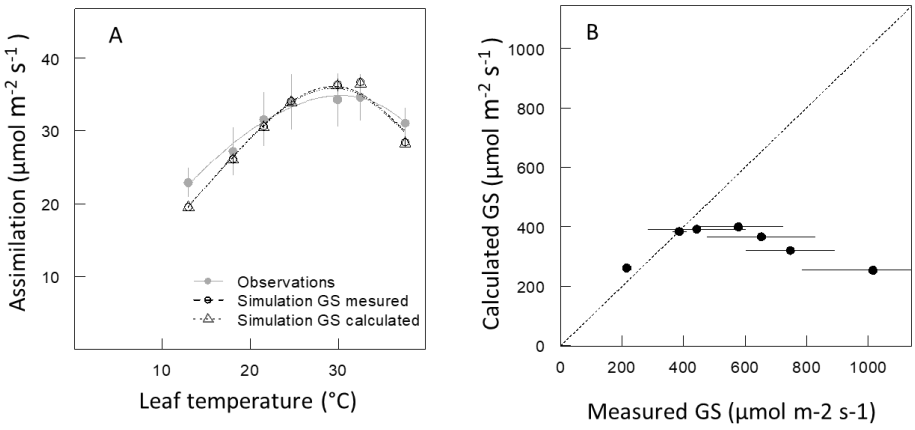

Figure 3.3 : Measured or predicted with our without accounting for stomatal conductance carbon assimilation at saturating light response to leaf temperature (A) and the relation between the measured and calculated (Eq. 3.14) stomatal conductance (B) for spring wheat cultivar Paragon grown at 28/24°C (treatment T28). **A**: A/T measured (grey full line, closed circle), predicted with GS as an input with Eq. 3.10 (dashed open circles) or predicted without accounting for g_s (dotted line, open triangles). Simulation of A with or the measured g_s as an input are similar and are so superposed on the figure. N_{leaf} = 2.92 g leaf^{-1}. Lines are non-parametric equation fitted to the data (spline). **B:** Relation between measured and calculated GS with Eq. 3.14. Data are mean ± s.d for *n* = 3 replicates.

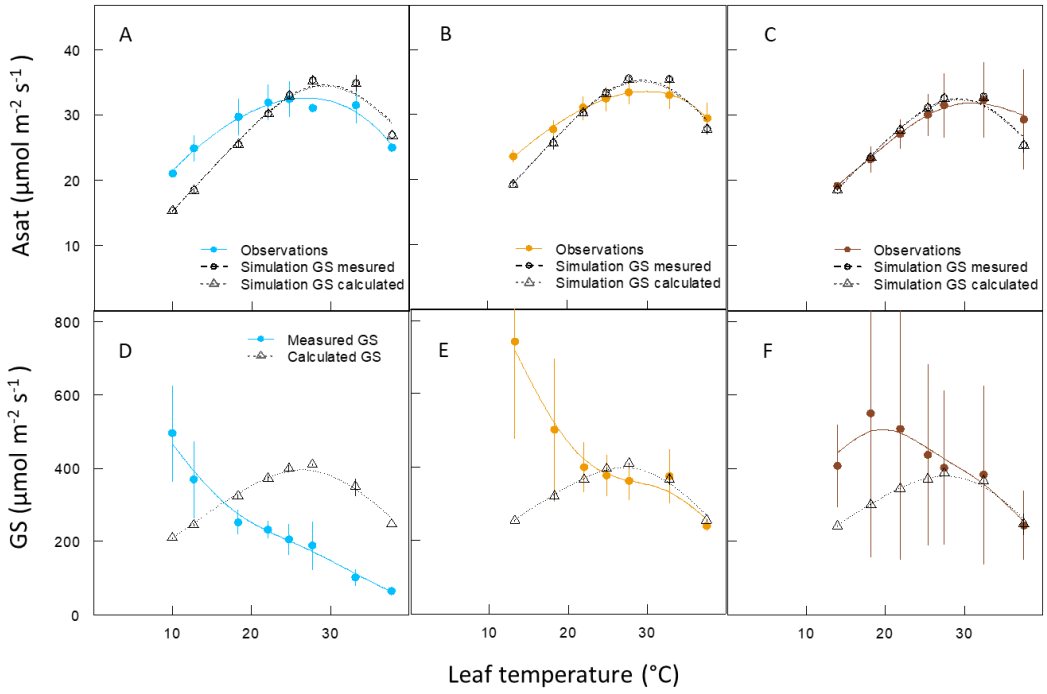

Figure 3.4: Measured or predicted with our without accounting for stomatal conductance carbon assimilation at saturating light response to leaf temperature (A to C), and measured or calculated stomatal conductance (D to F) response to leaf temperature for spring wheat cultivar Paragon grown at three different temperatures: 13/9°C (A and D ; T13), 23/19°C (B an E ; T23), or 33/29°C (C and F ; T33). **A to C:** A/T measured (grey full line, closed circle), predicted with GS as an input with Eq. 3.10 (dashed open circles) or predicted without accounting for GS with Eq 3.11 (dotted line, open triangles). Lines are non-parametric equation fitted to the data (spline). **D to F:** Measured (full colored lines, closed circles) or calculated with Eq 3.14 (dotted line, open triangles) stomatal conductance response to leaf temperature. Data are mean ± 1s.d for n=3 independent replicates.

one driven by the response of photosynthesis metabolism to temperature, and another by the response of stomatal conductance to temperature. This hypothesis was tested by simulating A_{sat} first with the measured g_s, then with an imposed g_s of 500 µmol m^{-2} s^{-1}, and finally without inquiring g_s as input of the model. All three sets of simulations resulted in similar A_{sat} values (Fig. 3.6A and B). Calculated g_s were lower than the observation, especially for T_{growth} = 23/19°C (Fig 3.6C and D) in which the calculated g_s was more than two times lower than the measured g_s. It indicated that g_s probably did not limit A_{sat} after these changes of temperature.

V. Discussion

1. Using a photosynthesis model allowed to test hypotheses about assimilation capacities response to temperature

a. Stomatal conductance did not drive the response of assimilation capacities to leaf temperature

The close correlation between g_s and A_{sat} makes difficult to uncorrelate one from another in experimental conditions (Nijs *et al.*, 1997; Del Pozo *et al.*, 2005). However, to be able to understand the mechanisms driving the responses of assimilation capacities to temperature and to temperature change, it was important to estimate the impact of g_s on assimilation. Ecophysiological models are a great tool to estimate the impact of a processes or an environmental variable on other processes (Ball *et al.*, 1987; Bernacchi *et al.*, 2013). Here, using a photosynthesis model combined with a diffusional model developed by Yin and Struik (2009), we showed that the observed changes of A/T with T_{growth} were probably not constrained by g_s. The observed results are therefore probably the result of the direct effect of temperature on enzyme activity, especially Rubisco (Medlyn *et al.*, 2002; Bernacchi *et al.*, 2003; Hikosaka *et al.*, 2006).

b. Quick acclimation to a change in growth temperature is due to the effect of temperature on metabolism

Results from Chapter 2 on the responses of assimilation capacities to a change of T_{growth} revealed two possible underlying processes of acclimation of photosynthesis to temperature: a control of A_{sat} when temperature decreased triggered by a decrease of gs, and an increase of A_{sat} with increasing temperature controlled by the temperature-enhanced metabolism. Here we first show

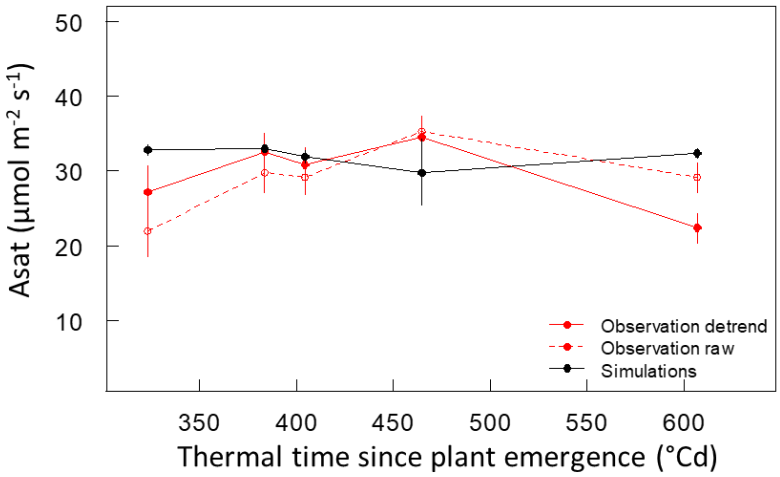

Figure 3.5: Time course of measured raw (dotted red line, open red circles), detrended (red line, closed circles) or predicted with GS as an input assimilation (black full line, closed black circles).

that this quick acclimation can be described by the current model, independently from the stomatal conductance. Since these results were obtained at saturating light, this indicates that the response of assimilation capacities to a change of T_{growth} was here again a result of the effect of temperature on the metabolism. However, it also indicated that the model could not explain the effects of long-term temperature, and that a probable acclimation of Vc_{max} to growth temperature needs to be taken into account.

Overall, these results confirm that the temperature-driven metabolism is the major underlying process of photosynthesis response to temperature, as it was already exposed by Law and Crafts-Brandner (1999); or Hikosaka *et al.* (2006).

2. Improving model simulation of the response of assimilation capacities to the temperature

The simulation of the response of A_{sat} to leaf temperature for wheat plants grown at different T_{growth} did not reflect the observed acclimation of T_{opt}. Thus, this acclimation of A/T to T_{growth} is a well-recognized behavior among plant species (Yamori *et al.*, 2013; Zaka *et al.*, 2016). Models need to better take into account this acclimation to be more performant.

In the model used here, the only effect of T_{growth} on assimilation capacities prediction was through the optimization of N_{leaf} to T_{growth}. Adapting N_{leaf} allowed modifying J_{max25} and Vc_{max25} according to the growth temperature. But the general shape of the Vc_{max} and J_{max} response to temperature were not modified. However, Vc_{max} response to temperature has already been shown to depend on T_{growth} especially through a modification of the curvature of the K_{mC} and K_{mO} relation to temperature (Kattge and Knorr, 2007). Including an effect of T_{growth} on the estimation of this variable could help improving the A/T acclimation to T_{growth}.

Another solution was recently proposed by Yin *et al.*, (2018) with a more mechanistic approach. This study is based on the reallocation of leaf nitrogen among photosynthetic protein (chlorophyll, electron transport system, Rubisco…) in response to an environmental change. They found that the optimal nitrogen partitioning involves a great investment in Rubisco under environment limiting the metabolism (e.g. low temperature), and to the opposite, the nitrogen partitioning was more directed to the chlorophyll when the energy supply was limiting (low light). This method allows predicting the rise of T_{opt} with T_{growth}.

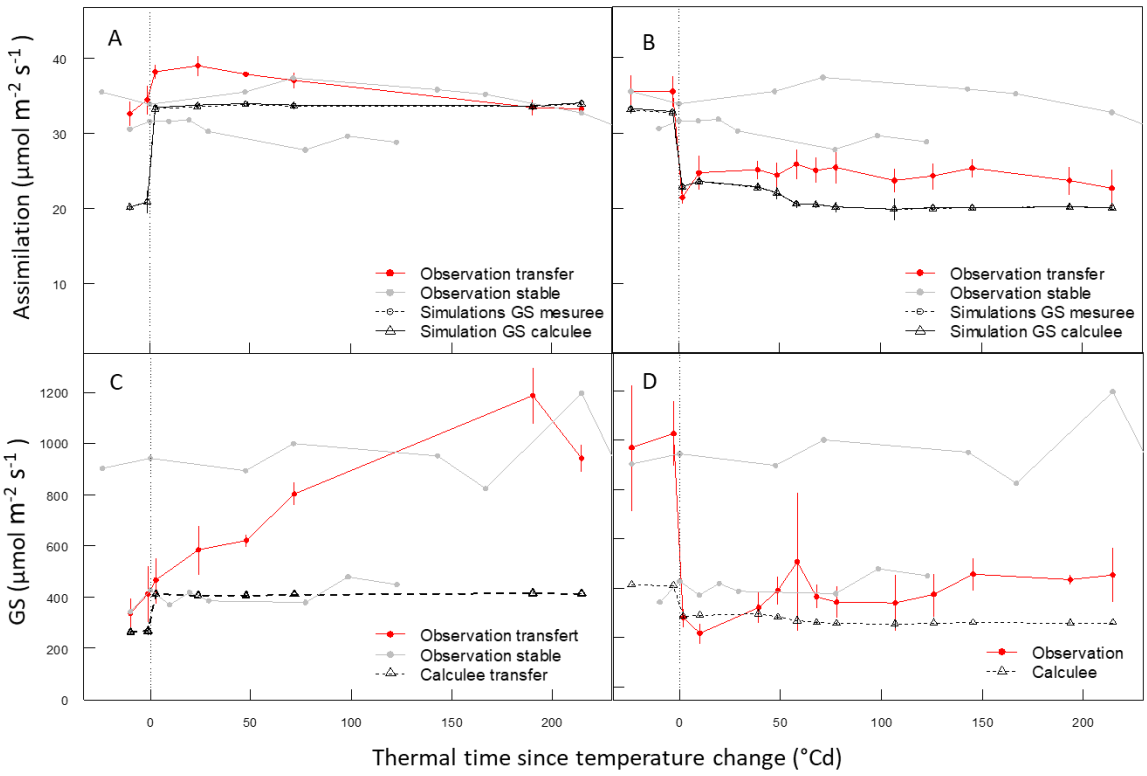

Figure 3.6 : Time course of measured (red line), predected wtih GS as an input (dashed black liene) or predicted without GS (dotted black line) leaf carbon assimilation (A and B); and stomatal conductance measured (red line) and calculated (dotted black line) (C and D) evolution in response to a change of growth temperature from 13/9°C to 23/19°C (A and C) or from 23/19°C to 13/9°C (B and D). Grey lines are carbon assimilation or stomatal conductance measured for the stable treatments 13LL (13/9°C) and 23HL (23/19°C).

3. The considered time scale reveals different needs on the consideration of acclimation assimilation capacities to temperature

When assimilation response to temperature is studied at the minute time scale, it presents different T_{opt} and A_{sat}^{opt} according to the growth temperature. The model was not able to predict such changes. However, the model predicted that assimilation capacities reached final values in a few hours only, as observed experimentally. This indicated that even if the model was not able to predict the responses of assimilation capacities to temperature change at a minute time-scale, it was sufficient to predict the observed change in assimilation capacities response to temperature changes at a several hours' time-scale. Thus, considering acclimation in models might not necessarily improve their predictions. We make the conclusion here that the higher the considered time-scale is, the less photosynthesis models need to be precise on their differentiation between leaf and growth temperature. The importance of choosing an appropriate time step for the prediction of assimilation capacities response to environment changes was also raised by Yin *et al.* (2018). Kirschbaum *et al.* (1997) showed a Rubisco-related activity change of 40 min, which could be a good basis to consider the full acclimation of assimilation capacities to temperature.

VI. Conclusion

The use of a FvCB –derived model combined with a diffusional model allowed us to answer the question rise in Chapter 2. We thus determined that: i) g_s is not limiting the assimilation response to short- and long-term change in temperature; ii) metabolism-related response to temperature is the underlying processes of assimilation capacities response to temperature. It also allowed to highlight the need of considering several time scale of temperature in assimilation and its underlying processes response to temperature to improve photosynthesis model predictions.

General discussion

The aim of my thesis was to improve crop model predictions by relying on less-empirical equations and by incorporating the effects of thermal history on plant processes. For both the effects of temperature changes on leaf appearance rate and carbon assimilation, we first used an experimental approach to build an ecophysiological hypothesis. Then, this hypothesis was challenged with the use of a model. Overall, this work brings new knowledge on plant responses to short and long-term changes of temperature. The hypothesis of carbon-driven leaf appearance rate was experimentally studied in Chapter 1 and used to improve a crop model evaluated in various field conditions. In Chapter 2, an experimental approach was built to study carbon assimilation response to long and short term changes of temperature. Based on this experimental work, several hypotheses were formulated and tested by simulation using a Farquhar-von Caemmerer-Berry (FvCB) type model (Chapter 3). In this last chapter of this thesis, I summarize the main findings of this work and then propose some perspectives for crop model improvement.

I. Leaf appearance rate is carbon limited

One of the major results of this thesis is the demonstration of a carbon limitation of leaf appearance rate in wheat. Since the source and sink processes linked to the hypothesis of carbon-limited development rate are common to all plants, we could hypothesize that this model can be generalized to other species. For instance, evidences of the effect of irradiance, temperature and plant density on leaf appearance rate have been reported for maize (Birch et al., 1998; Bos et al., 2000) and sorghum (Clerget et al., 2008).

The hypothesis of a carbon limitation may also apply for other plant development processes, which could be modelled with a formalism similar to that proposed in Chapter 2 for leaf appearance rate. For instance, tillering in sorghum has been shown to depend on internal plant competition for assimilates (Kim et al., 2010). The experimental approach used in this work with a factorial of environmental constraints to analyze leaf appearance rate could be adapted to analyze the environmental, developmental and trophic controls of the timing and rate of tiller appearance or senescence.

Our model of leaf appearance rate is closer to the underlying biological processes compared with simplistic linear models or models that consider empirical relationships between the latitude

and/or sowing date and the rate of leaf appearance (such as the model SiriusQuality before my thesis). Among the 15 wheat genotypes studied here, the intercept of the relationship between leaf appearance rate and photothermal coefficient was significantly different but not the slope. In our study, the other parameters of the model were considered constant and the values determined in control conditions were used to model leaf appearance rate in the field for both winter and spring cultivars. Further work is required to quantify the genetic variability of all parameters of the model. This step will be important to study the genetic mechanisms of leaf appearance rate but also to parametrize the model for new genotypes.

II. The fast change of photosynthesis after a change of growth temperature is driven by metabolism

This work precisely describes several responses of carbon assimilation to temperature. We distinguished several time-steps for the response of carbon assimilation to temperature. The first one is the response of assimilation to instantaneous temperature. The change of temperature is here at a minute time-scale, and the response is considered non-acclimated. Another response follows a change of growth temperature. Our results show that a change in growth temperature triggers a change of assimilation capacities within a few hours, with the new assimilation immediately reaching values of plants fully grown at the new temperature. This response to an hour time-step change in temperature are so not considered as acclimation *per se*, but as a direct effect of temperature on the underlying processes. Finally, there is an acclimation of assimilation to longer-term changes of temperature, meaning the assimilation of plant fully grown or grown after long-term changes at contrasted temperature.

We confirmed the existence of an acclimation of the short-term response of assimilation to temperature, with a modification of optimum temperature (T_{opt}) and assimilation at this temperature (A_{opt}^{sat}) over a large range of growth temperature (T_{growth}). The relation between T_{opt} and T_{growth} was linear but the increase of T_{opt} when T_{growth} increased was less important than previously reported for other C3 species (Yamori et al., 2003). Finally, we showed that the response of wheat plants to changes of temperature changed within a few hours.

Our experimental data and simulations using a FvCB-type model demonstrated that the short-term (non-acclimated) response of A_{sat} to temperature is not constrained by g_s, nor is A_{sat} response to a change of T_{growth}. We concluded that A_{sat} response to temperature is mainly driven by the direct effect of temperature on metabolism. These results thus indicate that including acclimation response of A_{sat} response to temperature to T_{growth} could improve photosynthesis model predictions (Thornley, 1998; Smith and Dukes, 2013; Perdomo *et al.*, 2016; Stinziano *et al.*, 2018; Yin *et al.*, 2018).

In the model used in Chapter 3, the only considered impact of T_{growth} was through a modification of N_{leaf} with T_{growth}, resulting in an insufficient acclimation of A_{satopt}. Yin et al (2018) proposed that N_{leaf} allocation between underlying processes of photosynthesis was modified by an environmental change. The proposed model was able to predict the acclimation of A_{sat} response to temperature to T_{growth}. Another solution has been proposed by Kaggde and Knorr (2007) with an empirical modification of Vc_{max} and J_{max} response to temperature with T_{growth}. A further work would be to evaluate the acclimation of Vc_{max} and J_{max} proposed by Kaggde and Knorr (2007) in the model used in this work. However, these authors considered T_{growth} as the mean temperature over the last 30 days, while our work highlights an acclimation of A_{sat} to T_{growth} within a few hours. Overall, the time step to consider in order to represent changes of T_{growth} needs to be tested in further model simulations.

III. The time scale to consider when studying responses to temperature depends on the studied process

Including acclimation responses to temperature in crop growth models implies a memory of the previous temperatures as well as a consideration of the immediate temperature to modulate plant responses, especially carbon assimilation. Indeed, a distinction needs to be made between the growth temperature and the instantaneous temperature. In control conditions, the growth temperature is generally stable over time, with usually a unique variation of temperature between day and night (Bunce, 1985). Thus, T_{growth} is considered as the mean day-time temperature, and the instantaneous temperature is the temperature recorded during specific measurements (*e.g.* recorded temperature during A_{sat}/T_{leaf} measurements). This distinction becomes more complex when working in field conditions, where the temperature naturally varies within hours and between days. Thus, a unique value for T_{growth} is perhaps not relevant and a more complex approach is probably needed.

In the case of leaf appearance rate, we observed a modification of the leaf appearance rate to a change of growth condition within 70°Cd (see Chapter 1). This experimentally observed time-window was successfully used to model LAR in field conditions. By contrast, when studying the response of assimilation to a change of T_{growth}, acclimation was observed within a few hours only. A shorter time window seems to be needed here. Since this acclimation seems to be a direct response of the metabolism, a 40 min time window based on the Rubisco-related activity could be used as suggested by Yin *et al.*, (2018). However, crop models generally calculate photosynthesis at an hour time-step. Considering that a change of A_{sat} in response to a change of T_{growth} happens within this time step, including a differentiation of the growth and the instantaneous temperature in crop models may not improve their prediction. In this case, considering a unique fully acclimated assimilation response to T_{growth} may be enough. However, when working at a finer time-scale, mean temperature over a 40 min time window could be assimilated to T_{growth}, while changes of temperature over a few minutes could be considered as the instantaneous temperature. This distinction could allow incorporating the acclimation of A_{sat}/T_{leaf} to T_{growth} and thus include a finer estimation of carbon assimilation in crop models (Smith and Dukes, 2013).

Overall, differencing growth temperature from instantaneous temperature presents a good solution to model acclimation of A_{sat}/T_{leaf} to T_{growth} that could improve small time-step model predictions. However, when working with hour time-scaled models, the differentiation might not be useful, and a general fully acclimated response of assimilation to T_{growth} might be enough to ensure good predictions.

IV. From empiric to mechanistic models through improvement of biological knowledge

Empirical models directly translate observed relations in equations while mechanistic models are based on the underlying mechanisms driving the observed relations. In various domains, both types of models have been shown to have similar results in some situations (Amphlett *et al.*, 1995 in cellular modelling; Strayer *et al.*, 2003 in ecosystem modeling; Dunne *et al.*, 2005 in ocean biology modelling). However, empiricism often constrains the range of situations for which models can be used. For instance, the use of thermal time to model leaf appearance rate only accounts for the effect of temperature (Jamieson *et al.*, 1995). Effects of other environmental variables such as photoperiod,

plant density or irradiance can be added by combining empirical models, but this results in complex models difficult to parametrize (Miglietta, 1991; Bindi *et al.*, 1995; Gauch *et al.*, 2003). By representing the underlying mechanisms, parameters of mechanistic models have a much clearer biological meaning and can often be measured. Mechanistic models are thus often easier to calibrate than empirical models. In this work, the parameters of the leaf appearance rate model measured in controlled conditions were used to model wheat crops in fluctuating conditions in the field in Arizona, USA and in Canterbury, New-Zealand. Such an understanding of mechanisms also allows using the model for complex questions such as the prediction of plant behavior in contrasted climates, non reproducible in experimental conditions, or to uncorrelate two linked plant processes as it was done in Chapter 2 with a coupled mechanistic photosynthesis-diffusional model.

For all these reasons, we need to build models closer to our understanding of biological processes. This implies a better understanding of these processes, going through an analysis of experimental results in various conditions. A special attention must be paid to build protocols specific to the question asked. These protocols should be reproducible to be able to go deeper or to cross-analyze different researches to improve our knowledge (Way and Yamori, 2014). For example, in this study we developed a standardized protocol to study acclimation response to temperature and a special attention has been paid to leaf appearance rate to get rid of potential confounding effects. This protocol is based on easily measurable traits and can be applied in many growth conditions and was used in different types of growth chambers. The produced data provided results on the underlying processes that can be used to improve crop growth models.

V. Further questions to improve temperature responses in crop growth models

Many questions are still remaining to understand plant processes response and acclimation to temperature. Future experiments should consider the impact of the development stage at which temperature is modified. Indeed, temperature was reported to have different impact on crop performances depending on the development stage (Al-Khatib and Paulsen, 1990; Asseng *et al.*, 2011). This, combined with the modified source/sink relation during plant development highlighted in Chapter 1, support the importance of the development stage on responses to temperature. Another major acclimating process that need to be considered in model is the respiration (Atkin and Tjoelker,

2003; Crous *et al.*, 2011; Peraudeau *et al.*, 2015). Studying respiration acclimation and response to temperature following the protocol exposed in this work could reveal new clues for modelling respiration acclimation.

In conclusion, this work provides a new vision for working on acclimation of plant processes to temperature. It gave new insights for including A_{sat} acclimation to temperature in models. It also presents a new mechanistic and robust model to simulate wheat development rate in a large range of conditions. Crop model consideration of responses to temperature still needs to be improved to ensure the goodness of their prediction. To achieve this, a better understanding of underlying plant processes is needed, and crop modelling needs to more rely on biological knowledge.

References

Abichou M, Fournier C, Dornbusch T, Chambon C, de Solan B, Gouache D, Andrieu B. 2018. Parameterising wheat leaf and tiller dynamics for faithful reconstruction of wheat plants by structural plant models. Field Crops Research **218**, 213–230.

Al-Khatib K, Paulsen GM. 1990. Photosynthesis and productivity during high-temperature stress of wheat genotypes from major world regions. Crop Science **30**, 1127–1132.

Amir J, Sinclair TR. 1991. A model of the temperature and solar-radiation effects on spring wheat growth and yield. Field Crops Research **28**, 47–58.

Amphlett JC, Baumert RM, Mann RF, Peppley BA, Roberge PR, Harris TJ. 1995. Performance modeling of the ballard mark IV solid polymer electrolyte fuel cell II . Empirical model development. Journal of The Electrochemical Society **142**, 9–15.

Arnone JA, Körner C. 1997. Temperature adaptation and acclimation potential of leaf dark respiration in two species of ranunculus from warm and cold habitats. Arctic and Alpine Research **29**, 122–125.

Asseng S, Ewert F, Rosenzweig C, *et al.* 2013. Uncertainty in simulating wheat yields under climate change. Nature Climate Change **3**, 827–832.

Asseng S, Foster I, Turner NC. 2011. The impact of temperature variability on wheat yields. Global Change Biology **17**, 997–1012.

Atkin OK, Bruhn D, Hurry VM, Tjoelker MG. 2005. The hot and the cold: unravelling the variable response of plant respiration to temperature. Functional Plant Biology **32**, 87–105.

Atkin OK, Tjoelker MG. 2003. Thermal acclimation and the dynamic response of plant respiration to temperature. Trends in Plant Science **8**, 343–351.

Baker CK, Gallagher JN, Monteith JL. 1980. Daylength change and leaf appearance in winter wheat. Plant, Cell & Environment **3**, 285–287.

Baker JT, Pinter PJ, Reginato RJ, Kanemasu ET. 1986. Effects of temperature on leaf appearance in spring and winter wheat cultivars. Agronomy Journal **78**, 605–613.

Ball JT, Woodrow IE, Berry JA. 1987. A model predicting stomatal conductance and its contribution to the control of photosynthesis under different environmental conditions. In: Biggins J, ed. Progress in Photosynthesis Research. Dordrecht: Springer Netherlands, 221–224.

Barnabás B, Jäger K, Fehér A. 2008. The effect of drought and heat stress on reproductive processes in cereals. Plant, Cell & Environment **31**, 11–38.

Bassu S, Asseng S, Motzo R, Giunta F. 2009. Optimising sowing date of durum wheat in a variable Mediterranean environment. Field Crops Research **111**, 109–118.

Bassu S, Brisson N, Durand JL, *et al.* 2014. How do various maize crop models vary in their responses to climate change factors? Global Change Biology **20**, 2301–2320.

Bauerle WL, Bowden JD, Wang GG. 2007. The influence of temperature on within-canopy acclimation and variation in leaf photosynthesis: spatial acclimation to microclimate gradients among climatically divergent Acer rubrum L. genotypes. Journal of Experimental Botany **58**, 3285–3298.

Bernacchi CJ. 2002. Temperature response of mesophyll conductance. Implications for the determination of rubisco enzyme kinetics and for limitations to photosynthesis in vivo. Plant Physiology **130**, 1992–1998.

Bernacchi CJ, Bagley JE, Serbin SP, Ruiz-Vera UM, Rosenthal DM, Vanloocke A. 2013. Modelling C_3 photosynthesis from the chloroplast to the ecosystem. Plant, Cell & Environment **36**, 1641–1657.

Bernacchi CJ, Pimentel C, Long SP. 2003. In vivo temperature response functions of parameters required to model RuBP-limited photosynthesis. Plant, Cell & Environment **26**, 1419–1430.

Berry J, Bjorkman O. 1980. Photosynthetic response and adaptation to temperature in higher plants. Annual Review of Plant Physiology **31**, 491–543.

Bindi M, Porter JR, Miglietta F. 1995. Comparison of models to simulate leaf appearance in wheat. European Journal of Agronomy **4**, 15–25.

Birch CJ, Vos J, Kiniry J, Bos HJ, Elings A. 1998. Phyllochron responds to acclimation to temperature and irradiance in maize. Field Crops Research **59**, 187–200.

Boese SR, Huner NPA. 1990. Effect of growth temperature and temperature shifts on spinach leaf morphology and photosynthesis. Plant Physiology **94**, 1830–1836.

Bonhomme R. 2000. Bases and limits to using 'degree.day' units. European Journal of Agronomy **13**, 1–10.

Boone MYL, Rickman RW, Whisler FD. 1990. Leaf appearance rates of two winter wheat cultivars under high carbon dioxide conditions. Agronomy Journal **82**, 718–724.

Bos HJ, Neuteboom JH. 1998. Morphological analysis of leaf and tiller number dynamics of wheat (Triticum aestivum L.): responses to temperature and light intensity. Annals of Botany **81**, 131–139.

Bos HJ, Tijani-Eniola H, Struik PC. 2000. Morphological analysis of leaf growth of maize: responses to temperature and light intensity. NJAS - Wageningen Journal of Life Sciences **48**, 181–198.

Brown H, Huth N, Holzworth D. 2018. Crop model improvement in APSIM: Using wheat as a case study. European Journal of Agronomy.

Bunce JA. 1985. Effects of day and night temperature and temperature variation on photosynthetic characteristics. Photosynthesis Research **6**, 175–181.

Bunce JA. 2000. Acclimation of photosynthesis to temperature in eight cool and warm climate herbaceous C3 species: Temperature dependence of parameters of a biochemical photosynthesis model. Photosynthesis Research **63**, 59–67.

Caemmerer SV. 2000. *Biochemical models of leaf photosynthesis*. Csiro Publishing.

Cai C, Li G, Yang H, *et al.* 2018. Do all leaf photosynthesis parameters of rice acclimate to elevated CO_2, elevated temperature, and their combination, in FACE environments? Global Change Biology **24**, 1685–1707.

Cao W, Moss DN. 1989. Daylength effect on leaf emergence and phyllochron in wheat and barley. Crop Science **29**, 1021–1025.

Cao W, Moss DN. 1991. Phyllochron change in winter wheat with planting date and environmental changes. Agronomy journal **83**, 396–401.

Challinor AJ, Wheeler TR. 2008. Use of a crop model ensemble to quantify CO_2 stimulation of water-stressed and well-watered crops. Agricultural and Forest Meteorology **148**, 1062–1077.

Chaves MM, Flexas J, Pinheiro C. 2009. Photosynthesis under drought and salt stress: regulation mechanisms from whole plant to cell. Annals of Botany **103**, 551–560.

Chenu K, Chapman SC, Tardieu F, McLean G, Welcker C, Hammer GL. 2009. Simulating the yield impacts of organ-level quantitative trait loci associated with drought response in maize: A “gene-to-phenotype” modeling approach. Genetics **183**, 1507–1523.

Chenu K, Van Oosterom EJ, McLean G, *et al.* 2018. Integrating modelling and phenotyping approaches to identify and screen complex traits: transpiration efficiency in cereals. Journal of Experimental Botany **69**, 3181–3194.

Christensen JH, Hewitson B, Busuioc A, *et al.* 2007. Regional climate projections. Climate Change, 2007: The Physical Science Basis. Contribution of Working group I to the Fourth Assessment Report of the Intergovernmental Panel on Climate Change. Cambridge: Cambridge University Press.

Clerget B, Dingkuhn M, Gozé E, Rattunde HFW, Ney B. 2008. Variability of phyllochron, plastochron and rate of increase in height in photoperiod-sensitive sorghum varieties. Annals of Botany **101**, 579–594.

Collatz GJ, Ball JT, Grivet C, Berry JA. 1991. Physiological and environmental regulation of stomatal conductance, photosynthesis and transpiration: a model that includes a laminar boundary layer. Agricultural and Forest Meteorology **54**, 107–136.

Crafts-Brandner SJ, Salvucci ME. 2000. Rubisco activase constrains the photosynthetic potential of leaves at high temperature and CO_2. Proceedings of the National Academy of Sciences **97**, 13430–13435.

Craufurd PQ, Qi A, Ellis RH, Summerfield RJ, Roberts EH, Mahalakshmi V. 1998. Effect of temperature on time to panicle initiation and leaf appearance in sorghum. Crop Science **38**, 942–947.

Crous KY, Quentin AG, Lin Y-S, Medlyn BE, Williams DG, Barton CVM, Ellsworth DS. Photosynthesis of temperate *Eucalyptus globulus* trees outside their native range has limited adjustment to elevated CO_2 and climate warming. Global Change Biology **19**, 3790–3807.

Crous KY, Zaragoza-Castells J, Löw M, Ellsworth DS, Tissue DT, Tjoelker MG, Barton CVM, Gimeno TE, Atkin OK. 2011. Seasonal acclimation of leaf respiration in *Eucalyptus saligna* trees: impacts of elevated atmospheric CO_2 and summer drought. Global Change Biology **17**, 1560–1576.

Daniel RM, Danson MJ, Eisenthal R, Lee CK, Peterson ME. 2008. The effect of temperature on enzyme activity: new insights and their implications. Extremophiles **12**, 51–59.

Davidson AM, Da Silva D, Saa S, Mann P, DeJong TM. 2016. The influence of elevated CO_2 on the photosynthesis, carbohydrate status, and plastochron of young peach (*Prunus persica*) trees. Horticulture, Environment, and Biotechnology **57**, 364–370.

De Reffye P, Houllier F, Blaise F, Barthelemy D, Dauzat J, Auclair D. 1995. A model simulating above- and below-ground tree architecture with agroforestry applications. Agroforestry Systems **30**, 175–197.

Dean C, Elzen P van den, Tamaki S, Dunsmuir P, Bedbrook J. 1985. Differential expression of the eight genes of the petunia ribulose bisphosphate carboxylase small subunit multi-gene family. The EMBO Journal **4**, 3055–3061.

Del Pozo A, Pérez P, Morcuende R, Alonso A, Martínez-Carrasco R. 2005. Acclimatory responses of stomatal conductance and photosynthesis to elevated CO_2 and temperature in wheat crops grown at varying levels of N supply in a Mediterranean environment. Plant Science **169**, 908–916.

Dell AI, Pawar S, Savage VM. 2011. Systematic variation in the temperature dependence of physiological and ecological traits. Proceedings of the National Academy of Sciences **108**, 10591–10596.

Dewar RC, Medlyn BE, Mcmurtrie RE. 1999. Acclimation of the respiration/photosynthesis ratio to temperature: insights from a model. Global Change Biology **5**, 615–622.

Dingkuhn M, Luquet D, Quilot B, Reffye P de. 2005. Environmental and genetic control of morphogenesis in crops: towards models simulating phenotypic plasticity. Australian Journal of Agricultural Research **56**, 1289–1302.

Dunne JP, Armstrong RA, Gnanadesikan A, Sarmiento JL. 2005. Empirical and mechanistic models for the particle export ratio. Global Biogeochemical Cycles **19**.

Dupraz C, Marrou H, Talbot G, Dufour L, Nogier A, Ferard Y. 2011. Combining solar photovoltaic panels and food crops for optimizing land use: Towards new agrivoltaic schemes. Renewable Energy **36**, 2725–2732.

Evans JR. 1983. Nitrogen and photosynthesis in the flag leaf of wheat (*Triticum aestivum* L.). Plant Physiology **72**, 297–302.

Evans JR, Poorter H. 2001. Photosynthetic acclimation of plants to growth irradiance: the relative importance of specific leaf area and nitrogen partitioning in maximizing carbon gain. Plant, Cell & Environment **24**, 755–767.

Evers JB, Vos J, Andrieu B, Struik PC. 2006. Cessation of tillering in spring wheat in relation to light interception and red : far-red ratio. Annals of Botany **97**, 649–658.

Evers JB, Vos J, Yin X, Romero P, Putten VD, L PE, Struik PC. 2010. Simulation of wheat growth and development based on organ-level photosynthesis and assimilate allocation. Journal of Experimental Botany **61**, 2203–2216.

Farooq M, Wahid A, Kobayashi N, Fujita D, Basra SMA. 2009. Plant drought stress: effects, mechanisms and management. In: Lichtfouse E,, In: Navarrete M,, In: Debaeke P,, In: Véronique S,, In: Alberola C, eds. Sustainable Agriculture. Springer Netherlands, 153–188.

Farquhar GD, Caemmerer S von, Berry JA. 1980. A biochemical model of photosynthetic CO2 assimilation in leaves of C3 species. Planta **149**, 78–90.

Farquhar GD, Sharkey and TD. 1982. Stomatal conductance and photosynthesis. Annual Review of Plant Physiology **33**, 317–345.

Flexas J, Carriqui M, Coopman R, Cago J, Galmès J, Martorelle S, Diaz-Espejo A. 2014. Stomatal and mesophyll conductance to CO_2 in different plant groups: underrated factors for predicting leaf photosynthesis responses to climate change? Plant Science **226**, 41–48.

Flexas J, Ribas-Carbó M, Diaz-Espejo A, Galmés J, Medrano H. 2008. Mesophyll conductance to CO2: current knowledge and future prospects. Plant, Cell & Environment **31**, 602–621.

Flood RG, Halloran GM. 1986. Genetics and physiology of vernalization response in wheat. In: Brady NC, ed. Advances in Agronomy. Academic Press, 87–125.

Fournier C, Durand JL, Ljutovac S, Schäufele R, Gastal F, Andrieu B. 2005. A functional-structural model of elongation of the grass leaf and its relationships with the phyllochron. The New Phytologist **166**, 881–894.

Frank AB, Bauer A. 1996. Temperature, nitrogen, and carbon dioxide effects on spring wheat development and spikelet numbers. Crop Science **36**, 659–665.

Friend DJC. 1965. Tillering and leaf production in wheat as affected by temperature and light intensity. Canadian Journal of Botany **43**, 1063–1076.

Galili S, Avivi Y, Feldman M. 1998. Differential expression of three RbcS subfamilies in wheat. Plant Science **139**, 185–193.

Gallagher JN. 1979. Field studies of cereal leaf growth I. Initiation and expansion in relation to temperature and ontogeny. Journal of Experimental Botany **30**, 625–636.

Gauch HG, Gene Hwang JT, Fick GW. 2003. Model evaluation by comparison of model-based predictions and measured values. Agronomy Journal **95**, 1442–1446.

Gautier H, Varlet-Grancher C. 1996. Regulation of leaf growth of grass by blue light. Physiologia Plantarum **98**, 424–430.

Gerbaud A, André M. 1980. Effect of CO_2, O_2, and light on photosynthesis and photorespiration in wheat. Plant Physiology **66**, 1032–1036.

Gifford R. 1995. Whole plant respiration and photosynthesis of wheat under increased CO_2 concentration and temperature long-term vs. short term distinctions for modelling.

Gillooly JF, Brown JH, West GB, Savage VM, Charnov EL. 2001. Effects of size and temperature on metabolic rate. Science **293**, 2248–2251.

Gutteridge S, Gatenby A. 1995. Rubisco synthesis, assembly, mechanism, and regulation. The Plant Cell **7**, 809–819.

Haldimann P, Feller U. 2004. Inhibition of photosynthesis by high temperature in oak (Quercus pubescens L.) leaves grown under natural conditions closely correlates with a reversible heat-dependent reduction of the activation state of ribulose-1,5-bisphosphate carboxylase/oxygenase. Plant, Cell & Environment **27**, 1169–1183.

Hansen N, Ostermeier A. 2001. Completely derandomized self-adaptation in evolution strategies. Evolutionary Computation **9**, 159–195.

Haun JR. 1973. Visual quantification of wheat development. Agronomy journal **65**, 116–119.

Hay RKM, Delécolle R. 1989. The setting of rates of development of wheat plants at crop emergence: Influence of the environment on rates of leaf appearance. Annals of Applied Biology **115**, 333–341.

He J, Le Gouis J, Stratonovitch P, *et al.* 2012. Simulation of environmental and genotypic variations of final leaf number and anthesis date for wheat. European Journal of Agronomy **42**, 22–33.

Henckel PA. 1964. Physiology of plants under drought. Annual Review of Plant Physiology **15**, 363–386.

Heslot N, Akdemir D, Sorrells ME, Jannink J-L. 2014. Integrating environmental covariates and crop modeling into the genomic selection framework to predict genotype by environment interactions. TAG. Theoretical and applied genetics. Theoretische und angewandte Genetik **127**, 463–480.

Hikosaka K, Ishikawa K, Borjigidai A, Muller O, Onoda Y. 2006. Temperature acclimation of photosynthesis: mechanisms involved in the changes in temperature dependence of photosynthetic rate. Journal of Experimental Botany **57**, 291–302.

Hoagland DR. 1950. *The water-culture method for growing plants without soil*. Berkeley, Calif: College of Agriculture, University of California.

Hoogenboom G. 2000. Contribution of agrometeorology to the simulation of crop production and its applications. Agricultural and Forest Meteorology **103**, 137–157.

Horsley SB, Gottschalk KW. 1993. Leaf area and net photosynthesis during development of P*runus serotina* seedlings. Tree Physiology **12**, 55–69.

IPCC, WG II. 2014. Fifth Assessment Report - Impacts, adaptation and vulnerability.

Jamieson PD, Brooking IR, Porter JR, Wilson DR. 1995. Prediction of leaf appearance in wheat: a question of temperature. Field Crops Research **41**, 35–44.

Jamieson P, Brooking I, Zyskowski R, Munro C. 2008. The vexatious problem of the variation of the phyllochron in wheat. Field Crops Research **108**, 163–168.

Jamieson PD, Semenov MA, Brooking IR, Francis GS. 1998. Sirius: a mechanistic model of wheat response to environmental variation. European Journal of Agronomy **8**, 161–179.

Johnson FH, Eyring H, Williams RW. 1942. The nature of enzyme inhibitions in bacterial luminescence: Sulfanilamide, urethane, temperature and pressure. Journal of Cellular and Comparative Physiology **20**, 247–268.

Kaiser WM. 1987. Effects of water deficit on photosynthetic capacity. Physiologia Plantarum **71**, 142–149.

Kattge J, Knorr W. 2007. Temperature acclimation in a biochemical model of photosynthesis: a reanalysis of data from 36 species. Plant, Cell & Environment **30**, 1176–1190.

Kim HK, van Oosterom E, Dingkuhn M, Luquet D, Hammer G. 2010. Regulation of tillering in sorghum: environmental effects. Annals of Botany **106**, 57–67.

Kim K, Portis AR. 2005. Temperature dependence of photosynthesis in Arabidopsis plants with modifications in rubisco activase and membrane fluidity. Plant and Cell Physiology **46**, 522–530.

Kimball BA, White JW, Wall GW, Ottman MJ, Martre P. 2018. Wheat response to a wide range of temperatures, as determined from the Hot Serial Cereal (HSC) Experiment. Open Data journal for Agricultural Research **4**, 16–21.

Kirby EJM. 1995. Factors affecting rate of leaf emergence in barley and wheat. Crop Science **35**, 11–19.

Kirby EJM, Appleyard M, Fellowes G. 1985. Leaf emergence and tillering in barley and wheat. Agronomie **5**, 193–200.

Kirschbaum MUF, Küppers M, Schneider H, Giersch C, Noe S. 1997. Modelling photosynthesis in fluctuating light with inclusion of stomatal conductance, biochemical activation and pools of key photosynthetic intermediates. Planta **204**, 16–26.

Krapp A, Stitt M. 1995. An evaluation of direct and indirect mechanisms for the “sink-regulation” of photosynthesis in spinach: Changes in gas exchange, carbohydrates, metabolites, enzyme activities and steady-state transcript levels after cold-girdling source leaves. Planta **195**, 313–323.

Kratsch HA, Wise RR. 2000. The ultrastructure of chilling stress. Plant, Cell & Environment **23**, 337–350.

Law RD, Crafts-Brandner SJ. 1999. Inhibition and acclimation of photosynthesis to heatstress is closely correlated with activation of Ribulose-1,5-bisphosphate carboxylase/oxygenase.

Lawlor DW, Cornic G. 2002. Photosynthetic carbon assimilation and associated metabolism in relation to water deficits in higher plants. Plant, Cell & Environment **25**, 275–294.

Leuning R. 1995. A critical appraisal of a combined stomatal-photosynthesis model for C3 plants. Plant, Cell & Environment **18**, 339–355.

Li T, Hasegawa T, Yin X, *et al.* 2015. Uncertainties in predicting rice yield by current crop models under a wide range of climatic conditions. Global Change Biology **21**, 1328–1341.

Lizaso JI, Boote KJ, Jones JW, Porter CH, Echarte L, Westgate ME, Sonohat G. 2011. CSM-IXIM: A new maize simulation model for DSSAT Version 4.5. Agronomy journal **103**, 766–779.

Lohraseb I, Collins NC, Parent B. 2017. Diverging temperature responses of CO_2 assimilation and plant development explain the overall effect of temperature on biomass accumulation in wheat leaves and grains. AoB Plants **9**.

Long SP. 1991. Modification of the response of photosynthetic productivity to rising temperature by atmospheric CO_2 concentrations: Has its importance been underestimated? Plant, Cell & Environment **14**, 729–739.

Long SP, Bernacchi CJ. 2003. Gas exchange measurements, what can they tell us about the underlying limitations to photosynthesis? Procedures and sources of error. Journal of Experimental Botany **54**, 2393–2401.

Longnecker N, Robson A. 1994. Leaf emergence of spring wheat receiving varying nitrogen supply at different stages of development. Annals of Botany **74**, 1–7.

Ly D, Chenu K, Gauffreteau A, Rincent R, Huet S, Gouache D, Martre P, Bordes J, Charmet G. 2017. Nitrogen nutrition index predicted by a crop model improves the genomic prediction of grain number for a bread wheat core collection. Field Crops Research **214**, 331–340.

Mäkelä A, Hari P, Berninger F, Hänninen H, Nikinmaa E. 2004. Acclimation of photosynthetic capacity in Scots pine to the annual cycle of temperature. Tree Physiology **24**, 369–376.

Martre P, Dambreville A. 2017. A model of leaf coordination to scale-up leaf expansion from the organ to the canopy. Plant Physiology, pp.00986.2017.

Martre P, Jamieson PD, Semenov MA, Zyskowski RF, Porter JR, Triboi E. 2006. Modelling protein content and composition in relation to crop nitrogen dynamics for wheat. European Journal of Agronomy **25**, 138–154.

Martre P, Yin X, Ewert F. 2017. Modeling crops from genotype to phenotype in a changing climate. Field Crops Research **202**, 1–4.

Masle J. 2000. The effects of elevated CO_2 concentrations on cell division rates, growth patterns, and blade anatomy in young wheat plants are modulated by factors related to leaf position, vernalization, and genotype. Plant Physiology **122**, 1399–1416.

Masle J, Doussinault G, Farquhar GD, Sun B. 1989*a*. Foliar stage in wheat correlates better to photothermal time than to thermal time. Plant, Cell & Environment **12**, 235–247.

Masle J, Doussinault G, Sun B. 1989*b*. Response of wheat genotypes to temperature and photoperiod in natural conditions. Crop Science **29**, 712–721.

McMaster GS, LeCain DR, Morgan JA, Aiguo L, Hendrix DL. 1999. Elevated CO_2 increases wheat CER, leaf and tiller development, and shoot and root growth. Journal of Agronomy and Crop Science **183**, 119–128.

McMaster GS, Wilhelm WW. 1995. Accuracy of equations predicting the phyllochron of wheat. Crop Science **35**, 30–36.

Medlyn BE, Dreyer E, Ellsworth D, *et al.* 2002. Temperature response of parameters of a biochemically based model of photosynthesis. II. A review of experimental data.

Miglietta F. 1991. Simulation of wheat ontogenesis. Climate Research **1**, 145–150.

Millet E, Welcker C, Kruijer W, *et al.* 2016. Genome-wide analysis of yield in Europe: allelic effects as functions of drought and heat scenarios. Plant Physiology, pp.00621.2016.

Miralles DJ, Richards RA. 2000. Responses of leaf and tiller emergence and primordium initiation in wheat and barley to interchanged photoperiod. Annals of Botany **85**, 655–663.

Monteith JL. 1977. Climate and the efficiency of crop production in Britain. Phil. Trans. R. Soc. Lond. B **281**, 277–294.

Moore BD, Cheng S-H, Sims D, Seemann JR. 1999. The biochemical and molecular basis for photosynthetic acclimation to elevated atmospheric CO_2. Plant, Cell & Environment **22**, 567–582.

Morison JIL, Gifford RM. 1983. Stomatal sensitivity to carbon dioxide and humidity: a comparison of two C3 and two C4 grass species. Plant Physiology **71**, 789–796.

Muchow RC, Carberry PS. 1990. Phenology and leaf-area development in a tropical grain sorghum. Field Crops Research **23**, 221–237.

Müller C, Elliott J, Levermann A. 2014. Food security: fertilizing hidden hunger. Nature Climate Change **4**, 540–541.

Murchie EH, Horton P. 1997. Acclimation of photosynthesis to irradiance and spectral quality in British plant species: chlorophyll content, photosynthetic capacity and habitat preference. Plant, Cell & Environment **20**, 438–448.

Nagai T, Makino A. 2009. Differences between rice and wheat in temperature responses of photosynthesis and plant growth. Plant and Cell Physiology **50**, 744–755.

Nash JE, Sutcliffe JV. 1970. River flow forecasting through conceptual models part I — A discussion of principles. Journal of Hydrology **10**, 282–290.

Nijs I, Ferris R, Blum H, Hendrey G, Impens I. 1997. Stomatal regulation in a changing climate: a field study using Free Air Temperature Increase (FATI) and Free Air CO_2 Enrichment (FACE). Plant, Cell & Environment **20**, 1041–1050.

Nix HA. 1976. Climate and crop productivity in Australia. Proceedings of the Symposium on Climate & Rice. International Rice Research Institute, 495–507.

Oguchi R, Hikosaka K, Hirose T. 2005. Leaf anatomy as a constraint for photosynthetic acclimation: differential responses in leaf anatomy to increasing growth irradiance among three deciduous trees. Plant, Cell & Environment **28**, 916–927.

Osonubi O, Davies WJ. 1980. The influence of plant water stress on stomatal control of gas exchange at different levels of atmospheric humidity. Oecologia **46**, 1–6.

Parent B, Leclere M, Lacube S, Semenov MA, Welcker C, Martre P, Tardieu F. 2018. Maize yields over Europe may increase in spite of climate change, with an appropriate use of the genetic variability of flowering time. Proceedings of the National Academy of Sciences **115**, 10642–10647.

Parent B, Tardieu F. 2012. Temperature responses of developmental processes have not been affected by breeding in different ecological areas for 17 crop species. New Phytologist **194**, 760–774.

Parent B, Tardieu F. 2014. Can current crop models be used in the phenotyping era for predicting the genetic variability of yield of plants subjected to drought or high temperature? Journal of Experimental Botany **65**, 6179–6189.

Parent B, Turc O, Gibon Y, Stitt M, Tardieu F. 2010. Modelling temperature-compensated physiological rates, based on the co-ordination of responses to temperature of developmental processes. Journal of Experimental Botany **61**, 2057–2069.

Peraudeau S, Lafarge T, Roques S, Quiñones CO, Clement-Vidal A, Ouwerkerk PBF, Van Rie J, Fabre D, Jagadish KSV, Dingkuhn M. 2015. Effect of carbohydrates and night temperature on night respiration in rice. Journal of Experimental Botany **66**, 3931–3944.

Perdomo JA, Carmo-Silva E, Hermida-Carrera C, Flexas J, Galmés J. 2016. Acclimation of biochemical and diffusive components of photosynthesis in rice, wheat, and maize to heat and water deficit: implications for modeling photosynthesis. Frontiers in Plant Science **7**, 1719.

Porter JR, Semenov MA. 2005. Crop responses to climatic variation. Philosophical Transactions of the Royal Society of London B: Biological Sciences **360**, 2021–2035.

R Core Team. 2017. R: a language and environment for statistical computing. R Foundation for Statistical Computing, Vienna, Austria. URL http://www.R-project.org/.

Reynolds JF, Acock B. 1997. Modularity and genericness in plant and ecosystem models. Ecological Modelling **94**, 7–16.

Rickman RW, Klepper BL. 1995. The phyllochron: where do we go in the future? Crop Science **35**, 44–49.

Rickman RW, Klepper B, Peterson CM. 1985. Wheat seedling growth and developmental response to incident photosynthetically active radiation. Agronomy Journal **77**, 283–287.

Rondanini D, Mantese A, Savin R, Hall AJ. 2006. Responses of sunflower yield and grain quality to alternating day/night high temperature regimes during grain filling: Effects of timing, duration and intensity of exposure to stress. Field Crops Research **96**, 48–62.

van Rooijen R, Aarts MGM, Harbinson J. 2015. Natural genetic variation for acclimation of photosynthetic light use efficiency to growth irradiance in Arabidopsis. Plant Physiology **167**, 1412–1429.

Rosenzweig C, Elliott J, Deryng D, *et al.* 2014. Assessing agricultural risks of climate change in the 21st century in a global gridded crop model intercomparison. Proceedings of the National Academy of Sciences **111**, 3268–3273.

Rosenzweig C, Parry ML. 1994. Potential impact of climate change on world food supply. Nature **367**, 133–138.

Rötter RP, Carter TR, Olesen JE, Porter JR. 2011. Crop–climate models need an overhaul. Nature Climate Change **1**, 175–177.

Sage RF. 1994. Acclimation of photosynthesis to increasing atmospheric CO_2: The gas exchange perspective. Photosynthesis Research **39**, 351–368.

Sage RF, Kubien DS. 2007. The temperature response of C3 and C4 photosynthesis. Plant, Cell & Environment **30**, 1086–1106.

Salvucci ME, Crafts-Brandner SJ. 2004. Inhibition of photosynthesis by heat stress: the activation state of Rubisco as a limiting factor in photosynthesis. Physiologia Plantarum **120**, 179–186.

Scafaro AP, Xiang S, Long BM, Bahar NHA, Weerasinghe LK, Creek D, Evans JR, Reich PB, Atkin OK. 2017. Strong thermal acclimation of photosynthesis in tropical and temperate wet-forest tree species: the importance of altered Rubisco content. Global Change Biology **23**, 2783–2800.

Sesták Z (Ed.). 1985. *Photosynthesis during leaf development*. Springer Netherlands.

Sharkey TD. 1985. Photosynthesis in intact leaves of C3 plants: physics, physiology and rate limitations. The Botanical Review **51**, 53–105.

Sharma RC. 1995. Tiller mortality and its relationship to grain yield in spring wheat. Field Crops Research **41**, 55–60.

Shewry PR. 2009. Wheat. Journal of Experimental Botany **60**, 1537–1553.

Simmons SR. 1987. Growth, development, and physiology. Wheat and Wheat Improvement **agronomymonogra**, 77–113.

Simpson GM. 1968. Association between grain yield per plant and photosynthetic area above the flag-leaf node in wheat. Canadian Journal of Plant Science **48**, 253–260.

Sinclair TR, Horie T. 1989. Leaf nitrogen, photosynthesis, and crop radiation use efficiency: a review. Crop Science **29**, 90.

Skinner RH, Nelson CJ. 1995. Elongation of the grass leaf and its relationship to the phyllochron. Crop science **35**, 4–10.

Slafer GA, Connor DJ, Halloran GM. 1994. Rate of leaf appearance and final number of leaves in wheat: effects of duration and rate of change of photoperiod. Annals of Botany **74**, 427–436.

Slafer GA, Rawson HM. 1995. Base and optimum temperatures vary with genotype and stage of development in wheat. Plant, Cell & Environment **18**, 671–679.

Slafer GA, Rawson HM. 1997. Phyllochron in wheat as affected by photoperiod under two temperature regimes. Functional Plant Biology **24**, 151–158.

Slayter RO, Morrow PA. 1977. Altitudinal variation in the photosynthetic characteristics of snow gum, *Eucalyptus pauciflora* sieb. ex Spreng. I. Seasonal changes under field conditions in the snowy mountains area of south-eastern australia. Australian Journal of Botany **25**, 1–20.

Smith NG, Dukes JS. 2013. Plant respiration and photosynthesis in global-scale models: incorporating acclimation to temperature and CO_2. Global Change Biology **19**, 45–63.

Smith NG, Dukes JS. 2017. Short-term acclimation to warmer temperatures accelerates leaf carbon exchange processes across plant types. Global Change Biology, 1–14.

Stinziano JR, Way DA, Bauerle WL. 2018. Improving models of photosynthetic thermal acclimation: which parameters are most important and how many should be modified? Global Change Biology **24**, 1580–1598.

Stitt M, Zeeman SC. 2012. Starch turnover: pathways, regulation and role in growth. Current Opinion in Plant Biology **15**, 282–292.

Strayer DL, Beighley RE, Thompson LC, Brooks S, Nilsson C, Pinay G, Naiman RJ. 2003. Effects of Land Cover on Stream Ecosystems: Roles of Empirical Models and Scaling Issues. Ecosystems **6**, 407–423.

Streck NA. 2003. Stomatal response to water vapor pressure deficit: an insolved issue. Current Agricultural Science and Technology **9**.

Tardieu F, Cabrera-Bosquet L, Pridmore T, Bennett M. 2017. Plant phenomics, from sensors to knowledge. Current biology: CB **27**, R770–R783.

Tardieu F, Simonneau T. 1998. Variability among species of stomatal control under fluctuating soil water status and evaporative demand: modelling isohydric and anisohydric behaviours. Journal of Experimental Botany **49**, 419–432.

Terashima I, Hanba YT, Tazoe Y, Vyas P, Yano S. 2006. Irradiance and phenotype: comparative eco-development of sun and shade leaves in relation to photosynthetic CO_2 diffusion. Journal of Experimental Botany **57**, 343–354.

Thomashow MF. 2003. Plant cold acclimation: freezing tolerance genes and regulatory mechanisms. Annual Review of Plant Physiology and Plant Molecular Biology **50**, 571–599.

Thornley JHM. 1998. Dynamic model of leaf photosynthesis with acclimation to light and nitrogen. Annals of Botany **81**, 421–430.

Tottman DR, Makepeace RJ, Broad H. 1979. An explanation of the decimal code for the growth stages of cereals, with illustrations. Annals of Applied Biology **93**, 221–234.

Trnka M, Rötter RP, Ruiz-Ramos M, Kersebaum KC, Olesen JE, Žalud Z, Semenov MA. 2014. Adverse weather conditions for European wheat production will become more frequent with climate change. Nature Climate Change **4**, 637–643.

Upchurch RG. 2008. Fatty acid unsaturation, mobilization, and regulation in the response of plants to stress. Biotechnology Letters **30**, 967–977.

Vile D, Pervent M, Belluau M, Vasseur F, Bresson J, Muller B, Granier C, Simonneau T. 2012. Arabidopsis growth under prolonged high temperature and water deficit: independent or interactive effects? Plant, Cell & Environment **35**, 702–718.

Volk T, Bugbee B. 1991. Modeling light and temperature effects on leaf emergence in wheat and barley. Crop Science **31**, 1218–1224.

Wall GW, Kimball BA, White JW, Ottman MJ. 2011. Gas exchange and water relations of spring wheat under full-season infrared warming. Global Change Biology **17**, 2113–2133.

Wang JY. 1960. A critique of the heat unit approach to plant response studies. Ecology **41**, 785–790.

Wang E, Engel T. 1998. Simulation of phenological development of wheat crops. Agricultural Systems **58**, 1–24.

Wang E, Martre P, Zhao Z, *et al.* 2017. The uncertainty of crop yield projections is reduced by improved temperature response functions. Nature Plants **3**.

Warton DI, Duursma RA, Falster DS, Taskinen S. 2012. smatr 3– an R package for estimation and inference about allometric lines. Methods in Ecology and Evolution **3**, 257–259.

Way DA, Oren R. 2010. Differential responses to changes in growth temperature between trees from different functional groups and biomes: a review and synthesis of data. Tree Physiology, tpq015.

Way DA, Yamori W. 2014. Thermal acclimation of photosynthesis: on the importance of adjusting our definitions and accounting for thermal acclimation of respiration. Photosynthesis Research **119**, 89–100.

Wheeler TR, Batts GR, Ellis RH, Hadley P, Morison JIL. 1996. Growth and yield of winter wheat (Triticum aestivum) crops in response to CO2 and temperature. The Journal of Agricultural Science **127**, 37–48.

White JW, Kimball BA, Wall GW, Ottman MJ. 2012. Cardinal temperatures for wheat leaf appearance as assessed from varied sowing dates and infrared warming. Field Crops Research **137**, 213–220.

Wilhelm WW, McMaster GS. 1995. Importance of the phyllochron in studying development and growth in grasses. Crop Science **35**, 1–3.

Wong SC, Cowan IR, Farquhar GD. 1979. Stomatal conductance correlates with photosynthetic capacity. Nature **282**, 424–426.

Xinyou Y, Laar HH van. 2005. *Crop systems dynamics: an ecophysiological simulation model for genotype-by-environment interactions*. Wageningen Academic Pub.

Yamasaki T, Yamakawa T, Yamane Y, Koike H, Satoh K, Katoh S. 2002. Temperature acclimation of photosynthesis and related changes in photosystem II electron transport in winter wheat. Plant Physiology **128**, 1087–1097.

Yamori W, Hikosaka K, Way DA. 2013. Temperature response of photosynthesis in C3, C4, and CAM plants: temperature acclimation and temperature adaptation. Photosynthesis Research **119**, 101–117.

Yamori W, Noguchi K, Hikosaka K, Terashima I. 2010. Phenotypic plasticity in photosynthetic temperature acclimation among crop species with different cold tolerances. Plant Physiology **152**, 388–399.

Yamori W, Noguchi K, Terashima I. 2005. Temperature acclimation of photosynthesis in spinach leaves: analyses of photosynthetic components and temperature dependencies of photosynthetic partial reactions. Plant, Cell and Environment **28**, 536–547.

Yin X, van Laar H h. 2005. *Crop systems dynamics*. Wageningen Academic Publishers.

Yin X, Schapendonk AHCM, Struik PC. 2018. Exploring the optimum nitrogen partitioning to predict the acclimation of C3 leaf photosynthesis to varying growth conditions. Journal of Experimental Botany.

Yin X, Struik PC. 2009. C3 and C4 photosynthesis models: an overview from the perspective of crop modelling. NJAS - Wageningen Journal of Life Sciences **57**, 27–38.

Yin X, Struik PC. 2010. Modelling the crop: from system dynamics to systems biology. Journal of Experimental Botany **61**, 2171–2183.

Yin X, Struik PC, Romero P, Harbinson J, Evers JB, Putten PELVD, Vos J. 2009. Using combined measurements of gas exchange and chlorophyll fluorescence to estimate parameters of a biochemical C3 photosynthesis model: a critical appraisal and a new integrated approach applied to leaves in a wheat (Triticum aestivum) canopy. Plant, Cell & Environment **32**, 448–464.

Zaka S, Ahmed LQ, Escobar-Gutiérrez AJ, Gastal F, Julier B, Louarn G. 2017. How variable are non-linear developmental responses to temperature in two perennial forage species? Agricultural and Forest Meteorology **232**, 433–442.

Zaka S, Frak E, Julier B, Gastal F, Louarn G. 2016. Intraspecific variation in thermal acclimation of photosynthesis across a range of temperatures in a perennial crop. AoB PLANTS **8**.

Zhao C, Liu B, Piao S, *et al.* 2017. Temperature increase reduces global yields of major crops in four independent estimates. Proceedings of the National Academy of Sciences **114**, 9326–9331.

Zhu J, Dai Z, Vivin P, Gambetta GA, Henke M, Peccoux A, Ollat N, Delrot S. 2018. A 3-D functional-structural grapevine model that couples the dynamics of water transport with leaf gas exchange. Annals of Botany **121**, 833–848.